



The University of  
**Nottingham**

# **PEGYLATION OF PACLITAXEL FOR INHALED CHEMOTHERAPY**

**Tian Luo, MSc.**

**Thesis submitted to the University of Nottingham  
for the degree of Doctor of Philosophy**

**Supervisors: Prof. Rita Vanbever  
Dr. Cynthia Bosquillon**

**June 2016**





## SUMMARY

Pulmonary delivery is considered an attractive route of drug administration for chemotherapeutic agents, with the advantages of high drug concentrations locally and low side effects systemically. However, fast clearance mechanisms result in short residence times of small molecule drugs in the lung. Moreover, the local toxicity induced by antineoplastic drugs is considered a major obstacle for the application of inhaled chemotherapy in the clinic.

In this study, we aimed at developing polyethylene glycol-paclitaxel (PEG-PTX) conjugates in order to retain paclitaxel within the lung, achieve its sustained release locally and reduce its toxicity to the lung. The conjugates were expected to present increased efficacy in the treatment of lung cancer, as compared to the quickly-cleared native drug.

Two structures of PEG-PTX conjugates with PEG molecular weights of 6 kDa and 20 kDa were synthesized. One structure was synthesized with azide linker using “click” chemistry and the other was synthesized with a succinic spacer. Conjugation to PEG improved the solubility of paclitaxel by up to four orders of magnitude. The conjugates showed good stability in phosphate buffer saline and in bronchoalveolar lavage at both molecular weights, but hydrolyzed quickly in mouse serum. The conjugates showed cytotoxicity to B16-F10 melanoma cells and LL/2 Lewis lung cancer cells but less than free paclitaxel or Taxol, the commercial paclitaxel formulation. The conjugates synthesized by

“click” chemistry were chosen for the evaluation *in vivo* because they were more stable in different media than the succinic conjugates.

Results *in vivo* showed that the conjugates increased the maximal tolerated doses of paclitaxel by up to 100-fold compared with Taxol following intratracheal instillation in healthy C57Bl/6 mice. The anti-tumor efficacy was assessed in the Lewis lung carcinoma cell-induced lung cancer murine model. It was enhanced significantly by delivering PEG-PTX conjugates to the lung, compared with Taxol delivered either intratracheally or intravenously. PEG-PTX 20 kDa (20 mg/kg PTX equivalent) showed equivalent anti-tumor efficacy as PEG-PTX 6 kDa delivered at a higher dose (50 mg/kg PTX equivalent). PEG-PTX conjugates increased biochemical and cellular markers of inflammation in the lung at their maximal tolerated doses. However, decreasing PEG-PTX 6k dose lowered local toxicity. Delivery of PEG-PTX conjugates to the lungs resulted in prolonged retention of the conjugate and sustained paclitaxel release in the lung over more than 48h. This study demonstrated that PEGylation offers a potential drug delivery system for inhaled chemotherapy with improved anti-tumor efficacy and reduced local toxicity.

## ACKNOWLEDGEMENTS

I would like to thank my supervisors Prof. Rita Vanbever and Dr. Cynthia Bosquillon for the guidance. I am very grateful for their scientific advice and insights, for the trust and independence they offered on me. I would also thank my supervisors Prof. Veronique Preat and Prof. Cameron Alexander for the help and inspiring discussions about this work.

I wish to thank Johannes for his help and advice on the chemistry in this thesis. I would not have completed the synthesis without his support.

I would like to thank Cristina for her help in animal experiments and useful advice on the *in vivo* study.

I would also thank Prof. Raphael Frédérick for offering the facilities in his lab for conjugate synthesis and precious advice. Many thanks to Prof. Giulio Muccioli for his help with the analysis of paclitaxel *in vivo* and insightful advice.

I also wish to thank my colleagues of the Advanced Drug Delivery and Biomaterials group in Université catholique de Louvain for creating a friendly and inspiring environment. I am very grateful to my dearest friends and lab mates: Laure, Marie-Julie, Harshad, Alessandra, Loic, Chiara, Aiswarya, Lungile, Pallavi, Michelle, Ana, Pauline, Dario, John and previous ADDDB colleagues Salome, Danielle, Kiran and Julie. I also appreciate the encouragement and help from Prof. Anne des Rieux, Fabienne, and Gaëlle in the lab.

I would like to express my thanks to the technical staff in ADDDB. Particularly Bernard, Kevin and Maria, thank you for working on the *in*

*vivo* study with me and all the generous support. Many thanks to Murielle and Jean-Pierre for the help with administrative stuff.

I would also thank other members of Université catholique de Louvain: Dr. Cecil Le Duff, Department of chemistry, for helping with analysis of NMR data; Vincent Stroobant, Ludwig Institute for Cancer Research, for the help with mass spectrum; Julien Masquelier and Pauline Bottemanne for the help with LC-MS and cytospin.

I would like to express my gratitude to the colleagues and friends in University of Nottingham: Sui Cheng, Francesca, Nora, Giovanna, Hiteshri, Vanessa, Joao, Kuldeep, Deepak, Keren, Sarah, Delian, Yewande, Emanuela, Jin Zhu, and Dr. Bowen Tian. Thank you for your kindness and support during my stay in Nottingham. The time spent with you was really wonderful!

I appreciate Dr. Ji Liu, University of Cambridge and Dr. Zhengyuan Zhou, Duke University for valuable advice on this thesis.

I would like to thank Erasmus Mundus NanoFar Program for offering me this opportunity to study in Belgium and UK. Many thanks to Prof. Frank Boury and Marion Toucheteau who made this happen!

Last but not least, I would like to express my sincere gratitude to my family for the understanding and support during these years. Thank you for always being considerate in my good and bad times. I would not have made it without you!

I dedicate this thesis to my beloved grandma Fengju Wang.

谨以此文献给我思念的姥姥王凤菊。

**ABBREVIATIONS**

BAL	Bronchoalveolar lavage
CYP-450	Cytochrome P450
$d_{aer}$	Aerodynamic diameter
$D_{mucus}$	Diffusion constant in mucus
DIC	N,N'-Diisopropylcarbodiimide
DMAP	4-Dimethylaminopyridine
DMEM	Dulbecco's Modified Eagle Medium
DMF	Dimethylformamide
DMSO	Dimethyl sulfoxide
DPBS	Dulbecco's phosphate-buffered saline
EPR	Enhanced permeability and retention
FBS	Fetal bovine serum
HBSS	Hank's balanced salt solution
HPLC	High Performance Liquid Chromatography
HSA	Human serum albumin
i.v.	Intravenously
i.t.	Intratracheally
ICRP	International commission on radiological protection
LDH	Lactate dehydrogenase
LC-MS	Liquid chromatography mass spectrometry
MEM-Alpha	Minimum Essential Medium Eagle Alpha
MTD	Maximum tolerated dose
MTT	3-(4, 5-Dimethylthiazol-2-yl)-2,5-

## ABBREVIATIONS

---

	Diphenyltetrazolium Bromide
MW	Molecular weight
NMR	Nuclear magnetic resonance
NSCLC	Non-small cell lung cancer
PEG	Polyethylene glycol
PEG-PCL	Poly (ethylene glycol)-b-polycaprolactone
PEG-DSPE	PEG-distearoyl phosphatidylethanolamine
P (DAPG-EOP)	P (2,4-diacetylphloroglucinol-EOP)
PEG-PTX	Polyethylene glycol-paclitaxel conjugate
PHPMA	Poly [N-(2-hydroxypropyl) methacryamide]
PGA	Polyglutamic acid
PTX	Paclitaxel
R.T.	Room temperature
SN38	7-ethyl-10-hydroxy-camptothecin
SEM	Standard error of the mean
$t_{1/2}$	Half-life
TLC	Thin layer chromatography
TOF-ES-MS	Electrospray ionisation time-of-flight mass spectrometry

## TABLE OF CONTENTS

<b>CHAPTER 1. INTRODUCTION .....</b>	<b>1</b>
1. Lung cancer and current therapies.....	3
1.1 Surgical resection .....	3
1.2 Radiotherapy .....	4
1.3 Chemotherapy .....	5
1.4 Other novel treatments .....	10
2. Inhaled chemotherapy.....	11
2.1 Advantages of inhaled chemotherapy.....	11
2.2 Physiological factors affecting local antitumor efficacy in the lungs.....	13
2.3 Safety issue of chemotherapeutics delivered to the lungs ..	20
2.4 Nanocarrier related issue.....	23
2.5 Pulmonary delivery of paclitaxel .....	24
3. PEGylation: an useful strategy for inhaled chemotherapy.....	26
3.1 Concept of PEGylation .....	27
3.2 PEGylation of chemotherapeutic agents.....	28
3.3 PEGylation for pulmonary delivery.....	33
4. Aim of the thesis.....	33

<b>CHAPTER 2. SYNTHESIS AND <i>IN VITRO</i> EVALUATION OF POLYETHYLENE GLYCOL-PACLITAXEL CONJUGATES FOR LUNG CANCER THERAPY .....</b>	<b>39</b>
1. Introduction .....	42
2. Materials and methods .....	48
2.1 Materials and instruments.....	48
2.2 Synthesis of PEG-N <sub>3</sub> 6 kDa and 20 kDa.....	49
2.3 Synthesis of PTX alkyne.....	50
2.4 Synthesis of PEG-N <sub>3</sub> -PTX conjugates 6 kDa and 20 kDa ..	51
2.5 Synthesis of PEG-suc 6 kDa and 20 kDa .....	52
2.6 Synthesis of PEG-suc-PTX conjugates 6 kDa and 20 kDa	53
2.7 Solubility .....	54
2.8 Stability of conjugates in PBS, BAL and serum of mice .....	54
2.9 Cytotoxicity .....	56
3. Results and discussion.....	58
3.1 Chemistry .....	58
3.2 Aqueous solubility and <i>in vitro</i> stability of PEG-PTX conjugates .....	61
3.3 Cytotoxicity .....	64
4. Conclusion .....	69

<b>CHAPTER 3. PEGYLATION OF PACLITAXEL LARGELY IMPROVES ITS SAFETY AND ANTI-TUMOR EFFICACY FOLLOWING PULMONARY DELIVERY IN A MOUSE MODEL OF LUNG CARCINOMA.....</b>	<b>71</b>
1. Introduction .....	75
2. Materials and methods .....	78
2.1 Materials .....	78
2.2 PEG-PTX conjugates and Taxol .....	79
2.3 Animals .....	80
2.4 Maximum tolerated doses of PEG-PTX conjugates delivered intratracheally .....	81
2.5 Local toxicity of PEG-PTX conjugates in the lungs .....	81
2.6 Anti-tumor efficacy of PEG-PTX conjugates against Lewis lung carcinoma .....	83
2.7 Kinetics of <i>in vivo</i> distribution in the respiratory tract .....	84
2.8 Statistics .....	86
3. Results .....	86
3.1 Conjugation to PEG increased the MTD of paclitaxel post-intratracheal delivery .....	86
3.2 Local toxicity studies of PEG-PTX conjugates in the lungs .....	89
3.3 PEG-PTX conjugates increased anti-tumor efficacy in a murine model of lung carcinoma.....	95
3.4 PEG-PTX conjugates prolonged the retention time of paclitaxel in the lungs .....	97

4. Discussion.....	98
<b>CHAPTER 4. DISCUSSION AND CONCLUSION.....</b>	<b>103</b>
1. Main achievements .....	105
1.1 Outcomes of the thesis .....	105
1.2 Synthesis of PEG-conjugated paclitaxel with cleavable linkage for pulmonary application .....	107
1.3 Increased anti-tumor efficacy and prolonged lung retention of chemotherapeutics .....	109
1.4 Improved MTD and reduced local toxicity for inhaled chemotherapy.....	110
1.5 Summary .....	111
2. Perspectives.....	112
2.1 Long-term toxicity .....	112
2.2 Improvement of polymer-drug conjugation strategy.....	113
2.3 Mechanisms involved in the lung retention of PEGylated paclitaxel.....	114
<b>APPENDIX .....</b>	<b>117</b>
<b>REFERENCES .....</b>	<b>119</b>

---

**LIST OF FIGURES**

Fig.1 Molecule structure and 3-D structure of paclitaxel.....	5
Fig. 2 Illustration of the gradients in oxygen, nutrients and energy, and drug concentration in solid tumor cells. ECM, extracellular matrix (adapted from (14) ). .....	6
Fig. 3 Predicted particle deposition in total and in different respiratory regions for light exercise (nose breathing) based on ICRP deposition model. Average data from males and females (39).....	15
Fig. 4 Illustration of mucociliary clearance. The mucus absorbs large particles and, with the assistance of the cilia and cough, the harmful particles are exhaled (adapted from (42) ). .....	16
Fig. 5 Diffusion constants in mucus compared with PBS as a function of hydrodynamic diameter of the diffusing particles (40).....	17
Fig. 6 The half-life of drug absorption is depended on the lipophilicity. P represents the octanol/water partition coefficient. Half-life represents the time taken for absorption of 50% of the initial dose through the lung following intratracheal administration in rats (45).....	19
Fig. 7 The half-life of drug absorption through the lung is related to the molecular weight. Molecules characterized as lipid-insoluble or as lipid-soluble are shown as squares and triangles, respectively. Molecules with active uptake are shown as inverted triangles (45). .....	19
Fig. 8 PEG-paclitaxel synthesized by Greenwald <i>et al.</i> Paclitaxel was conjugated to a bi-functional PEG by ester bonds (adapted from (80) ). .....	30
Fig. 9 PLA-PEG-PLA/paclitaxel conjugate (83).....	31
Fig. 10 The drug release mechanism of PEGylated docetaxel (NKTR-	

---

105) (85).....	32
Fig. 11 Normalized absorption profiles of prednisolone in the isolated perfused rat lungs obtained with (□) prednisolone alone, (○) mPEG2000-Pred and (Δ) PEG2000-Pred <sub>2</sub> . Prednisolone concentration (nmol L <sup>-1</sup> ) measured in perfusate was divided by the actual delivered dose (nmol) to give a relative prednisolone fraction (L <sup>-1</sup> ). Data are presented as mean ± SD, n = 3. (91) .....	35
Fig. 12 Structure-active relationships (SARs) of paclitaxel (77) .....	37
Fig. 13 Two structures of PEG-PTX conjugates developed in this thesis. ....	38
Fig. 14 Synthetic routes of PEG-PTX conjugates. <b>A. “Click” chemistry route:</b> PTX (compound 1) was modified with pentynoic acid at C-2' group to obtain PTX-alkyne (compound 2). PEG-N <sub>3</sub> 6 kDa and 20 kDa (compounds 5a and 5b) were synthesized from PEG with 2 hydroxyl ends by tosylation followed by azidation. PTX-alkyne was then conjugated to PEG-N <sub>3</sub> 6 kDa and 20 kDa via “click” chemistry respectively to obtain the final conjugates PEG-N <sub>3</sub> -PTX 6 kDa and 20 kDa (compounds 6a and 6b). <b>B. Succinic spacer route:</b> succinic acid was linked to PEG 6 kDa and 20 kDa via esterification to obtain PEG-suc 6 kDa and 20 kDa (compounds 7a and 7b). PEG-suc-PTX 6 kDa and 20 kDa (compounds 8a and 8b) were then obtained by esterification of PEG-suc and PTX at C-2' position.....	47
Fig. 15 <sup>1</sup> H NMR spectrum of PEG-suc-PTX, PEG-N <sub>3</sub> -PTX 6 kDa and PTX.....	60
Fig. 16 Stability profiles of conjugates in bronchoalveolar lavage (A) and serum of mouse (B). ....	63

Fig. 17 Cell metabolic activities of PEG-PTX conjugates and Taxol on LL/2 Lewis lung cancer cells (A) and B16-F10 melanoma cells (B). Results are shown as the mean of 3 independent tests (8 measurements each test) and standard deviation. ....66

Fig. 18 Cytotoxicity of PEG reagents on LL/2 cells after 72 hour incubation at the concentration of 2.5 µg/mL (PTX equiv.). Results are shown as the mean of 3 independent tests (8 measurements per test) and standard deviation. \* p<0.05, when compared with control group. # p<0.05, when compared with triton 1% (Mann-Whitney). ....69

Fig. 19 Body weights of mice receiving PEG-PTX conjugates and Taxol intratracheally and intravenously. (A) PEG-PTX 6k conjugate delivered intratracheally at different doses, (B) PEG-PTX 20k conjugate delivered intratracheally, (C) Taxol delivered intratracheally at different doses, (D) Taxol delivered intravenously at different doses. Mean ± SEM are shown, n=6 mice per group.....88

Fig. 20 Local toxicity of PEG-PTX conjugates, Taxol, free PEG-N<sub>3</sub> 6k and Cremophor EL. (A) Total protein (B) LDH level (C) total cell numbers (D) macrophage numbers (E) neutrophil numbers and (F) lymphocyte numbers in BAL at different time points post intratracheal instillation of PEG-PTX conjugates, Taxol, PEG-N<sub>3</sub> 6k and Cremophor EL. Mean and SEM are shown, n=4-6 mice per group, \* p< 0.05, \*\* p< 0.01, compared with control group (Mann-Whitney). ....91

Fig. 21 Representative pictures showing foamy macrophages in (A) PEG-PTX 20k group 7 days post-delivery and their absence in (B) PBS control group (colored by Diff Quick®, magnification × 40 under optical microscope). ....93

---

Fig. 22 Representative pictures showing lung morphology post intratracheal delivery of PBS control (A), Taxol 0.5 mg/kg (B), PEG-PTX 6k 50 mg/kg (C), PEG-PTX 20k 20 mg/kg (D), PEG-PTX 0.5 mg/kg (E), and PEG-N <sub>3</sub> 50 mg/kg (F) (Hematoxylin-Eosin staining). .....	94
Fig. 23 Efficacy assessment of PEG-PTX conjugates and Taxol delivered by intratracheal instillation or intravenous injection in a murine model of Lewis lung carcinoma. (A) Representative images of mouse lungs. (B) Numbers of LL/2 tumor cells per milligram lung tissue. (C) Body weights of mice. Mean ± SEM are given, n=6-7. * $p < 0.05$ ; NS, no significant difference (Mann-Whitney). Similar results were obtained in two independent experiments.....	96
Fig. 24 PTX and PEG-PTX 20k recovered from the respiratory tract 0h, 24h and 48h post intratracheal administration. (A) PTX amount in BAL and (B) PTX amount in the lungs in mice having received PEG-PTX 20k (20 mg/kg PTX equiv.) and Taxol (0.5 mg/kg). (C) Amount of PTX expressed as a percentage of the total dose recovered from BAL, lungs and serum at time 0. (D) Amount of PEG-PTX 20k expressed as a percentage of the total dose recovered from BAL and lungs at time 0. * $p < 0.05$ , when compared with Taxol group (Mann-Whitney); BQ, below quantification limit. ....	98
Fig. 25 Illustration of possible release mechanism of PTX from conjugates in the lungs. ....	102

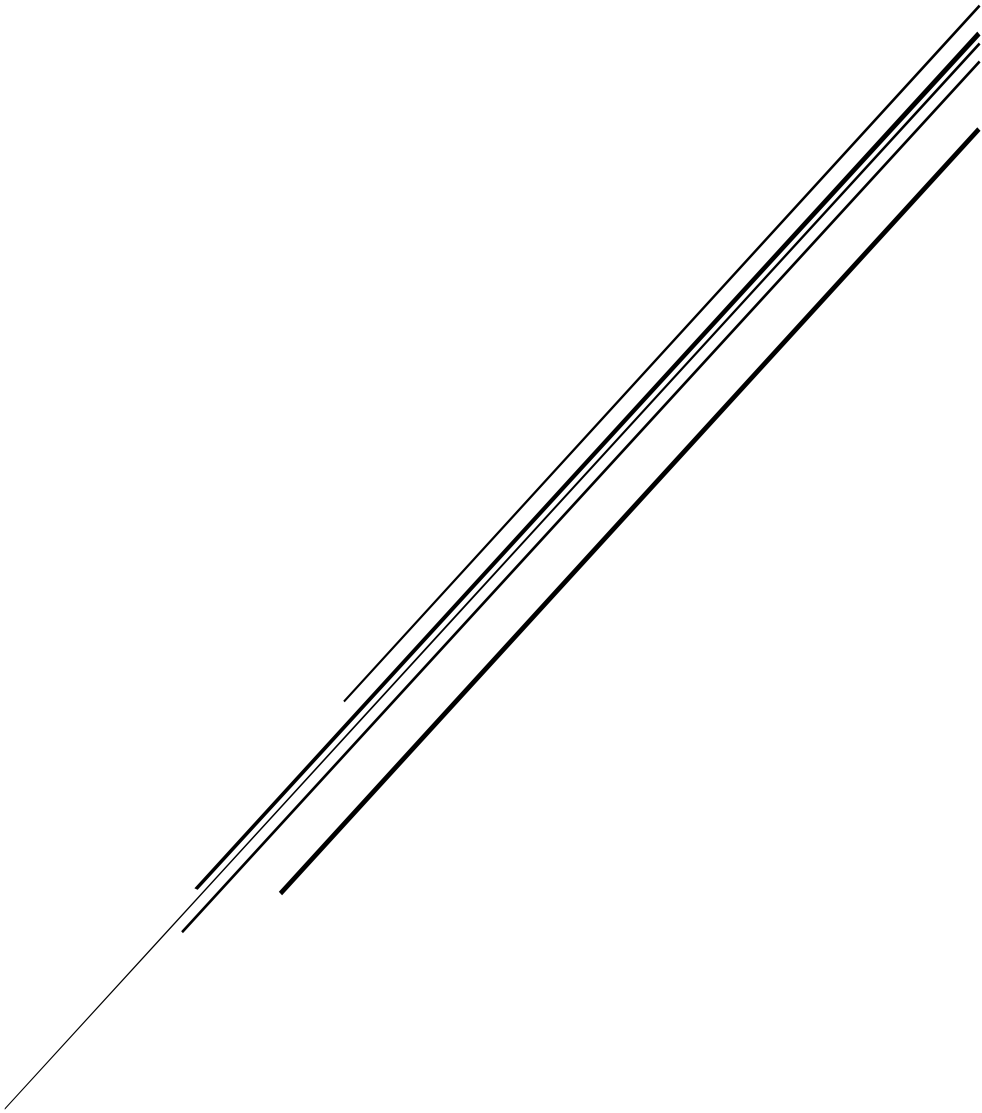
## LIST OF TABLES

Table 1. Anti-cancer agents in delivery systems now on the market (adapted from (19)).	8
Table 2. Polymer drug conjugates presented in clinical trials or on the market (adapted from (20, 21)).	9
Table 3. Half-lives of conjugates in different media	62
Table 4. IC <sub>50</sub> values of all the conjugates calculated based on the data of MTT test.	65
Table 5. MTD of PEG-paclitaxel conjugates and Taxol post i.t. or i.v. injection.	89

## LIST OF TABLES

---

# CHAPTER 1. INTRODUCTION



千里之行，始于足下。  
A journey of a thousand miles begins with a single step.



## **1. Lung cancer and current therapies**

Lung cancer is the most common cancer worldwide and causes a large number of death 1.4 million per year (1). More than half a million patients are diagnosed with lung cancer each year and about 80% is non-small cell lung cancer (NSCLC), including adenocarcinomas, large cell carcinomas, and squamous cell carcinomas (2). Primary lung cancers mainly originate from lung epithelial cells and result from smoking and exposure to contaminants. Metastasis of other cancers (e.g., breast and prostate cancer) are also frequently found in the lungs (3). Most patients are diagnosed with lung cancer when the cancer has become locally advanced or spread distantly. The typical treatments for lung cancer are surgical resection, radiotherapy and chemotherapy.

### **1.1 Surgical resection**

Surgical resection is commonly regarded as the most effective treatment for early stage NSCLC limited to the lung and surrounding glands with tumor cells. Most surgeries have shown five-year survival rate from 55% to 72% in patients with localized stage I NSCLC, and 29% to 51 for patients with stage II NSCLC (4). But only about 20% of tumors are suitable for resection (5). Moreover, there is no convincing evidence to certify that surgeries improve survival of patients compared with other treatments, for instance, radiotherapy or chemotherapy.

If a limited resection is performed to individuals with localized cancers, the chance of local recurrence will increase. A more extensive resection could decrease this risk. Chemotherapy sometimes is combined with surgery. However, chemotherapy followed by surgery showed no better effect than chemotherapy followed by radical radiotherapy in terms of overall survival (4).

## **1.2 Radiotherapy**

Patients who are not suitable for surgical resection due to comorbidities (e.g., heart disease) are treated with conventional radiotherapy for early stage lung cancer. Results are not ideal because conventional radiotherapy is not effective to 60-70% of patients with primary lung tumor (6). Generally, the combination of cytotoxic chemotherapy and radiotherapy could improve efficacy compared with radiotherapy alone. Recent research results from clinical trials using advanced irradiation delivery techniques have demonstrated that patients treated with these modified therapies together with cisplatin-based chemotherapy have a superior long-term survival compared with those who were only treated with radiotherapy or chemotherapy (7, 8). However, the combination treatment is usually accompanied with increased toxicity in the radiation field. More hematological toxicity is often observed in patients receiving combination treatments (9).

### 1.3 Chemotherapy

Chemotherapy has been widely used to treat non-small cell lung cancer. It can be administered as single treatment or combined with surgery or radiotherapy in radical or palliative treatment. Chemotherapy after radiotherapy or surgery can help patients live longer. Combinations of different anti-cancer drugs in chemotherapy tend to work better than a single drug. Cisplatin and carboplatin play an important role in the treatment of both small cell lung cancer and non-small cell lung cancer, and the combination with gemcitabine, etoposide, vinorelbine, paclitaxel (Taxol) (Fig. 1), docetaxel (Taxotere) or doxorubicin are frequently used in treating non-small cell lung cancer (2, 10, 11).

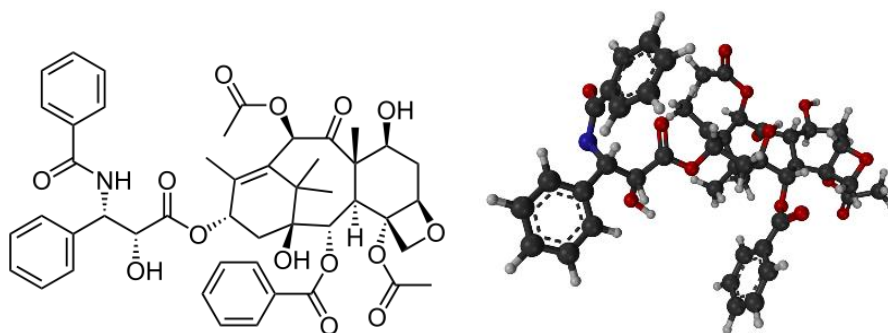


Fig. 1 Molecule structure and 3-D structure of paclitaxel.

Generally, chemotherapy prolongs the survival of patients with advanced NSCLC by 3 to 6 months compared with best supportive care (12). Combination of platinum with other chemotherapeutics can improve survival compared with best supportive care or single treatment of cisplatin. However, there is only 2-month extension of

median survival time. Survival at 1 year only has an increased probability of 10% to 20%. The addition of bevacizumab, an angiogenesis inhibitor, to platinum treatment has prolonged survival time of 2 months compared with chemotherapy alone (13). The unsatisfactory clinical efficacy of chemotherapy can be attributed to the low local drug concentration in the lung tumor and the severe dose-limiting side effects.

It is reviewed in (14) that the inefficient drug penetration from blood vessels in solid tumors leads to unsatisfactory anti-tumor effectiveness. The limited drug penetration is illustrated in Fig. 2. The oxygen, nutrients and energy, and drug concentration were in decreased gradients from the blood vessel to the tumor region.

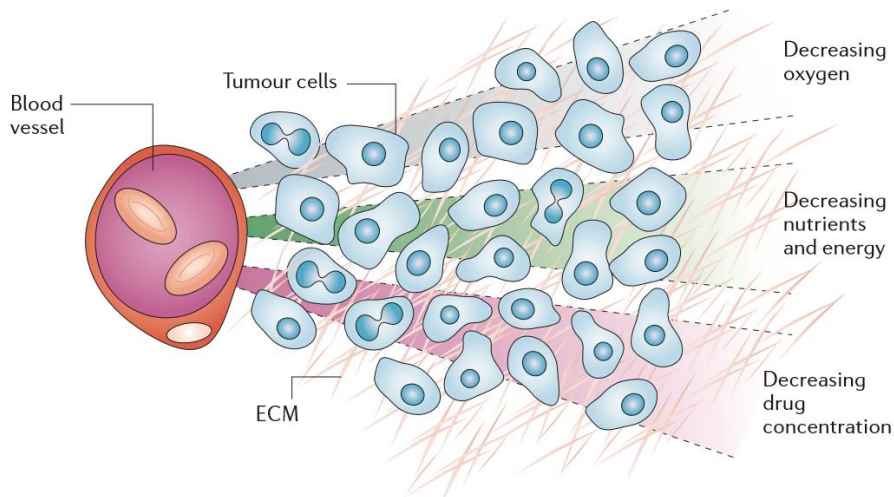


Fig. 2 Illustration of the gradients in oxygen, nutrients and energy, and drug concentration in solid tumor cells. ECM, extracellular matrix (adapted from (14) ).

Most chemotherapy is administered by the systemic route, so side effects are severe. The most common adverse drug reactions are induced by the effects of chemotherapeutic agents on rapidly dividing cells. Therefore, hair loss, white and red blood cell-count lowering may occur. Mouth sores and nausea may also happen (15). In addition to these common drug reactions, peripheral neurotoxicity is a dose-limiting and disabling side effect of many frequently used anti-cancer agents, in particular, paclitaxel, cisplatin, vincristine, oxaliplatin, and docetaxel. Specifically, systemic administration of paclitaxel usually induces myelosuppression and hyper sensibility reactions in addition to peripheral neuropathy.

Many anticancer agents have unsatisfactory pharmaceutical and pharmacological attributes, i.e., poorly water solubility, instability, irritating feature or fast metabolism. Different drug delivery systems have been developed for chemotherapeutics including liposomes, nanoparticles, polymeric micelles, and polymer-drug conjugates. Liposomal doxorubicin (Doxil), and nanoparticle albumin-bound paclitaxel (Abraxane) are two widely used formulations for cancer therapy now on the market. Doxil was the first nanoscale delivery system approved in US. It is approved for the treatment of AIDS-related Kaposi's sarcoma in the year of 1995. Then it was approved for treatment of ovarian cancer and multiple myeloma in US in the year of 1999 and 2007, respectively. The dramatic reduction of cardiotoxicity as well as the passive tumor targeted effect were the

main benefits of this liposomal formulation (16). Abraxane is approved for the treatment of metastatic breast cancer in 2005. Because the harmful excipient Cremophor EL was excluded in this formulation, the main advantage of Abraxane was the improved toxicity profile (17, 18). Drug delivery systems of traditional anti-cancer agents now on market are summarized in Table 1.

Table 1. Anti-cancer agents in delivery systems now on the market (adapted from (19)).

Anti-cancer agents	Delivery systems	Trade names	Clinical application	Year of approval
Doxorubicin	Liposome	Doxil	AIDS-related Kaposi's sarcoma	1995 US
			Ovarian cancer	1999
			Multiple myeloma	2007
Daunorubicin	Liposome	DaunoXome	AIDS-related Kaposi's sarcoma	1996 US
Cytarabine	Liposome	Depocyt	Lymphomatous meningitis	1999 US
Paclitaxel	Albumin-bound	Abraxane	Metastatic breast cancer	2005 US
Vincristine	Liposome	Marqibo	Acute lymphoblastic leukemia	2012 US
Paclitaxel	Micelle	Genexol-PM	Breast cancer Small cell lung cancer	2007 Korea

Table 2. Polymer drug conjugates presented in clinical trials or on the market (adapted from (20, 21)).

Conjugates	Name	Company	Indication	Status
PEG-irinotecan	NKTR-102	Nektar	Solid tumor	Phase II/III
PEG-SN38	EZN-2208	Enzon	Solid tumor	Phase II
PEG-docetaxel	NKTR-105	Nektar	Solid tumor	Phase I
PEG-camptothecin	Pegamotecan		Gastric cancer	Phase II
PEG-paclitaxel		Enzon	Solid tumor	Phase I (terminated)
PHPMA-platinum	AP5280	Access Pharmaceuticals	Various malignancies	Phase II
PHPMA-DACH-oxaliplatin	ProLinda	Access Pharmaceuticals	Ovarian cancer	Phase II
Fleximer-camptothecin	XMT-1001	Mersana	Gastric cancer, lung cancer	Phase I
Carboxymethyl dextran-T2531	Delimotecan	Daiichi Pharmaceuticals	Various malignancies	Phase I
Cyclodextrin-camptothecin	CRLX101	Cerulean	Advance solid tumor	Phase II
Polyglutamic acid-camptothecin	CT-2106	Cell Therapeutics	Colon cancer, ovarian cancer	Phase I/II
Polyglutamic acid-paclitaxel	Opaxio, CT-2103	Cell Therapeutics	Lung cancer, ovarian cancer	Phase III
HSA-methotrexate	MTX-HSA	Klinge Pharma	Kidney cancer	Phase II
Carboxymethyl dextran polyalcohol polymer-DX-8591	DE-310	Ontario Institute for Cancer Research	Various malignancies	Phase I/II
HPMA-paclitaxel	PNU166945	Pharmacia & Upjohn	Solid tumor	Phase I (terminated)

HSA, human serum albumin.

In addition to nano-carrier based systems, polymer-drug conjugate is another effective approach to improve therapeutic properties of anti-cancer drugs. Polymer-drug conjugates can benefit from the enhanced permeability and retention (EPR) effect when injected intravenously due to the relatively large particle size. Polymer-drug conjugates define that therapeutics are covalently linked to polymer carriers and are able to be released in active forms. Hydrophilic polymers PEG, N-2-Hydroxypropyl methacrylamide (PHPMA), and polyglutamic acid (PGA) are frequently involved in this strategy. Table 2 summarized the polymer drug conjugates in clinical trials or already on market currently.

#### **1.4 Other novel treatments**

Different from traditional nonspecific chemotherapy, targeting alternations in oncogene-driven cancers and immune-oncology are two main trends in novel cancer therapy. These targeting treatments have achieved therapeutic effects that improved survival of patients in some type of cancers.

*EGFR downregulating treatments.* Epidermal growth factor (EGF) and its receptor (EGFR) are crucial for the progression of solid tumors. EGFR is highly expressed in NSCLC (22). Various parts of the EGFR pathway is related with the growth of tumor cells in lung cancer. Thus, EGFR pathway is an attractive target for the treatment of lung cancer. Currently, two major approaches downregulating EGFR-signalling are anti-EGFR antibodies and EGFR tyrosine kinase inhibitors. Cetuximab (Erbix<sup>®</sup>) is the representative of anti-EGFR antibodies and gefitinib

(Iressa<sup>®</sup>) is the representative of EGFR tyrosine kinase inhibitors.

*Immunotherapy.* Many solid tumors are immunogenic. Tumor related antigens resulting from gene mutations are generated during the malignancy (23). These antigens could be recognized by the immune system. Tumor antigen – specific T cells responses are then initiated (23). However, cancer cells can form immune-suppressive networks, which disturbs the generation of tumor-reactive T cells and T-cell trafficking (24). Therefore, immune-suppressive inhibitory molecules (e.g., cytotoxic T lymphocyte antigen-4 (CTLA-4), programmed cell death protein-1 (PD-1), and programmed death-ligand 1 (PD-L1)) are the most popular targets for cancer immunotherapy (25). PD-1/L1 blockers showed very promising clinical results with better toxicity profile compared with conventional chemotherapy, particularly in melanoma, NSCLC and kidney cancer. PD-1 inhibitor nivolumab (Opdivo<sup>®</sup>) achieved encouraging long-term overall survival results in patients with NSCLC, which demonstrated its superior clinical efficacy (26).

## **2. Inhaled chemotherapy**

### **2.1 Advantages of inhaled chemotherapy**

Inhaled chemotherapy is considered very promising to treat lung cancer because of the targeted delivery with less systemic side effects. The concept of “magic bullet” therapy proposed by Paul Ehrlich 100 years ago illustrates the ideal approach to treat cancer, that is, the therapeutics toxic to tumors are targeted to cancer cells without

causing damage to healthy tissues and cells (27). Aerosol chemotherapy could achieve the targeted delivery with fewer side effects which is the main function of this “magic bullet”. Local exposure of the lungs to chemotherapeutics could be achieved. Moreover, because the anticancer agents are delivered locally, the dosages should be much lower than following intravenous injection, which results in higher drug concentrations at the site of lung malignancy and lower drug entry into the systemic circulation. Consequently, systemic side effects could be minimized due to the relatively low plasma level of anti-neoplastic drugs. Finally, inhaled chemotherapy could also increase the convenience and compliance of the patients compared with intravenous injection.

Many proof of concept studies have been done in the field of inhaled chemotherapy. This approach was first investigated by Tatsumura *et al.* in 1983 using 5-fluorouracil administered to patients by a supersonic nebulizer (28). They found remarkable anti-tumor responses in patients and only trace amounts of 5-fluorouracil were found in the serum samples of tested patients. In 1993, Tatsumura *et al.* also evaluated 5-fluorouracil in dogs by inhalation and obtained high concentrations of drug in trachea, hilar bronchi, and regional lymph nodes (29). In the following 2 decades, various chemotherapeutics were studied for efficacy and safety in either animals or humans (30-32). A study was conducted in dogs with spontaneously occurred primary and metastatic tumors in the lungs to investigate the safety and anti-tumor efficacy of inhaled paclitaxel or doxorubicin (33). Anti-tumor efficacy was demonstrated without any

acute systemic side effects, i.e., myelosuppression, nausea, and vomiting associated in any dogs. They also revealed that a combination of both the intravenous and inhaled routes of administering chemotherapeutics enhanced anti-tumor efficacy without increasing overall toxicity. These studies based on dogs showed that inhaled chemotherapy as a novel therapeutic approach could have potential efficacy and safety in humans with lung cancer or lung metastasis of other types of cancers. The most recent clinical phase II trial in inhaled chemotherapy was conducted with aerosolized doxorubicin combined with intravenously delivered platinum (34). It showed acceptable toxicity, however, the response rate did not meet the objective. Therefore, this treatment was not pursued further.

Nevertheless, the development and application of inhaled formulations for lung cancer face several challenges. The lung itself has a sophisticated structure and a very efficient defense system which easily clears the substances entering the lung. Moreover, safety issues remain major concerns for inhaled chemotherapy. These challenges will be discussed in the following sections 2.2 and 2.3.

## **2.2 Physiological factors affecting local antitumor efficacy in the lungs**

Although inhaled chemotherapy sounds reasonable and attractive theoretically, it is not easy to achieve the ideal efficacy. Obstacles present in the complexity of lung physiology, including lung barriers, epithelial absorption and enzyme systems.

## 2.2.1 Lung barriers

### Airway geometry and particle deposition

The lung is the site for frequent gas exchange with the environment and is consequently exposed to numerous pathogens daily. It has a complex structure and includes anatomical barriers to avoid the invasion of particles into the lung, thus decreasing the accessibility of drugs to the lung. The human lung has been described as a tree of which the trachea, bronchi and bronchioles are the branches and the alveoli are the leaves (35). The branched nature of the airways leads to the impaction of particles in the respiratory tract. Moreover, the humid environment in the airways facilitates the growing of hygroscopic particle size and then their deposition in the different areas of the lung (36).

Large particles (aerodynamic diameter,  $d_{aer} > 5 \mu\text{m}$ ) deposit in the upper respiratory tract by inertial impaction. Particles with 1 to 5  $\mu\text{m}$   $d_{aer}$  settles down in the central and distal tracts by gravitational settling. Most particles with 0.1 and 1  $\mu\text{m}$   $d_{aer}$  are exhaled (37). Ultrafine particles (<100 nm) quickly deposit in the alveolar region by random Brownian movement. Particles below 10 nm deposit in the tracheo-bronchial region because of high diffusion coefficients (38). Fig. 3 illustrates the total and regional deposition predicted by the International Commission on Radiological Protection (ICRP) deposition model. The ICRP model was used to estimate the dose to human organs after the inhalation of radioactive particles. Three levels of exercise were included in this model: sitting, light exercise, and

heavy exercise (39).

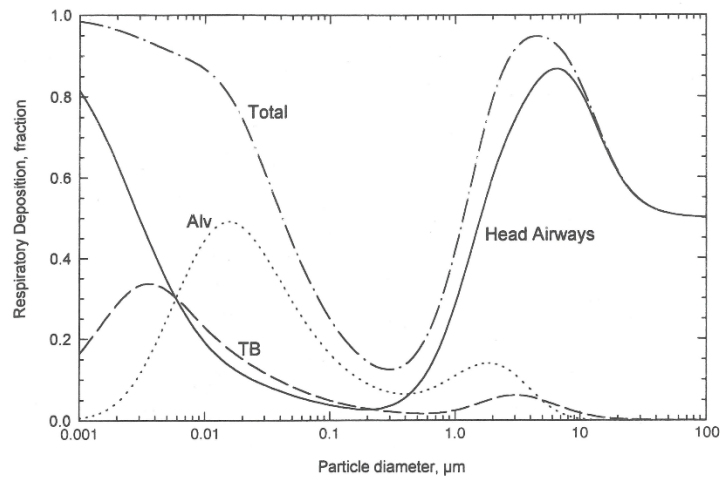


Fig. 3 Predicted particle deposition in total and in different respiratory regions for light exercise (nose breathing) based on ICRP deposition model. Average data from males and females (39).

### Mucus barrier

After deposition in the lung, the particles are trapped in another barrier, the mucus. The mucus is a viscoelastic gel composed of 95% water, 2% mucin, 1% albumin, immunoglobulins and enzymes and < 1% lipids. Mucin is a glycoprotein with a fibrous structure which provides the gel property of the mucus (40).

Mucociliary escalator and phagocytosis are considered as two major mechanisms of the clearance of particles in the lung. The mucus is secreted continuously and it has a transport velocity around 10-100 μm/s which facilitates the mucociliary clearance (40), resulting in the

movement of mucus and particles trapped in it to the oropharynx, where they are swallowed or expelled out (Fig. 4). Phagocytosis by alveolar macrophages is the major pathway to eliminate microparticles and large proteins depositing in the alveoli. However, particles smaller than 200 nm are not efficiently cleared by phagocytosis, which may then cause nanotoxicity (41). These highly defensive mechanisms protect the lung from hazardous pathogens and particles, however, they become major obstacles for drugs to be delivered to the targeted site in the lung. Mucociliary clearance has been considered to be the cause of the short retention times of nanoparticles that administered to the airways.

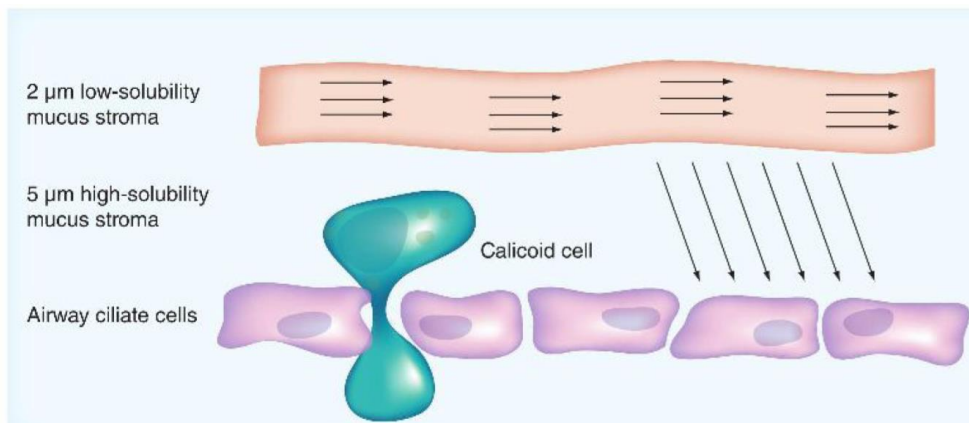


Fig. 4 Illustration of mucociliary clearance. The mucus absorbs large particles and, with the assistance of the cilia and cough, the harmful particles are exhaled (adapted from (42) ).

Particles that escape from mucociliary clearance of the mucus then start to diffuse throughout. The speed of diffusion in mucus is related to the particle size. A study has tested the diffusion constants of

particles with various sizes in fresh samples of human cervico-vaginal mucus. The results were presented as the ratio of diffusion constant in mucus,  $D_{\text{mucus}}$ , divided by the diffusion constant in PBS,  $D_{\text{pbs}}$  (Fig. 5). It was observed that soluble globular protein with particle size less than 100 nm could diffuse freely through the mucus ( $D_{\text{mucus}}/D_{\text{pbs}} = 1$ ). PEGylated nanoparticles with size of 500 nm can still diffuse through mucus but at a slow rate. As particle diameter increases, the speed of diffusion is slowed down (43). Because the general properties of mucus secreted from various epithelia are similar, i.e., they are viscoelastic gel containing mucin, water, salts, lipid and protein, this cervico-vaginal model could be used to predict the diffusion of particles in the lungs. Therefore, choosing a specific size for particles to escape or to stay in the mucus could fulfill different purposes when designing drug delivery systems (44).

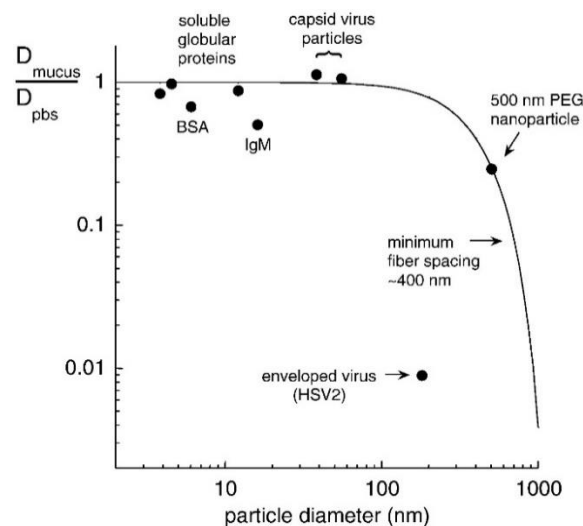


Fig. 5 Diffusion constants in mucus compared with PBS represented as a function of hydrodynamic diameter of the diffusing particles (40).

### **2.2.2 Epithelial absorption**

Absorption occurs when the drug solubilized in the mucus passes through the epithelium. It has been previously investigated that the lung is highly permeable to a number of drugs. Water solubility, lipophilicity, and molecular weight play important roles. Small lipophilic molecules ( $\log P > 0$ ) have a very short half-life for absorption (around 1 minute). Small hydrophilic molecules ( $\log P < 0$ ) have half-lives around 1 hour (Fig. 6) (45). Hydrophilic macromolecules are absorbed much more slowly into the blood stream than hydrophilic small molecule drugs (Fig. 7). By using a large molecule carrier to form stable delivery systems, the local residence time as well as the local concentration of anticancer agents could be improved. For instance, Polyethylene glycol (PEG) with large molecular weight ( $mw > 5$  kDa) has been shown to be retained in the lung for up to 7 days (46). This prolonged retention time in the lung can be utilized to achieve sustained drug release in the lung by conjugating small molecule drugs to macromolecules.

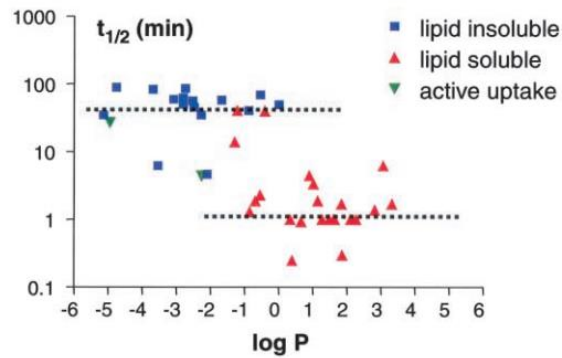


Fig. 6 The half-life of drug absorption is depended on the lipophilicity.  $P$  represents the octanol/water partition coefficient. Half-life represents the time taken for absorption of 50% of the initial dose through the lung following intratracheal administration in rats (45).

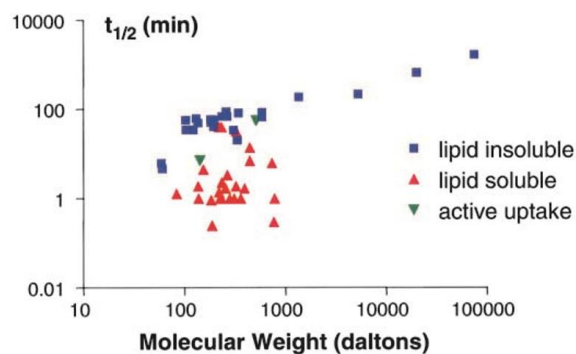


Fig. 7 The half-life of drug absorption through the lung is related to the molecular weight. Molecules characterized as lipid-insoluble or as lipid-soluble are shown as squares and triangles, respectively. Molecules with active uptake are shown as inverted triangles (45).

At the tumor site, changes in some physical factors could affect drug diffusion and absorption. For example, tumors lack functional lymphatics. The lymphatic drainage is absent, which results in increased high interstitial fluid pressure in tumors (47). Consequently, the diffusion and distribution of drugs in tumor can be affected, resulting in reduced convection and limited distribution of drugs.

### **2.2.3 Enzymatic system of the lung**

Although the lung is not a major site for metabolism, all the metabolizing enzymes existing in the liver are found in the lung but in lower amounts. The groups of metabolizing enzymes identified include phase I CYP-450s, phase II conjugating enzymes, ubiquitous esterase and other enzymes. The regional distribution of these enzymes is heterogeneous and there are differences between cell types, even within the same airway section. The nonspecific esterase is widely distributed in the lung tissue. It is present at a high level in alveolar macrophages and to a lesser extent in alveolar type I and II cells. Esterase can act on esters, amides and thioesters, which allows the delivery of prodrugs containing such linkers to be one strategy for inhaled chemotherapy (48).

### **2.3 Safety issue of chemotherapeutics delivered to the lungs**

Although various anti-cancer drugs and delivery systems have been designed and tested for pulmonary delivery, the concerns of efficacy versus toxicity to the lung tissue remain debatable. Firstly, pulmonary toxicity reactions could happen when using chemotherapeutic agents

such as paclitaxel, and docetaxel. This may occur during or after treatment (24). Furthermore, local delivery of high doses of chemotherapeutic agents can increase the risk of drug-induced disease in the lung in patients who usually already have impaired lung functions as a result of tobacco-related illness (25). Moreover, the occupational exposure to health professionals during treatment is also an issue. The nebulized drug must, for instance, be administered in a well-ventilated room (26).

Lung injury can be induced after administration of chemotherapeutics either by i.v. Infusion or inhalation. Patients are found to have lung interstitial fibrosis and pneumonitis while receiving systemic chemotherapy. Inhalation of chemotherapeutics forces the lung to be exposed directly to the cytotoxic drug, which would generate even more safety problems. Drug induced damage could happen both in the airways and in the lung parenchyma (42).

*Airways damages.* Bronchoconstriction, which is a lung's defense mechanism, is the major symptom observed after the inhalation. This can be found immediately after administration. Nonproductive cough is consequently found and the can last several minutes to months. Bronchitis obliteration is another dangerous symptom induced by inhalation of drugs (49). Neutrophil infiltration and granuloma tissue generation can be found in the airway. Peripheral neuropathy can also be observed as the neurological adverse effect (50). It is recommended that pre-administration of inhaled corticosteroids could help to moderate the airways symptoms (47).

*Lung parenchyma damages.* Noncardiologic pulmonary edema can occur as an acute toxicity effect induced by interaction of cytotoxic with the lung parenchyma. Acute respiratory distress can also be observed as a symptom (51). Diffuse pneumonitis and interstitial fibrosis can be found either as an acute or chronic injury. The pathological alterations behind these adverse effects are: pneumocyte cells type I which covering the alveoli surface are destroyed; pneumocyte cells type II, which is the ancestors of type I, being reproduced in a larger number; However, abnormal type I cells are finally produced due to toxicity burden and the limited time. Hypersensitivity pneumonitis is another drug induced disease which can be observed either in acute or chronic forms. Fever and nonmucus productive cough are usually found as symptoms. In this case, eosinophil infiltration in the alveoli and interstitial lung tissue is usually observed (42).

Study of inhaled doxorubicin and paclitaxel based on dogs showed acute pulmonary toxicity, including nonproductive cough, which was observed in 50% of the tested dogs (33). This side effect was presumably associated with the direct interaction of doxorubicin with the airways, which resulted in the damages of airways. Mild pneumonitis, multifocal interstitial fibrosis and alveolar histiocytosis which represents the lung parenchyma damages were also found.

In a phase I clinical trial of inhaled doxorubicin on patients with metastatic tumors to the lungs, the most frequent pulmonary side effect was cough (31). Dyspnea, chest pain, wheezing, hoarseness, hemoptysis, and bronchospasm were also observed. Sever pulmonary adverse effects i.e., hypoxia and respiratory distress were

observed in a limited number of patients. One patient received the high dose of doxorubicin (9.4 mg/kg) died during the study. The patient was a 50-year-old male with bronchoalveolar carcinoma involving both lungs. He experienced severe shortness of breath and decreased oxygen saturation following the first dose of inhaled doxorubicin. Autopsy showed that mucinous bronchoalveolar carcinoma was extensively presented in the lungs and acute obstructive pneumonia was observed. The author attributed the death to the acute obstructive pneumonia secondary to extensive tumor load and tumor evading into the larger airways.

#### **2.4 Nanocarrier related issue**

Nanocarrier systems are widely investigated to deliver anti-cancer drugs by the pulmonary route but there is also safety issues related to nanoparticles. After administration into the lungs, some nanoparticles may be transported to sites out of the lungs and reach non-targeted tissues. These properties can lead to potential toxicity as well. In some cases, nanoparticles are translocated into interstitial sites, where they obtain access to the blood circulation via lymphatics, leading to distribution to the whole body (52-54). Furthermore, the ultrafine nanoparticles are not easy to be phagocytized by macrophages as mentioned before, therefore, they are difficult to be eliminated from the alveoli (55). This kind of nanoparticles could stay either in epithelial cells or transport to the interstitium, consequently, long-term accumulation and toxicity issues could be aroused by them(56). Moreover, the toxicity data *in vitro* is hard to predict the performance

of nanoparticles *in vivo* in lungs. Studies by Sayes *et al.* that demonstrated very little correlation between *in vitro* and *in vivo* toxicities of nanoscaled zinc oxide and fullerenes (57, 58).

## **2.5 Pulmonary delivery of paclitaxel**

Paclitaxel is one of the most effective broad-spectrum chemotherapeutic agents. It was originally obtained from the needle and bark of pacific yew tree. The antitumor mechanism of paclitaxel results from the stabilization of microtubules. This inhibits cell growth by preventing cytoskeletal microtubule depolymerization, leading to the cessation of the cell cycle (59). Paclitaxel has been widely used in clinics for the treatment of a wide spectrum of cancer, such as small and non-small cell lung cancer, ovarian cancer, breast cancer, bladder cancer, and colon cancer (60). However, the clinical application of paclitaxel is limited due to its low aqueous solubility. There is no functional group on the structure of paclitaxel to form salt to increase its dissolution rate in aqueous solutions (60, 61). The current commercial paclitaxel formulation used in the clinic is Taxol, which is formulated with 1:1 mixture of Cremophor EL and ethanol and causes serious side effects, including hypersensitivity reaction, cardiotoxicity and neurotoxicity (62).

Taxol is administered by the intravenous route, which is not ideal for attaining high local drug concentrations in the lungs. In addition, the formulation contains an excipient which triggers serious side effects. Furthermore, it is clear that administration of free antineoplastic agents by aerosol delivery can improve drug accumulation in the lung tumor,

but cannot change the toxicity. Therefore, effective and safe pulmonary delivery systems of paclitaxel are in need for the clinic.

In recent years, several delivery systems of paclitaxel have been developed and demonstrated potential for pulmonary delivery. In these works, paclitaxel was incorporated into different biodegradable carriers to form micelles, liposomes, solid lipid nanoparticles or microspheres. In particular, polymeric nanoparticles fabricated from polymers like poly (ethylene glycol)-*b*-polycaprolactone (PEG-PCL) copolymers, PEG-distearoyl phosphatidylethanolamine (PEG-DSPE), alginate, and polyphosphoester polymer p(2,4-diacetylphloroglucinol - EOP) (P(DAPG-EOP)) have been widely studied (63, 64).

Paclitaxel liposomes for aerosol treatment was first developed in 2001 by Koshkina *et al.* (63). The pharmacokinetics of paclitaxel liposomes after inhalation and intravenous administration was compared in murine models at the same doses. In the inhalation group, higher local concentrations and slow clearance of the drug in the lungs were detected. These drug carriers enhance the solubility of paclitaxel by encapsulating it and providing a hydrophilic surface. The polymeric carriers protect paclitaxel from degradation before reaching the targeted site. Local delivery of these paclitaxel systems to the lungs could increase the drug concentrations in the tissue, thus improving the therapeutic index and reducing the exposure to irrelevant organs and tissues. Furthermore, if sustained release is attained, the dosage will be decreased drastically and frequent administration will be avoided.

Although many pulmonary delivery systems have been developed for paclitaxel, very few achieved sustained drug release in the lung for a long period. In Gill's research (65), paclitaxel was encapsulated in poly(ethylene oxide)-block-distearoyl phosphatidylethanolamine (PEG<sub>5000</sub>-DSPE) micelles. Paclitaxel PEG-DSPE micelles were delivered to the lungs of Sprague–Dawley rats directly by intratracheal instillation and the tissue distribution and plasma pharmacokinetics of the drug were monitored. Initially, a similar drug concentration was measured in the lung following paclitaxel delivery using PEG-DSPE micelles and Taxol, but after 12h, a much higher paclitaxel concentration was found in the lungs with the micelles, which indicated a sustained release of paclitaxel.

### **3. PEGylation: an useful strategy for inhaled chemotherapy**

Attaining a sustained release of drug in the lung would be of great benefit. A sustained-release formulation of a chemotherapeutic agent could maintain drug concentrations at an effective levels in the lungs for a long period of time and avoid peaks in local drug concentration, consequently improving the cancer treatments and reducing toxicity to lung tissues (66). However, attaining sustained-drug release in the lung is challenging. The lung has highly efficient defense mechanisms to clear solutes and particulates as described earlier in this chapter (67). Different strategies to obtain sustained drug release in the lungs have been tested in animal models, including tumor-bearing animals. These include PEGylation, dendrimers, biodegradable polymeric

microspheres, liposomes, lipid particles, and micelles (68-72). In this thesis, we focus on PEGylation of a small molecule anti-cancer drugs for pulmonary delivery. Therefore, the concept of PEGylation, its use in chemotherapy and pulmonary delivery will be discussed in details in the following text.

### **3.1 Concept of PEGylation**

Polyethylene glycol (PEG) is a macromolecule which can be significantly hydrated in water because of the hydrogen bonds with water. PEGylation defines linking one or more PEG to a protein, peptide or small molecular drug (73). Depending on its size, PEG can be transported and absorbed across the epithelia membranes in the lung. Using PEG to formulate small molecule drugs could theoretically prolong the retention of drugs in the lung and thus possibly achieve sustained release of drugs. PEG is nontoxic and FDA has approved its usage in formulations. PEGylation of small molecules can be classified according to the general configuration of the system (linear, branched, dendrimeric, etc.) or the type of linkage between components (ester, amide, biodegradable, nonbiodegradable, etc.) (74).

PEG-drug conjugates have several advantages: 1) The improvement of the solubility of hydrophobic drugs, 2) prolongation of residence time in the body, 3) reduction of degradation by metabolic enzymes, and 4) minimization of protein immunogenicity.

PEG-drug conjugates can be designed as controlled release systems

which are able to release the drugs from conjugates to meet specific needs (75). This function can be fulfilled by designing different types of linkers. For instance, using particular linkers or bonds sensitive to pH could result in the specific release of drug inside the cells. N-cisaconityl acid spacer and hydrazone linkages could be hydrolyzed at the acidic pH of endosomes. H-Gly-Phe-Leu-Gly-OH or H-Gly-Leu-Phe-Gly-OH spacers could result in breakdown in lysosome by acid proteases or aminopeptidases (76).

The typical problem in small drugs PEGylation is the low drug loading percentage due to PEG only possessing one or two functional terminal groups. To overcome this limitation, dendrimeric structures or branched PEG have been developed. However, these structures may cause a decrease in solubility after drug loading. Furthermore, synthesis of dendrimer-like or branched PEG remains difficult in terms of cost and industrial production (77).

### **3.2 PEGylation of chemotherapeutic agents**

Solid tumors have the unique anatomy and pathophysiology which are different from normal tissues. Tumor tissues present selective extravasation of macromolecules due to the hypervascularity and increased permeability of tumor blood vessels. This feature of solid tumors is called enhanced permeability and retention (EPR) effect (78). For antineoplastic drug, PEGylation could provide a passive targeting to solid tumors through the EPR effect when injected intravenously. For pulmonary delivery, PEGylation could simply improve the drug's pharmacokinetic profile by slowing down the drug clearance from the

lungs. Usually PEG-drug conjugates are considered as macromolecular prodrugs, because the loaded drugs are not active unless released from the conjugate.

Various anti-cancer drugs on the market have been PEGylated. These drugs include paclitaxel, docetaxel, doxorubicin, gemcitabine, and camptothecin. There are several PEGylated chemotherapeutics under clinical trials from the two leading companies focusing on polymer-drug conjugates, i.e., Nektar Therapeutics and Enzon Pharmaceutical. PEG-irinotecan (NKTR-102) and PEG-docetaxel (NKTR-105) from Nektar, and PEG-SN38 (SN 38, 7-ethyl-10-hydroxy-camptothecin) (EZN-1108) from Enzon are now in clinical trials for solid tumors (20, 73, 79). The recent developments of PEGylated paclitaxel and docetaxel, two important anti-neoplastic drugs in the taxane family, will be discussed in the following text.

### **Paclitaxel**

The clinical application of paclitaxel is limited by the poor aqueous solubility and the serious side effects. PEGylated paclitaxel could increase its aqueous solubility and at the same time minimize its side effects. Linkage to a macromolecule could enable paclitaxel reaching the tumor tissue via the EPR effect following intravenous injection. Furthermore, sustained release could be obtained due to the slow clearance of large PEG molecules from the lung.

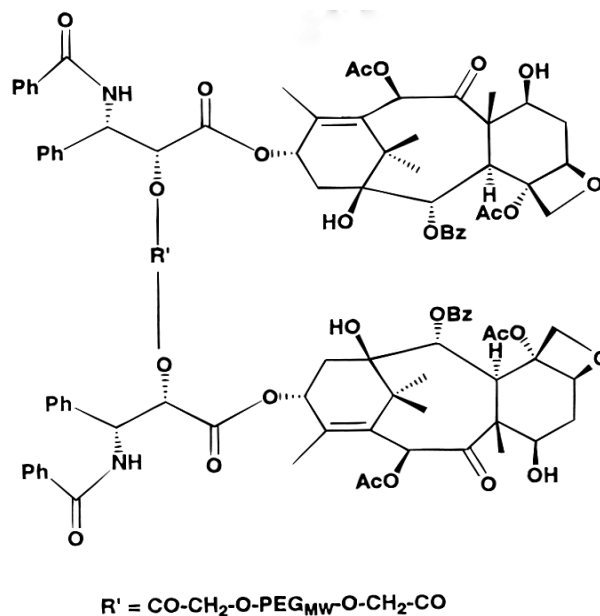


Fig. 8 PEG-paclitaxel synthesized by Greenwald *et al.* Paclitaxel was conjugated to a bi-functional PEG by ester bonds (adapted from (80) ).

In 1996, Greenwald *et al.* synthesized several PEG-paclitaxel conjugates with different molecular weights of 6 kDa, 20 kDa and 40 kDa (Fig. 8) (80). Paclitaxel was covalently linked to PEG by esterification. Then this PEG-paclitaxel has been involved in clinical trial phase I for solid tumor and lymphomas with pharmaceutical company Enzon in 2001. However, the phase I clinical trials was terminated in 2003 based on a strategic analysis of the program's potential returns against the associated costs, competitive risks, and development time (77, 81). Pendri *et al.* (82) developed PEG-conjugated paclitaxel-2 $\phi$ -glycinate. Glycine was used as a spacer. The prodrug is structured with an amide bond between glycine and PEG and an ester bond between glycine and paclitaxel. This water-soluble

form of paclitaxel showed lower toxicity and enhanced antitumor activity compared with the native drug in a P388/0 murine leukemia model following intraperitoneal injection. The author attributed these advantages to the tripartite nature of the conjugate. The prodrug would first break down at the amide bond and release the glycine ester-paclitaxel moiety extracellularly, due to the high levels of aminopeptidases and lysosomal acid proteases. Then, the rapid cleavage of the ester bond between paclitaxel and glycine would release the free drug.

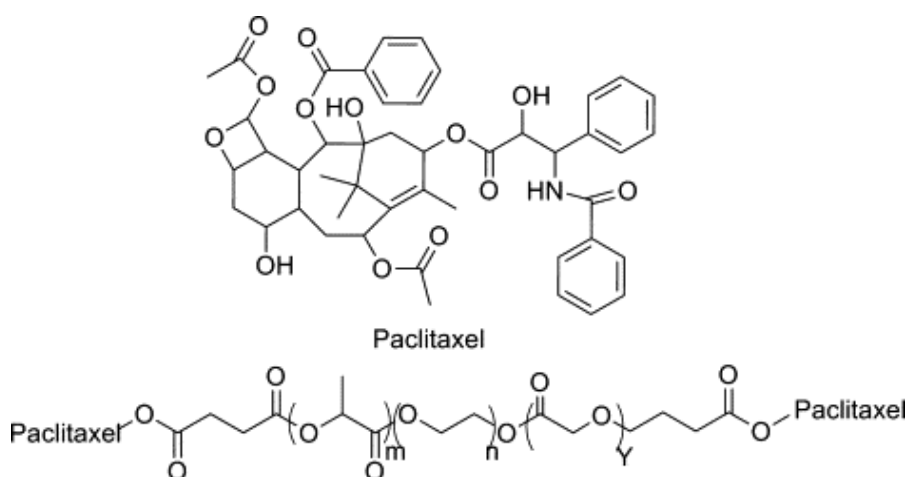


Fig. 9 PLA-PEG-PLA/paclitaxel conjugate (83).

Another example is a poly(lactic acid)-b-poly(ethylene glycol)-b-poly(lactic acid) (PLA-PEG-PLA)/paclitaxel conjugate synthesized by Xie *et al.* (Fig. 9) (83). This conjugate can self-assemble into micelles in an aqueous phase. It was shown that the conjugate had high cytotoxicity against Hela cancer cells, which indicated that paclitaxel had been released in an active form and the anti-tumor efficacy had been maintained.

## Docetaxel

Docetaxel is an anti-mitotic chemotherapeutics for treatments of non-small cell lung cancer, advanced or metastatic breast cancer, gastric cancer and hormone-refractory prostate cancer. Docetaxel is sold on the market as Taxotere or Docecad.

PEGylated docetaxel (NKTR-105) was produced by Nektar with multi-arm PEG (Fig. 10). In the preclinical study in rats and dogs, NKTR-105 improved the PK profile of docetaxel by reducing its peak concentrations and prolonging its half-life. NKTR-105 showed superior activity over docetaxel in murine models of human lung, colon, and prostate carcinomas. A significant and prolonged delay in tumor growth was observed in the group receiving NKTR-105 (84, 85). This conjugate has entered phase I clinical studies for investigation of its safety property.

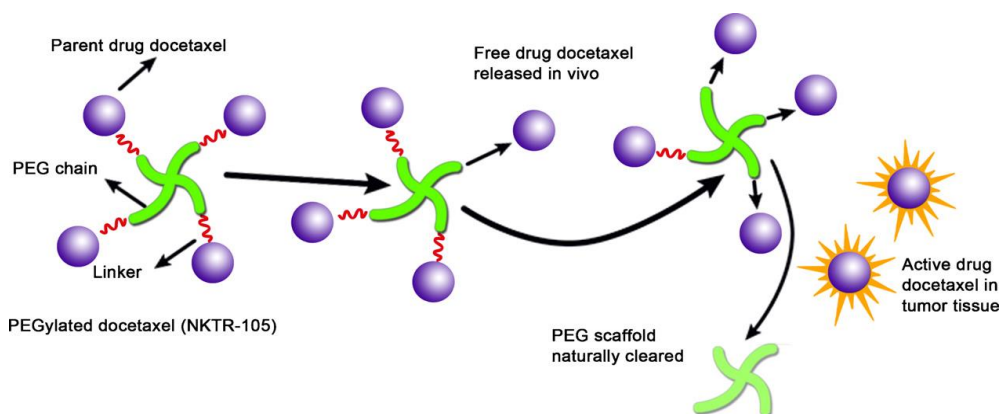


Fig. 10 The drug release mechanism of PEGylated docetaxel (NKTR-105) (85).

### 3.3 PEGylation for pulmonary delivery

PEGylation has been used in pulmonary delivery to attain sustained drug release in the lungs. PEGylation of proteins are commonly used to protect the therapeutics from degradation and thereby enhance the local efficacy. For instance, monomethoxy-PEG-750-insulin showed long  $t_{1/2}$  for 12h, which is twice as long as that detected for regular insulin (86). In addition, PEGylated antibody fragments such as anti-interleukin-17A (IL-17A) F(ab')<sub>2</sub> and anti-IL-13 Fab' greatly prolonged the presence of these fragments in the lungs. The PEGylated antibody fragments were retained in the lungs for up to 4 h post-delivery and persisted in the lungs for more than 2 days. However, the clearance of the unconjugated proteins commenced immediately after administration and was mostly completed within one day (87).

Christopher J. Morris *et al.* (88) tested the hypothesis that PEGylation of an inhaled antimicrobial peptide could reduce its pulmonary toxicity while offering stable and effective antimicrobial activity. They administered the PEGylated peptide via the airways in an isolated perfused rat lung (IPRL) model and concluded that PEGylation may enhance the lung biocompatibility of antimicrobial peptides.

Besides, PEGylation of excipients is widely used to increase drug retention and enhance efficacy. For instance, different formulations of PEGylated liposomes loaded with antisense oligonucleotides, and small interfering RNA were developed and delivered intratracheally to mice (89). Recently, the behavior of PEGylated dendrimers was studied in the lungs (90). The authors explored the potential of

PEGylated polylysine dendrimers as drug carriers for pulmonary application and the relationship between dendrimer size, absorption of the particles and retention in the lungs. Approximately 20–30% of the relatively small PEGylated dendrimers (<22 kDa) were absorbed in to systemic circulation within 48 h compared with only 2% absorption of a large dendrimer (78 kDa) within 7 days. As the molecular weights of the dendrimers increase, the absorption slows down. Prolonged retention in the lung can be achieved.

However, reports on pulmonary delivery of PEGylated small molecule drugs are rare in the literature. PEG-prednisolone conjugates were developed for asthma and chronic obstructive pulmonary disorder therapies and assessed *in vitro* and *ex vivo* in isolated and perfused rat lung (91). PEGylated prednisolone showed reduced maximum blood concentration ( $C_{max}$ ) and prolonged absorption as compared to the free drug. The  $C_{max}$  of PEG-prednisolone was reduced by a factor 3 and  $t_{max}$  increased by 45%, compared to prednisolone. The  $t_{1/2}$  absorption from the lung was 1 min with prednisolone and 8 min with PEG-prednisolone (Fig. 11).

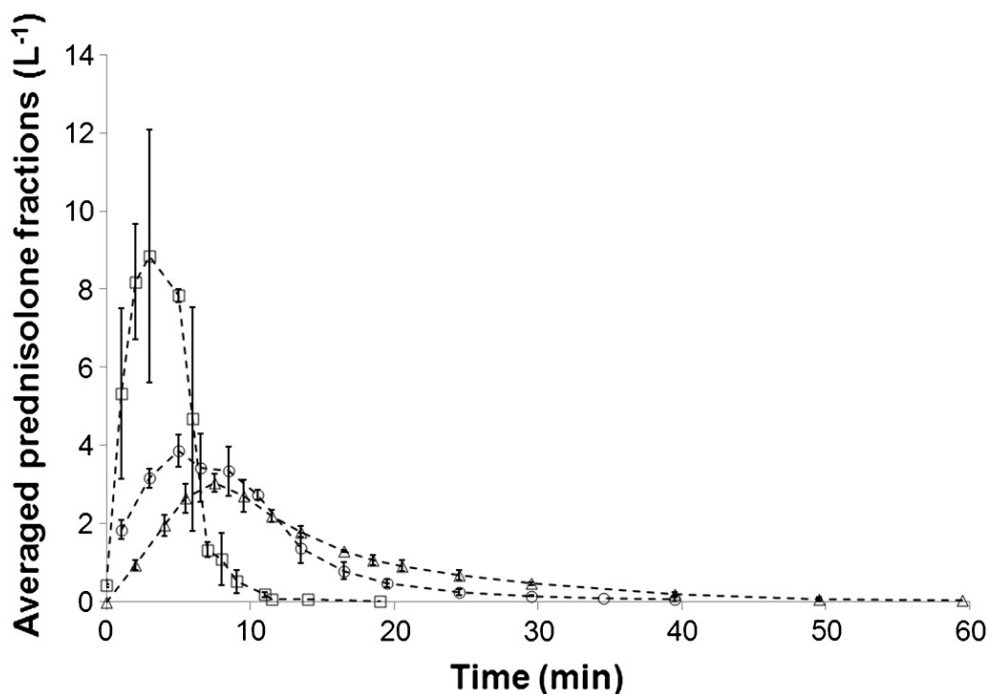


Fig. 11 Normalized absorption profiles of prednisolone in the isolated perfused rat lungs obtained with (□) prednisolone alone, (○) mPEG2000-Pred and (Δ) PEG2000-Pred<sub>2</sub>. Prednisolone concentration ( $\text{nmol L}^{-1}$ ) measured in perfusate was divided by the actual delivered dose ( $\text{nmol}$ ) to give a relative prednisolone fraction ( $\text{L}^{-1}$ ). Data are presented as mean  $\pm$  SD,  $n = 3$ . (91)

Up to date, there is no report about PEGylated anti-cancer drugs for inhaled chemotherapy though they have been widely investigated by the intravenous route. Therefore, exploration of the pulmonary delivery of PEGylated small molecular chemotherapeutics is needed.

#### **4. Aim of the thesis**

The objective of this project is to explore the application of polymer drug conjugates in inhaled chemotherapy. PEGylation of anti-neoplastic drugs was chosen as a strategy. Polyethylene glycol (PEG)-paclitaxel conjugates (PEG-PTX) for pulmonary delivery were designed in order to achieve improved anti-cancer efficacy with reduced local toxicity. PEG-PTX were expected to present sustained release of PTX in the treatment of lung cancer, as compared to the quickly-cleared native drug.

Paclitaxel (854 Da) was designed to link to PEG of large molecular weights (6 kDa and 20 kDa) by an ester bond. As the hydrolysis of the ester bond proceeds, PTX will be released progressively in the lung fluid. Our hypothesis was that the macromolecule will permit paclitaxel retention in the airspaces for a prolonged time period, as compared to free paclitaxel. The present strategy would be beneficial for cancer therapy, because improved tumor exposure to anti-neoplastic drugs would be achieved by sustained drug release from conjugates.

Paclitaxel was chosen as a model drug for our project. It is used in first-line treatments of lung cancer. It is poorly-water soluble and conjugation with PEG, a highly hydrophilic polymer, will increase its solubility. PEG (molecular weights 6k Da and 20k Da) has been chosen because it is proved that large PEG (molecular weight > 5 kDa) has a long retention time (7 days) in the lung tissue, which could enable a sustained drug release from PEG-paclitaxel conjugate in the

lung (46). Meanwhile, it is nontoxic and non-biodegradable but it can be eliminated by renal and hepatic pathways. It has already been approved for human use in dosage forms for intravenous, oral and inhalation applications.

2'-OH on paclitaxel was chosen to be conjugated to PEG by an ester bond. 7-OH and 1-OH were not chosen because of the steric hindrance. Although 2'-OH is necessary for the activity of paclitaxel, as the hydrolysis of the ester bond proceeds, paclitaxel will be released in active form (Fig. 12). Two structures of the conjugates were designed: 1) paclitaxel was conjugated to PEG by "click" chemistry; 2) a succinic spacer was used to link paclitaxel to PEG (Fig. 13).

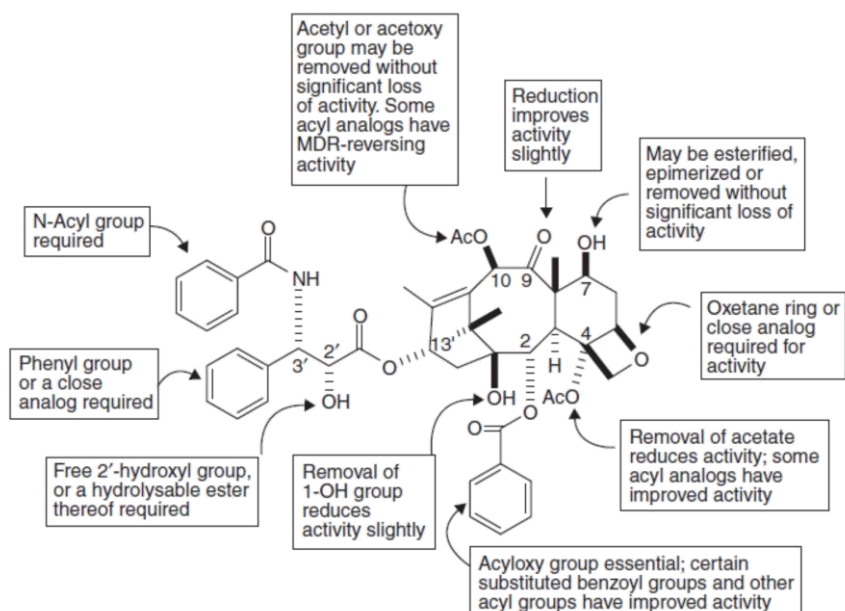


Fig. 12 Structure-active relationships (SARs) of paclitaxel (77)

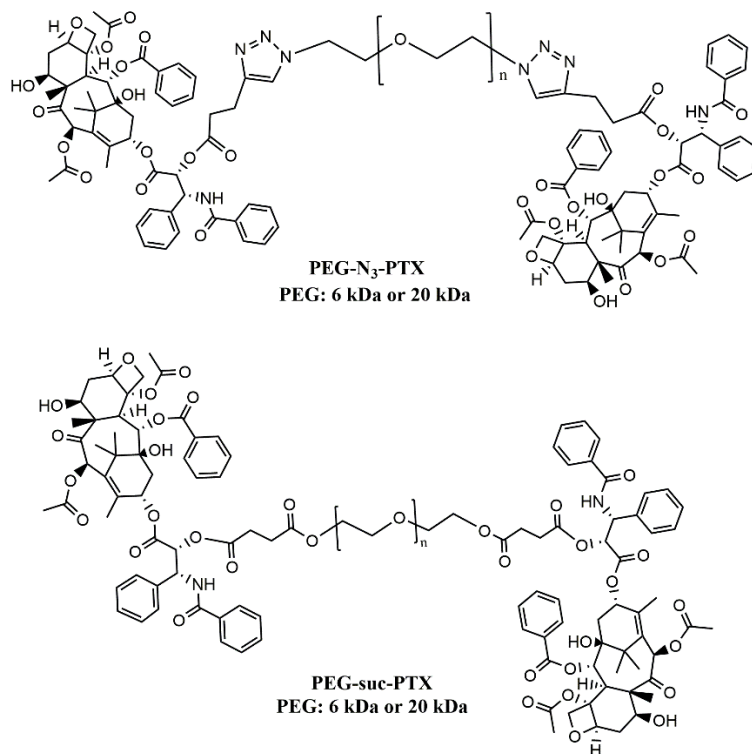
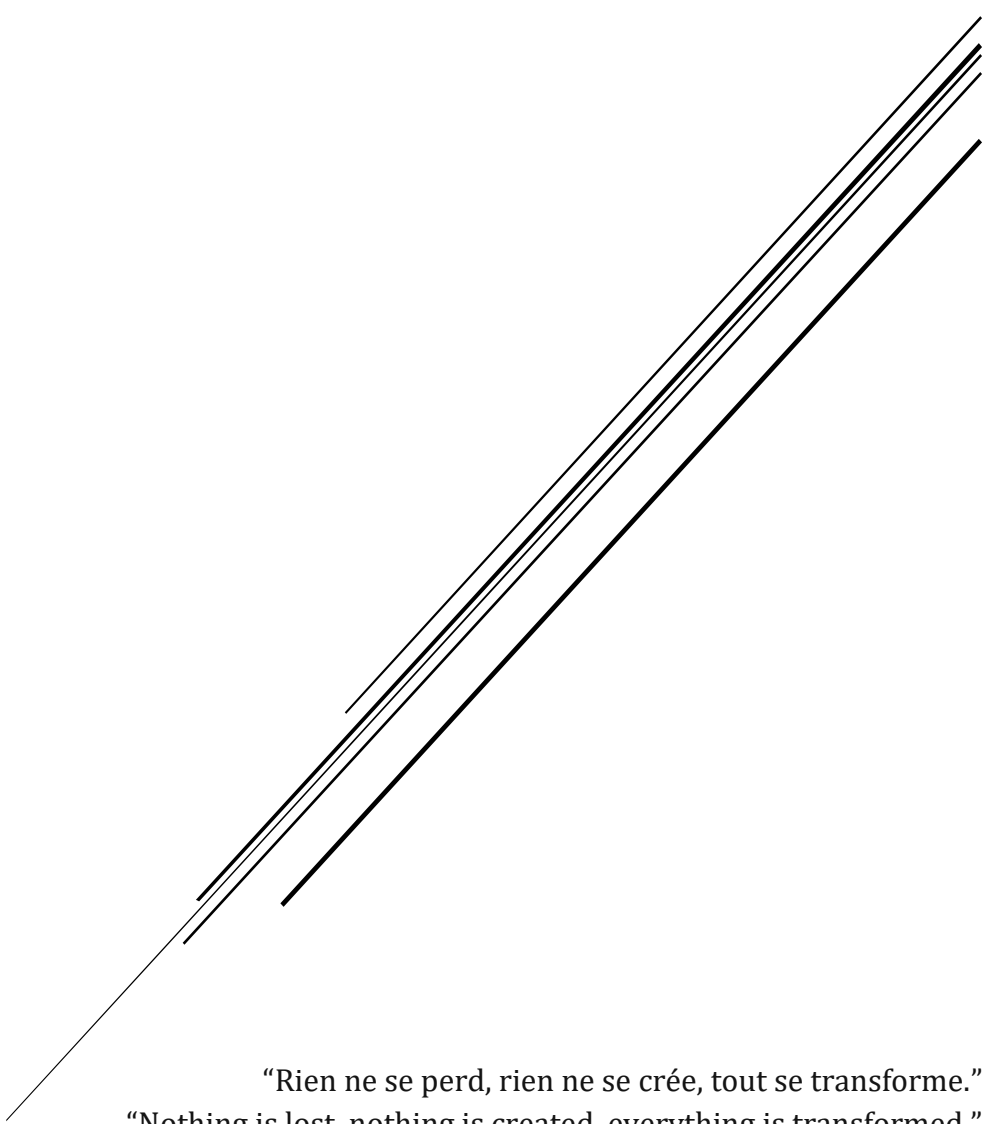


Fig. 13 Two structures of PEG-PTX conjugates developed in this thesis.

In this thesis, PEG-PTX were synthesized and characterized physico-chemically. The *in vitro* evaluation was conducted to investigate stability of PEG-PTX in different medium and cytotoxicity to cancer cells. Afterwards, acute toxicity of PEG-PTX was investigated in mice to determine the maximum tolerated doses. Local toxicological studies were conducted on mice to understand the toxicity of PEG-PTX to the lungs. Further, Anti-tumor efficacy of PEG-PTX was studied on a murine lung carcinoma model. The efficacy of intratracheally and intravenously administrated treatments were compared. Finally, *in vivo* release of paclitaxel and the retention of PEG-PTX conjugates in mouse lungs were investigated.

**CHAPTER 2.  
SYNTHESIS AND *IN VITRO* EVALUATION OF  
POLYETHYLENE GLYCOL-PACLITAXEL  
CONJUGATES FOR LUNG CANCER THERAPY**



“Rien ne se perd, rien ne se crée, tout se transforme.”  
“Nothing is lost, nothing is created, everything is transformed.”

— *Antoine Lavoisier*



## **ABSTRACT**

Pulmonary drug delivery is considered an attractive route of drug administration for lung cancer chemotherapy. However, fast clearance mechanisms result in short residence time of small molecule drugs in the lung. Therefore, achieving a sustained presence of chemotherapeutics in the lung is very challenging. In this study, we synthesized two different polyethylene glycol-paclitaxel ester conjugates with molecular weights of 6 kDa and 20 kDa in order to achieve sustained release of paclitaxel in the lung. One structure was synthesized with azide linker using “click” chemistry and the other structure was synthesized with a succinic spacer. The physicochemical and biological properties of the conjugates were characterized *in vitro*. Conjugation to PEG improved the solubility of paclitaxel by up to four orders of magnitude. The conjugates showed good stability in phosphate buffer saline pH 6.9 (half-life  $\geq$  72 h) and in bronchoalveolar lavage (half-life of 3 to 9 h) at both molecular weights, but hydrolyzed quickly in mouse serum (half-life of 1 to 3 h). The conjugates showed cytotoxicity to B16-F10 melanoma cells and LL/2 Lewis lung cancer cells but less than free paclitaxel or Taxol, the commercial paclitaxel formulation. These properties imply that the conjugates have the potential to retain paclitaxel in the lung for a prolonged duration and to sustain its release locally for a better efficacy.

Adapted from : *Synthesis and in vitro evaluation of polyethylene glycol-paclitaxel conjugates for lung cancer therapy. Pharmaceutical Research. 16 Mar 2016.*

Authors : Tian Luo • Johannes Magnusson • Véronique Préat • Raphael Frédérick • Cameron Alexander • Cynthia Bosquillon • Rita Vanbever

## 1. Introduction

Lung cancer is the most common cancer worldwide and caused 1.6 million deaths in 2012 (92). Systemic chemotherapy is widely used in the treatment of lung cancer, but the clinical efficacy is unsatisfactory as a result of the low local drug concentrations in the lung tumors and the severe dose-limiting side effects. Pulmonary delivery of chemotherapeutic agents is considered an attractive route of administration, with the advantages of high drug concentrations locally and low side effects systemically. However, small molecules have very short half-lives of absorption from the lung to the systemic circulation (93). In general, small hydrophilic compounds ( $\log P < 0$ ) have a half-life to absorption of approximately 1 hour, whereas lipophilic small molecules ( $\log P > 0$ ) are absorbed in approximately 1 minute. This rapid systemic absorption results in a short residence time of chemotherapeutics in the lung. In addition, inhalation of chemotherapeutics alone would lead to transient high drug concentrations locally and unacceptable toxicity to the lung tissue (94). Therefore, drug carriers could provide promising application for the pulmonary administration of anti-cancer agents in lung cancer with prolonged drug retention and sustained drug release locally as well as with reduced lung toxicity compared to the pulmonary delivery of the free drug (95).

Several nanocarrier-based pulmonary delivery systems have been developed and evaluated as potential treatment for lung cancer after inhalation, such as polymeric nanoparticles of doxorubicin and

liposomes of paclitaxel (PTX) (32, 96). However, the control of the release kinetics is difficult to achieve with these delivery systems. Moreover, the absorption of the therapeutics across pulmonary epithelia to lung tumors and the drug distribution in tumors are expected to be decreased due to the relatively large size and surface charges of these nanocarrier systems (97, 98).

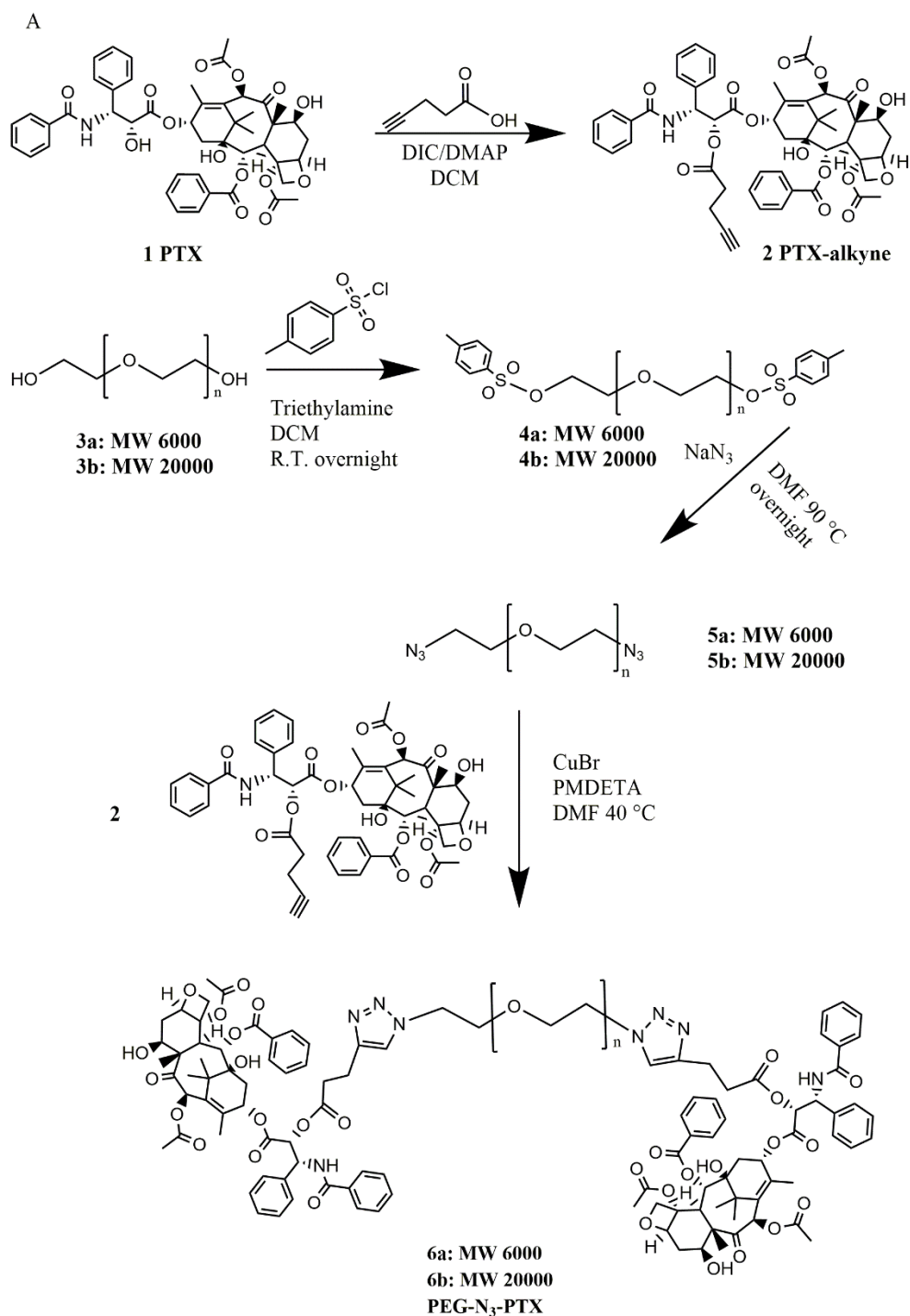
Conjugation of drugs to macromolecules by means of esterification provides a possible mechanism by which drugs could be retained in the lung due to the long residence times of macromolecules in the airspaces (93). Polyethylene glycol (PEG) is widely used in drug delivery and it has been shown that PEG with large molecular weight (MW > 5 kDa) can be retained in the lung for up to 7 days (99). This could enable a sustained release of a drug conjugated to PEG by hydrolysis of the ester bond between the polymer and the drug (87, 91, 99). Moreover, the polymer-drug conjugates will be taken into the cells by endocytosis (100, 101), which could possibly avoid multi-drug resistance mediated by efflux pumps (102, 103). As compared to carrier particles and micelles, drug loading is relatively high for conjugates (10-30%) (104). In addition, as the conjugates will be delivered in solution, the size of this carrier will be very small (< 10 nm), which will not generate the problem of tumor access.

PTX is a first-line drug for lung cancer treatment but it is poorly water soluble. Taxol, the commercial formulation of PTX, contains Cremophor EL to increase the drug solubility. However, Cremophor EL is well-known for its severe toxicity and its impact on PTX

pharmacokinetics. Cremophor EL alters PTX pharmacokinetic behaviour to a non-linear profile (105-107). Conjugation to highly hydrated PEG could largely increase PTX solubility without inducing unexpected toxicity (108, 109). In fact, PEG is nontoxic and it can be eliminated by mucociliary clearance and by renal and hepatic pathways (87). It has already been approved for human use in dosage forms for intravenous, oral and inhalation applications (110). Several studies have reported the synthesis of polymer-PTX conjugates in the literature. For instance, poly (L-glutamic acid)-PTX (Opaxio™) has already reached phase III clinical trials for ovarian cancer (111) and this conjugate showed reduced toxicity when locally delivered to the lung of mice (112). There are also various studies on PEG-PTX conjugates in the literature (80, 113-116). However, the pulmonary application of PEGylated PTX for lung cancer and the evaluation of its properties for lung cancer therapy both *in vitro* and *in vivo* have not been explored.

Therefore, the aim of this study was to develop water soluble and stable PEG-PTX conjugates for pulmonary application in lung cancer. Two conjugates with either an azide linker (PEG-N<sub>3</sub>-PTX) or a succinic linker (PEG-suc-PTX) were designed with 6 kDa and 20 kDa MW PEG (Fig. 14). Linear PEGs were modified with PTX at both hydroxyl ends to increase the drug load in the final products. PTX was linked to the PEG molecule via an ester bond at the C-2' position on PTX side chain. Although the hydroxyl on the C-2' is necessary for PTX activity, the chemical and enzymatic hydrolysis of the conjugate in the lung could offer a progressive release of active PTX with free C-2' hydroxyl.

Moreover, the C-2' position on PTX does not present steric hindrance as the hydroxyl 1-OH and 7-OH on the taxane ring do and could permit a high conversion rate. We used "click" chemistry in one of the synthetic routes because of the high efficiency of the azide and alkyne reaction. Moreover, the triazole formed between alkyne and PEG-azide is very stable and cannot hydrolyze before the ester bond. Consequently, the free PTX will release from the conjugate in an active form. All the conjugates were characterized physically and chemically and stability as well as cytotoxicity were evaluated *in vitro*.



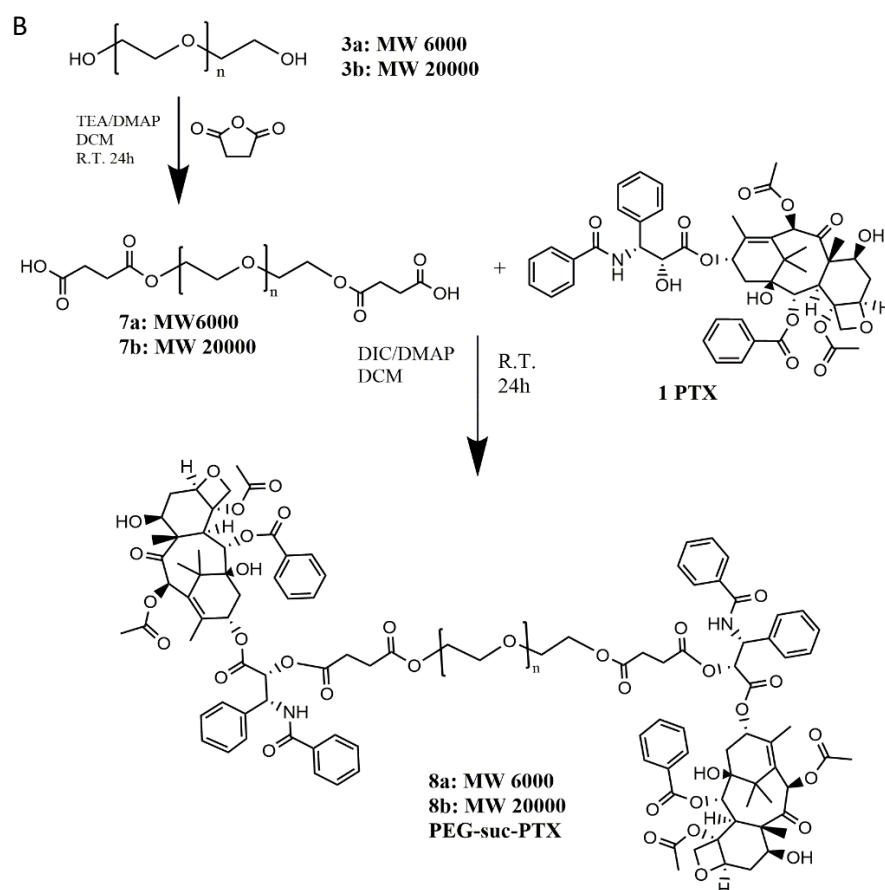


Fig. 14 Synthetic routes of PEG-PTX conjugates. **A. “Click” chemistry route:** PTX (compound 1) was modified with pentynoic acid at C-2’ group to obtain PTX-alkyne (compound 2). PEG-N<sub>3</sub> 6 kDa and 20 kDa (compounds 5a and 5b) were synthesized from PEG with 2 hydroxyl ends by tosylation followed by azidation. PTX-alkyne was then conjugated to PEG-N<sub>3</sub> 6 kDa and 20 kDa via “click” chemistry respectively to obtain the final conjugates PEG-N<sub>3</sub>-PTX 6 kDa and 20 kDa (compounds 6a and 6b). **B. Succinic spacer route:** succinic acid was linked to PEG 6 kDa and 20 kDa via esterification to obtain PEG-suc 6 kDa and 20 kDa (compounds 7a and 7b). PEG-suc-PTX 6 kDa and 20 kDa (compounds 8a and 8b) were then obtained by esterification of PEG-suc and PTX at C-2’ position.

## 2. Materials and methods

### 2.1 Materials and instruments

PEG with two hydroxyl terminals and MW of 6 kDa and 20 kDa were purchased from Iris Biotech (Marktredwitz, Germany). Paclitaxel was purchased from Chemieliva (Chongqing, China). Taxol was obtained from Bristol-Myers Squibb. N,N'-diisopropylcarbodiimide (DIC), 4-dimethylaminopyridine (DMAP), tyrosol chloride, trimethylamine (TEA), dichloromethane, dimethyl sulfoxide (DMSO), acetonitrile, dimethylformamide (DMF), and Cremophor EL (Kolliphor® EL) were all purchased from Sigma Aldrich (Gillingham, UK). Hank's balanced salt solution (HBSS) and Dulbecco's phosphate-buffered saline (DPBS) were purchased from Life Technologies (Paisley, UK). The thiazolyl blue tetrazolium bromide (MTT) was from Sigma Aldrich (St. Louis, MO, USA). Spectra/Por® 7 Tubing (Spectrum Laboratories, Inc, Rancho Dominguez, CA, US) was used to carry out all the dialysis work.

Nuclear magnetic resonance (NMR) spectra were recorded on a Bruker 400 MHz spectrometer. Chemical shifts are reported in ppm ( $\delta$  units) downfield from internal tetramethylsilane. Electrospray ionisation time-of-flight mass spectrometry (TOF-ES-MS) was performed by WATERS-2795 (Waters, UK) and analyzed by MassLynx software.

## 2.2 Synthesis of PEG-N<sub>3</sub> 6 kDa and 20 kDa

PEG-N<sub>3</sub> was obtained by tosylation followed by azidation. PEG 6kDa (1 g, 0.167 mmol, 1.0 equiv.) was dissolved in 5 mL toluene and evaporated to dryness for 3 cycles to remove water. The dried PEG was dissolved in 5 mL dichloromethane under Argon. The solution was cooled to 0 °C, then tosyl chloride (0.191 g, 1 mmol, 6 equiv.) and triethylamine (0.139 mL, 1 mmol, 6.0 equiv.) were added. The solution was kept at 0 °C for 2 hours and then warmed up to room temperature and stirred overnight. The reaction solution was poured into cool diethyl ether 3 times to precipitate PEG-bis-tosyl ester. The product was then filtered and dried under vacuum overnight. The same method and reaction scale were applied for PEG 20 kDa. The yield was 80% at both PEG MW. Compounds 4a and 4b: <sup>1</sup>H NMR (400 MHz, D<sub>2</sub>O, δ in ppm) δ 7.79 (d, J = 8.5 Hz, 4H), 7.45 (d, J = 7.9 Hz, 4H), 4.20 (d, J = 4.4 Hz, 4H), 3.62 (m, PEG). δ 7.79 and 7.45 ppm represented the phenyl protons on the tosyl groups. δ 4.2 ppm represented the terminal -CH<sub>2</sub> on PEG which was linked to the tosyl group.

PEG-bis-tosyl ester 6 kDa (1.0 g, 0.167 mmol, 1.0 equiv.) and NaN<sub>3</sub> (0.106 g, 1.67 mMol, 10.0 equiv.) were dissolved in 5 mL DMF. The mixture was stirred at 90 °C under argon atmosphere overnight. The product was precipitated in diethylether to remove DMF. Precipitates were dissolved in 10 mL water, and transferred to pre-wetted dialysis bags MWCO 2000 Da. Dialysis was carried out against deionized water overnight under stirring to remove excess sodium azide and

DMF. The product was finally freeze dried. The same method and reaction scale were applied to PEG-tosyl 20 kDa. The yield was 80% at both PEG MW. Compounds **5a** and **5b**:  $^1\text{H}$  NMR ( $\text{CDCl}_3$ ,  $\delta$  in ppm)  $\delta$  3.77 – 3.58 (m, PEG backbone), 3.41 (t,  $J = 5.0$  Hz, 4H, PEG-O- $\text{CH}_2$ - $\text{CH}_2$ - $\text{N}_3$ ). FT-IR: 2916.74, 2113.73, 1644.69, 1469.55, 1349.95, 1297.95, 1251.61, 1097.31, 949.52, 840.07.

### 2.3 Synthesis of PTX alkyne

The synthesis of PTX alkyne has previously been described (117). PTX (50 mg, 0.059 mmol, 1.0 equiv.) was dissolved in 5.0 mL anhydrous dichloromethane under Argon. 4-Pentynoic acid (6.9 mg, 0.07 mmol, 1.2 equiv.), DIC (11.1 mg, 0.08 mmol, 1.5 equiv.) and DMAP (3.5 mg, 0.03 mmol, 0.5 equiv.) were dissolved in dichloromethane under nitrogen. The resulting solution was left to stir under Argon at room temperature overnight. The product was purified using a silica gel column, and hexane/ethyl acetate 1:1 was used as eluent. Thin layer chromatography was used to track the product. Samples containing PTX were combined and the solvent was removed by vacuum. The product was dried under vacuum overnight. The yield was 65%. Compound **2**:  $^1\text{H}$  NMR ( $\text{CDCl}_3$ ,  $\delta$  in ppm)  $\delta$  8.19 (d,  $J = 7.4$  Hz, 2H, 2-OBz), 7.79 (d,  $J = 7.5$  Hz, 2H, 3'-NBz), 7.68 (t,  $J = 7.4$  Hz, 1H, 2-OBz), 7.58 – 7.51 (m, 3H, 2-OBz, 3'-NBz), 7.47 – 7.35 (m, 7H, 2-OBz, 3'-ph, 3'-NBz), 6.32 (s, 1H, C10-H), 6.28 (t,  $J = 8.9$  Hz, 1H, C13-H), 6.00 (dd,  $J = 9.2, 3.0$  Hz, 1H, C3'-H), 5.71 (d,  $J = 7.1$  Hz, 1H, C2-H), 5.55 (d,  $J = 3.1$  Hz, 1H, C2'-H), 5.00 (d,  $J = 7.7$  Hz, 1H, C5-H), 4.51 – 4.43 (m, 1H, C7-H), 4.34 (t,  $J = 7.1$  Hz, 1H, C20- $\text{H}_a$ ), 4.26 –

4.20 (m, 1H, C20-H<sub>b</sub>), 3.84 (d,  $J = 7.1$  Hz, 1H, C3-H), 2.71 (m, 2H, HC≡C-CH<sub>2</sub>-CH<sub>2</sub>-COO-PTX), 2.60 (m, 2H, HC≡C-CH<sub>2</sub>-CH<sub>2</sub>-COO-PTX), 2.53 (m, 1H, C6-H<sub>a</sub>), 2.51 (m, 1H 7-OH), 2.48(s, 3H, C4-OAc), 2.39 (m, 1H, C14-H<sub>a</sub>), 2.26 (s, 3H, C10-OAc), 2.20 (m, 1H, C14-H<sub>b</sub>), 1.97 (s, 3H, C18-Me), 1.94 (m, 1H, C6-H<sub>b</sub>), 1.91 (s, 1H, HC≡C-CH<sub>2</sub>-CH<sub>2</sub>-COO-PTX), 1.68 (s, 3H, C19-Me), 1.26 (s, 3H, C17-Me) 1.15 (s, 3H, C16-Me). Signal of  $\delta$  5.55 ppm showed that an ester bond was formed at the desired C2' position on the paclitaxel side chain.  $\delta$  4.51 – 4.43 ppm represented the C7 proton, which stayed at the same position as the starting material paclitaxel. This verified that no ester bond formed at C7 position. Finally, signals of  $\delta$  2.71 and 2.60 ppm showed the presence of –CH<sub>2</sub>-CH<sub>2</sub>- on the pentynoic group and the signal of  $\delta$  1.91 ppm demonstrated the alkyne proton. These information confirmed that pentynoic acid was successfully linked on the C2' position of paclitaxel. MS  $m/z$  (ES+) calculated from C<sub>52</sub>H<sub>55</sub>NO<sub>15</sub> : 934.4 (M+H<sup>+</sup>) (PTX-alkyne + H<sup>+</sup>), 856.3 (fragment of PTX).

#### 2.4 Synthesis of PEG-N<sub>3</sub>-PTX conjugates 6 kDa and 20 kDa

PEG-N<sub>3</sub> 6 kDa (100 mg, 0.016mmol, 1.0 equiv.), PTX alkyne (39 mg, 0.04 mmol, 2.5 equiv.) and PMDETA (10  $\mu$ L, 0.05 mmol, 3.0 equiv.) were dissolved in 4 mL DMF under nitrogen, and then degassed for 10 min. Copper bromide (7 mg, 0.1 mmol, 3.0 equiv.) and sodium ascorbate (19.5 mg, 0.2 mmol, 6.0 equiv.) were dissolved in 1 mL DMF in another vial under nitrogen and degassed for 10 min. The mixture of copper bromide and sodium ascorbate were added into the reaction flask under nitrogen and degassed for another 10 min. The reaction

was stirred at 45 °C overnight. The conjugate was first purified by precipitation in cold diethylether to remove PTX and catalysts, and then by dialysis against water to remove copper bromide. The 20k conjugate was produced with the same method. The yield was 70% at both PEG MW. Compounds **6a** and **6b** : <sup>1</sup>H NMR (CDCl<sub>3</sub>, δ in ppm) δ 8.14 (d, *J* = 7.4 Hz, 4H, 2-OBz), 7.82 (d, *J* = 7.5 Hz, 4H, 3'-NBz), 7.62 (t, *J* = 7.4 Hz, 4H, 2-OBz), 7.56 – 7.45 (m, 10H, 2-OBz, 3'-NBz, 3'-ph), 7.42 – 7.33 (m, 12H, triazole, 2-OBz, 3'-ph, 3'-NBz), 6.28 (s, 2H, C10-H), 6.19 (t, *J* = 8.9 Hz, 2H, C13-H), 5.94 (dd, *J* = 8.6, 3.7 Hz, 2H, C3'-H), 5.67 (d, *J* = 7.0 Hz, 2H, C2-H), 5.44 (d, *J* = 3.7 Hz, , 2H, C2'-H), 4.96 (d, *J* = 8.5 Hz, 2H, C5-H), 4.53 – 4.39 (m, 6H, PEG-O-CH<sub>2</sub>-CH<sub>2</sub>-triazole, C7-H), 4.31 (d, *J* = 8.5 Hz, 2H, C20-H<sub>a</sub>), 4.19 (d, *J* = 8.5 Hz, 2H, C20-H<sub>b</sub>), 3.80(m, 6H, C3-H, PEG-O-CH<sub>2</sub>-CH<sub>2</sub>-triazole), 3.55-3.75 (m, PEG), 3.03 (m, 4H, PEG-triazole-CH<sub>2</sub>-CH<sub>2</sub>-CO-PTX), 2.85 (m, 4H, PEG-triazole -CH<sub>2</sub>-CH<sub>2</sub>-CO-PTX), 2.60 – 2.52 (m, 2H, C6-H<sub>a</sub>), 2.50 (d, *J* = 3.9 Hz, 2H, 7-OH), 2.42 (s, 6H, C4-OAc), 2.29 (dd, *J* = 15.4, 9.4 Hz, 2H, C14-H<sub>a</sub>), 2.23 (s, 6H, C10-OAc), 2.06 (dd, *J* = 15.4, 8.9 Hz, 2H, C14-H<sub>b</sub>), 1.92 (s, 6H, C18-Me), 1.86 (m, 2H, C6-H<sub>b</sub>), 1.68 (s, 6H, C-19), 1.22 (s, 6H, C17-Me), 1.13 (s, 6H, C16-Me).

## 2.5 Synthesis of PEG-suc 6 kDa and 20 kDa

PEG 6 kDa (1.0 g, 0.167 mmol, 1.0 equiv.) was dissolved in 5 mL toluene and evaporated 3 times to remove water. The dried PEG was dissolved in dichloromethane under Argon. The solution was cooled to 0 °C, succinic anhydride was added (100 mg, 1 mmol, 6.0 equiv.). TEA (0.14 mL, 1 mmol, 6.0 equiv.) was dropped with a syringe. The reaction

was then kept on ice for 1 hour and was stirred at room temperature overnight. The PEG-suc was purified by precipitation in cold diethylether 3 times. The precipitates were dried under vacuum at room temperature overnight. The same method and reaction scale were applied to PEG 20 kDa. The yield was 80% at both PEG MW. Compounds **7a** and **7b**:  $^1\text{H NMR}$  ( $\text{CDCl}_3$ ,  $\delta$  in ppm)  $\delta$  4.22 (t,  $J = 25.0$  Hz, 4H, PEG-O-CH<sub>2</sub>-CH<sub>2</sub>-O-succinic acid), 3.94 – 3.36 (m, PEG backbone), 2.71 (d,  $J = 54.4$  Hz, 8H, PEG-COO-CH<sub>2</sub>-CH<sub>2</sub>-COOH).

## 2.6 Synthesis of PEG-suc-PTX conjugates 6 kDa and 20 kDa

PEG-suc 6 kDa (100 mg, 0.017 mmol, 1.0 equiv.), PTX (37 mg, 0.04 mmol, 2.5 equiv.) and DMAP (5 mg, 0.04 mmol, 2.5 equiv.) were dissolved in 1.5 mL DCM under nitrogen. The reaction flask was placed on ice and DIC (2.0  $\mu\text{L}$ , 0.04 mmol, 2.5 equiv.) was added into the flask. The reaction was then stirred overnight at room temperature. The conjugate was purified by precipitation in cold diethylether 3 times and dried under vacuum. The 20k conjugate was produced with the same method but with higher PTX ratio (equiv. 4.0). The yield was 70% at both PEG MW. Compounds **8a** and **8b**:  $^1\text{H NMR}$  ( $\text{CDCl}_3$ ,  $\delta$  in ppm)  $\delta$  8.10 (m, 4H, 2-OBz), 7.85 (m, 4H, 3'-NBz), 7.62 (t,  $J = 7.4$  Hz, 4H, 2-OBz), 7.56 – 7.45 (m, 10H, 2-OBz, 3'-NBz, 3'-ph), 7.42 – 7.33 (m, 10H, 2-OBz, 3'-ph, 3'-NBz), 7.33 (t,  $J = 6.8$  Hz, 2H, 3'-NBz), 7.07 (t,  $J = 9.0$  Hz, 2H, 3'-NH), 6.29 (s, 2H, C10-H), 6.23 (t,  $J = 8.7$  Hz, C13-H, 1H), 5.97 (dd,  $J = 9.1, 3.0$  Hz, 2H, C3'-H), 5.68 (d,  $J = 7.1$  Hz, 2H, C2-H), 5.49 (d,  $J = 5.5$  Hz, 2H, C2'-H), 4.97 (d,  $J = 7.9$  Hz, 2H, C5-H), 4.45 (m, 2H, C7-H), 4.32 (d,  $J = 8.4$  Hz, 2H, C20-H<sub>a</sub>), 4.20 (d,  $J = 8.5$  Hz,

2H, C20-H<sub>b</sub>), 4.10 (m, 4H, PEG-O-CH<sub>2</sub>-CH<sub>2</sub>-O-succinic) 3.51-3.80 (m, PEG backbone), 2.80 – 2.69 (m, 4H, PEG-COO-CH<sub>2</sub>-CH<sub>2</sub>-COO-PTX), 2.64 (m, 4H, PEG-COO-CH<sub>2</sub>-CH<sub>2</sub>-COO-PTX), 2.56 (m, 2H, C6-H<sub>a</sub>), 2.50 (d, *J* = 3.9 Hz, 2H, 7-OH), 2.44 (s, 6H, C4-OAc), 2.36 (dd, *J* = 15.4, 9.3 Hz, 2H, C14-H<sub>a</sub>), 2.23 (s, 6H, C10-OAc), 2.15 (dd, *J* = 15.4, 8.9 Hz, 2H, C14-H<sub>b</sub>), 1.98 (s, 6H, C18-Me), 1.86 (m, 2H, C6-H<sub>b</sub>), 1.68 (s, 6H, C19-Me), 1.24 (s, 6H, C17-Me), 1.13 (s, 6H, C16-Me).

## 2.7 Solubility

The solubility of the conjugates was estimated by adding increasing amounts of conjugates to 0.1 mL ultrapure water at room temperature until saturation (116, 118). Solubility was estimated by the weights added in 3 parallel experiments.

## 2.8 Stability of conjugates in PBS, BAL and serum of mice

The conjugates were dissolved in 5 mL PBS at pH 6.9 and pH 7.4 respectively (final concentration of PTX 20 µg/mL). The solutions were incubated at 37 °C in a water bath with shaking. 200 µL samples were withdrawn at pre-determined time points. The samples were then diluted with acetonitrile and centrifuged at 15000×g for 10 min before High Performance Liquid Chromatography (HPLC) analysis.

Female NMRI mice (6 to 8 week-old; Elevage Janvier, Le Genest-St-Isle, France) were used to collect serum and bronchoalveolar lavage (BAL). Blood samples were collected from the orbital sinus of the mice. The blood samples were kept in the fridge (4 °C) overnight and centrifuged at 12000×g. The serum supernatant was then taken and

stored at -20 °C. BAL was performed after euthanizing the mice by cervical dislocation. One ml of HBSS was injected into the trachea and left for 15 s. 0.5 mL of the fluid was then withdrawn and re-injected into the lung. All the BAL liquid was removed from the lung afterwards. This procedure was repeated twice until a total of 3 mL HBSS was injected. The BAL was then centrifuged at 4500×g for 10 min to remove the cells. The supernatant was collected and stored at -20 °C. All experimental procedures were performed in compliance with guidelines of Institutional Animal Care and Use Committee of the Université catholique de Louvain (Permit number: 2012/UCL/MD/006). Animals were anesthetized before manipulation and efforts were made to minimize animal suffering.

The 6 kDa and 20 kDa conjugates were dissolved in 200 µL BAL in Eppendorf tubes at the concentration of 50 µg/mL and 35 µg/mL (PTX equiv.). Conjugates were also dissolved in 40 µL serum at the same concentrations as above. All the samples were then incubated at 37 °C. These tubes were taken out for analysis at different time points. 200 µL acetonitrile were added into the samples which were then centrifuged at 15000×g for 10 min before HPLC analysis. The percentages of conjugates remaining in BAL or serum over time were calculated by comparing with the amount recovered at 0 hour. The degradation half-lives of the conjugates were calculated from time vs. residual amount curves by assuming first-order kinetics. HPLC was carried out using the Hewlett Packard series 1100 system (Agilent Technologies, Palo Alto, CA) using a reverse phase C<sub>18</sub> column (NUCLEOSIL® 300-5 C18 · 5 µm particles · 300 Å pores,

250mm×4.6mm, MACHEREY-NAGEL GmbH & Co. KG, Düren, Germany). The mobile phase was acetonitrile and water eluted at 1 mL/min using a gradient protocol as follows: a linear gradient from acetonitrile 40% to 60% for 20 minutes, a linear gradient from acetonitrile 60% to 40% for 5 minutes. Absorbance of the column effluent was monitored at 227 nm (116). A standard curve was established in the range of 5-100 µg/mL of PTX dissolved in acetonitrile (correlation coefficient of  $R^2 = 0.9995$ , LOD = 1.52 µg/ml, LOQ = 5.01 µg/ml). Samples of 20 µL were injected. The areas under the peaks of conjugates and paclitaxel were monitored. The retention time of paclitaxel was 13 min according to this analytical method. PEG chain does not have a significant UV absorbance. After conjugation with paclitaxel, the PEG-PTX conjugates had retention times of 19-20 min for 6k and 15-16 min for 20k. The peaks of the mono- and di-conjugates were not separated in the method.

## 2.9 Cytotoxicity

The *in vitro* cytotoxicity of the conjugates was tested on LL/2 Lewis lung carcinoma cell line (ATCC<sup>®</sup> CRL-1642<sup>™</sup>) and B16-F10 melanoma cell line (ATCC<sup>®</sup> CRL-6475<sup>™</sup>) using the MTT assay. LL/2 cells were cultured in Dulbecco's Modified Eagle Medium (DMEM, Life Technologies, Belgium) and B16-F10 melanoma cells were cultured in Minimum Essential Medium Eagle Alpha (MEM Alpha, Life Technologies, Belgium). Both media were supplemented with 10% fetal bovine serum and 1% antibiotics (Pen Strep, Life Technologies, Belgium). The cells were maintained in a 5% CO<sub>2</sub> humidified

atmosphere at 37 °C.

Cells were seeded in 96 plates at a density of 100 cells/well for LL/2 and 1000 cells/well for B16-F10. Cells were then incubated with the 4 conjugates, and Taxol dissolved in 100 µL full culture medium at different concentrations ( $6 \times 10^{-6}$ -2.5 µg/mL, PTX equivalent) for 72 hours. PTX was also tested at the same concentrations by diluting PTX stock solution in DMSO (500 µg/mL) with culture medium. Less than 0.5% of DMSO was present in the final culture medium. Then, the medium was removed and the cells were incubated with MTT 0.5 mg/mL in culture medium without FBS for 3 hours. MTT was aspirated off and DMSO was added to dissolve the formazan crystal. The absorbance was then measured at 560 nm with the spectrophotometer Multiskan EX (Thermo Scientific, US). Untreated cells were taken as control with 100% metabolic activity and cells incubated with Triton X-100 1% were used as positive control. The toxicity of PEG reagents (PEG, PEG-N<sub>3</sub> 6 kDa and 20 kDa, PEG-suc 6 kDa and 20 kDa) was evaluated on LL/2 cells at a concentration corresponding to 2.5 µg/mL PTX in the conjugates. Cremophor EL/ethanol was also tested on LL/2 cells at a concentration corresponding to 2.5 µg/mL PTX in Taxol. DMSO 0.5% in culture medium (corresponding to 2.5 µg/mL PTX) was tested on LL/2 cells as a control. The IC<sub>50</sub> was calculated using the regression equation from the plot showing the cell metabolic activity versus the log of concentration.

### **Statistics**

All the results were shown as mean ± standard deviation. Mann-

Whitney test was conducted to demonstrate statistical differences ( $p < 0.05$ ); IC<sub>50</sub> values of cytotoxicity were calculated from the dose-response signal curve by regression function with variable hill slopes. The Pearson correlation coefficient was calculated using the Excel function CORREL. Graphpad Prism as well as Microsoft Excel 2010 were used for data processing.

### 3. Results and discussion

#### 3.1 Chemistry

PEG-N<sub>3</sub>-PTX conjugates 6 kDa and 20 kDa were obtained using “click” chemistry. PTX was first modified by pentynoic acid to obtain an alkyne group, while PEG was activated to PEG-azide by tosylation followed by azidation. DMF was chosen as the solvent because of the satisfactory solubility of PTX, PEG as well as copper bromide in this solvent. As shown in Fig. 15, C2'-H on PTX shifted from  $\delta$  4.8 (a, Fig. 15) to  $\delta$  5.5 (a', Fig. 15) in <sup>1</sup>H NMR spectra, which indicates the formation of the ester bond.

PEG-suc-PTX conjugates 6 kDa and 20 kDa were obtained using a typical method of esterification. First, succinic acid was added to the PEG backbone to introduce carboxyl groups and also to act as a spacer between PTX and PEG. PTX was then conjugated to PEG under the catalysts DIC/DMAP in DCM. As shown in Fig. 15, C2'-H shifted from  $\delta$  4.8 (a, Fig. 15) to  $\delta$  5.5 (a'', Fig. 15). No downfield shift was observed in <sup>1</sup>H-NMR for either of the C2 (i, Fig. 15) or C7 (e, Fig. 15) protons in both PEG-N<sub>3</sub>-PTX and PEG-suc-PTX structures, which

indicates that PTX was conjugated to PEG on the C2'. Therefore, the data confirm that it was not necessary to protect the 7-OH and 1-OH on PTX because the steric hindrance makes these two hydroxyls not easy to access for esterification (119). On the contrary, if the goal was to modify the 7-OH, the protection of 2'-OH on the side chain of PTX would be necessary (120). The PTX substitution reached 90% for both structures at both molecular weights.

The drug loading in the conjugates was calculated by dividing PTX mass by the whole molecule mass according to the ratio of PTX substitution calculated with <sup>1</sup>H NMR. It reached 20% and 7% (w/w) in all the structures of 6 kDa and 20 kDa conjugates, respectively. The molecular ratio of PTX in PEG-PTX conjugates was approximately 1.8 PTX for 1 PEG molecule in both structures and both molecular weights.

The structure of the azide conjugate is novel with a hydrolysable ester bond and a stable triazole link between PEG and PTX. The ester bond ensures that paclitaxel can be released in an intact form and the triazole link enhances the stability of the conjugate. Although various polymer-paclitaxel conjugates have been prepared, few studies have been performed in the field of pulmonary drug delivery. In the case of the pulmonary delivery of polymer-drug conjugates, a long residence time of the conjugates in the lungs is crucial for attaining sustained local drug concentrations. Herein, we used high molecular weight PEG in the conjugates, with the expectation that it should contribute to a long drug residency in the lungs (99). Then, the progressive release of paclitaxel by hydrolysis of the ester bond should result in sustained local drug concentrations.

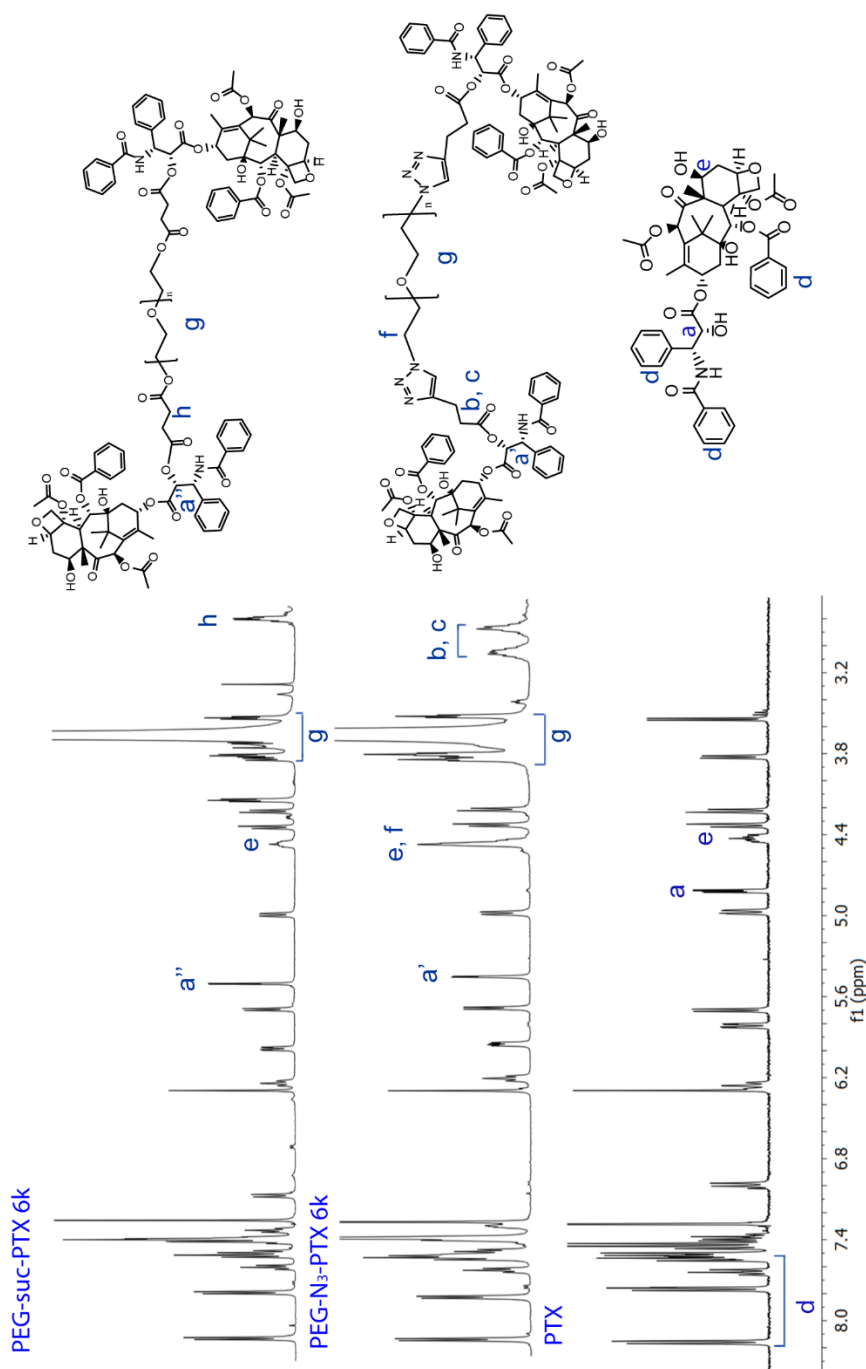


Fig. 15 <sup>1</sup>H NMR spectrum of PEG-suc-PTX, PEG-N<sub>3</sub>-PTX 6 kDa and PTX.

### **3.2 Aqueous solubility and *in vitro* stability of PEG-PTX conjugates**

The PEGylation of PTX greatly increased the aqueous solubility of PTX. The reported solubility of PTX in water in the literature is 0.5 µg/mL. PEG-N<sub>3</sub>-PTX and PEG-suc-PTX 6 kDa conjugates showed a highly increased solubility of 30 mg/mL and 25 mg/mL PTX equivalent (i.e., 145 mg/mL and 118 mg/mL conjugates). Although PEG is a hydrophilic molecule, the solubilities of the 20 kDa conjugates were lower (73 mg/mL for PEG-N<sub>3</sub>-PTX 20 kDa and 61 mg/mL for PEG-suc-PTX 20 kDa, or 5.8 mg/mL and 4.9 mg/mL PTX equivalent, respectively). Conjugation increased the solubility of paclitaxel in pure water by 3-4 orders of magnitude. The solvation of the PEG chain probably decreases with the increase of PEG molecular weight, due to the crystalline structure of the polymer chain. The lower solubility with higher PEG molecular weight was also found in previous reports on PEG-PTX prodrugs (80, 116).

The *in vitro* stability tests were performed in PBS at pH 6.9 and 7.4, BAL and mouse serum. All the conjugates showed better stability in PBS pH 6.9 than in PBS pH 7.4. The pH of 6.9 is the pH of the lung lining fluid in humans (121), while the pH of 7.4 is the physiological pH of human blood. As shown in Table 3 and Fig.16, the half-lives of these conjugates were longer than 72 hours in PBS pH 6.9, but decreased significantly in BAL and serum. The PEG-N<sub>3</sub>-PTX conjugates were more stable than the PEG-suc-PTX conjugates. In our strategy, PEG-N<sub>3</sub>-PTX was designed due to the superiority of the stability of the

triazole ring over the ester bond. The triazole ring is very stable and could not hydrolyze before the ester bond. Thus, free PTX will be released from the conjugate in an active form. However, there are two ester bonds between PTX and PEG in the structure of PEG-suc-PTX, which leads to increased possibilities for hydrolysis. As a result, the stability of the PEG-N<sub>3</sub>-PTX conjugates should increase compared with the PEG-suc-PTX conjugates, which is consistent with the results obtained.

Table 3. Half-lives of conjugates in different media

Conjugates	t <sub>1/2</sub> PBS pH 6.9 (h)	t <sub>1/2</sub> PBS pH 7.4 (h)	t <sub>1/2</sub> BAL (h)	t <sub>1/2</sub> Serum (h)
PEG-N <sub>3</sub> -PTX 6k	>72	>72	8.6±1.1	3.2±0.8
PEG-N <sub>3</sub> -PTX 20k	>72	>72	7.2±1.0	3.5±0.6
PEG-suc-PTX 6k	>72	10.0±2.5*	2.5±0.1*	1.1±0.2*
PEG-suc-PTX 20k	>72	36.1±4.1	4.0±0.4	1.0±0.1

Means ± SD are given, n=3. \* p<0.05, PEG-suc-PTX 6k versus 20k (Mann-Whitney).

In BAL and PBS pH 7.4, the 20 kDa succinic conjugate presented longer half-life than the 6 kDa (p < 0.05 Mann-Whitney). However, for the azide conjugates, increased stability was not observed for the 20 kDa conjugate. In serum, all conjugates had short half-lives. The PEG-N<sub>3</sub>-PTX azide conjugates showed better stability than the PEG-suc-PTX succinic conjugates at both MW in serum. Both 6 kDa and 20 kDa molecular weights of conjugates presented similar stability in serum for both structures. Although in the literature, the hydrolysis rate of

conjugates does not correlate with MW (80, 113, 116), the stability of PEG-suc-PTX conjugates at pH 7.4 and in BAL was dependent on MW in our study. The increased stability of the 20 kDa PEG-suc-PTX might result from the increased steric hindrance created by PEG and thereby, decreased accessibility of esterase for hydrolysis.

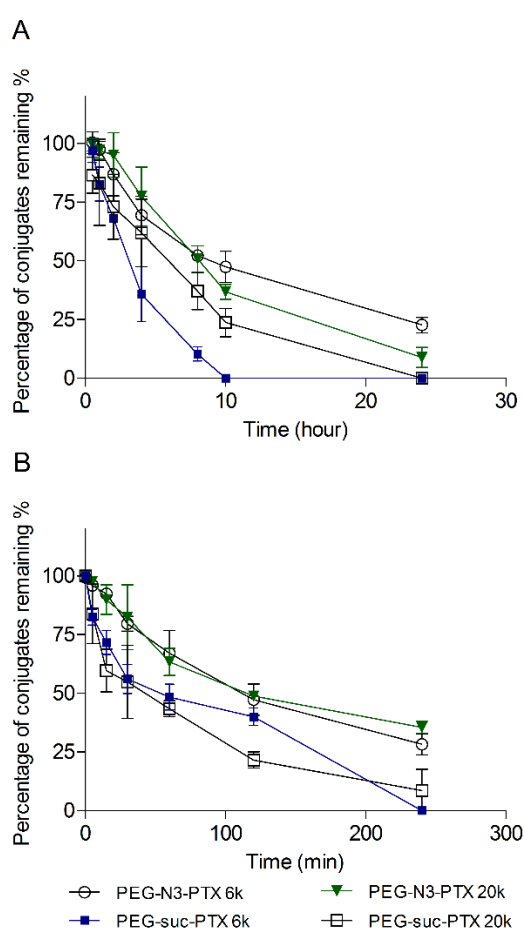


Fig. 16 Stability profiles of conjugates in bronchoalveolar lavage (A) and serum of mouse (B).

### 3.3 Cytotoxicity

The cytotoxicity of the conjugates was evaluated on LL/2 Lewis lung carcinoma cells and B16-F10 melanoma cells, which are widely used cell lines to establish a lung cancer model or a lung metastasis model in mice (122-124). The conjugates and Taxol were incubated at 37 °C with the cells for 72 hours in order to provide enough time for PTX release. Free PTX was also tested as a control. All the conjugates showed cytotoxicity on both cell lines but lower than Taxol and free PTX. Taxol had a similar cytotoxic profile as free PTX but with higher IC<sub>50</sub>. The IC<sub>50</sub> of all the conjugates were 5-fold higher compared with Taxol and more than 7-fold higher compared with free PTX (Table 4, Fig. 17). This is likely due to the slow release of PTX from the conjugates. However, the statistical test was not able to show a correlation between the *in vitro* release of the four conjugates in all the media tested and the cytotoxicity (Pearson correlation,  $p > 0.05$  for all). The sensitivity of these two cell lines to PTX cannot be compared because the numbers of cells seeded were different in the tests in order to reach the linear detection range of the UV absorbance.

The cellular internalization process is supposed to be different for free paclitaxel and Taxol, which comprises nanomicelles. Taxol showed a slightly increased IC<sub>50</sub> value compared with free paclitaxel. In the case of the 4 conjugates, as molecular mass of conjugates increased, the cellular internalization likely involved endocytosis instead of diffusion of free PTX. This change of mechanism along with the slow release of

PTX from the conjugates might lead to the increase of IC<sub>50</sub>. An increase of the IC<sub>50</sub> after conjugation of anti-cancer drugs to polymers has previously been reported (113). PTX was turned to a prodrug by PEGylation at the 2'-OH which is a necessary group for cytotoxicity (125). Thus the prodrug temporally lost cytotoxicity. After the hydrolysis of the ester bond between PTX and PEG, PTX was released in a non-conjugated form and began to interfere with the cell cycle and led to cell death.

Table 4. IC<sub>50</sub> values of all the conjugates calculated based on the data of MTT test

IC <sub>50</sub> of conjugates on different cancer cells (µg/mL PTX equiv.)		
	LL/2	B16-F10
PEG-N <sub>3</sub> -PTX 6k	0.0203 ± 0.0064 *	0.0567 ± 0.0110 *
PEG-N <sub>3</sub> -PTX 20k	0.0286 ± 0.0058 *	0.0521 ± 0.0134 *
PEG-suc-PTX 6k	0.1789 ± 0.0551 *	0.3050 ± 0.0363 *
PEG-suc-PTX 20k	0.0226 ± 0.0039 *	0.0809 ± 0.0083 *
Taxol	0.0039 ± 0.0006 *	0.0100 ± 0.0005 *
PTX	0.0022 ± 0.0005	0.0069 ± 0.0009

Means ± SD are given, n=3, 8 measurements each test. \* p<0.05, conjugates or Taxol versus PTX group, respectively (Mann-Whitney).

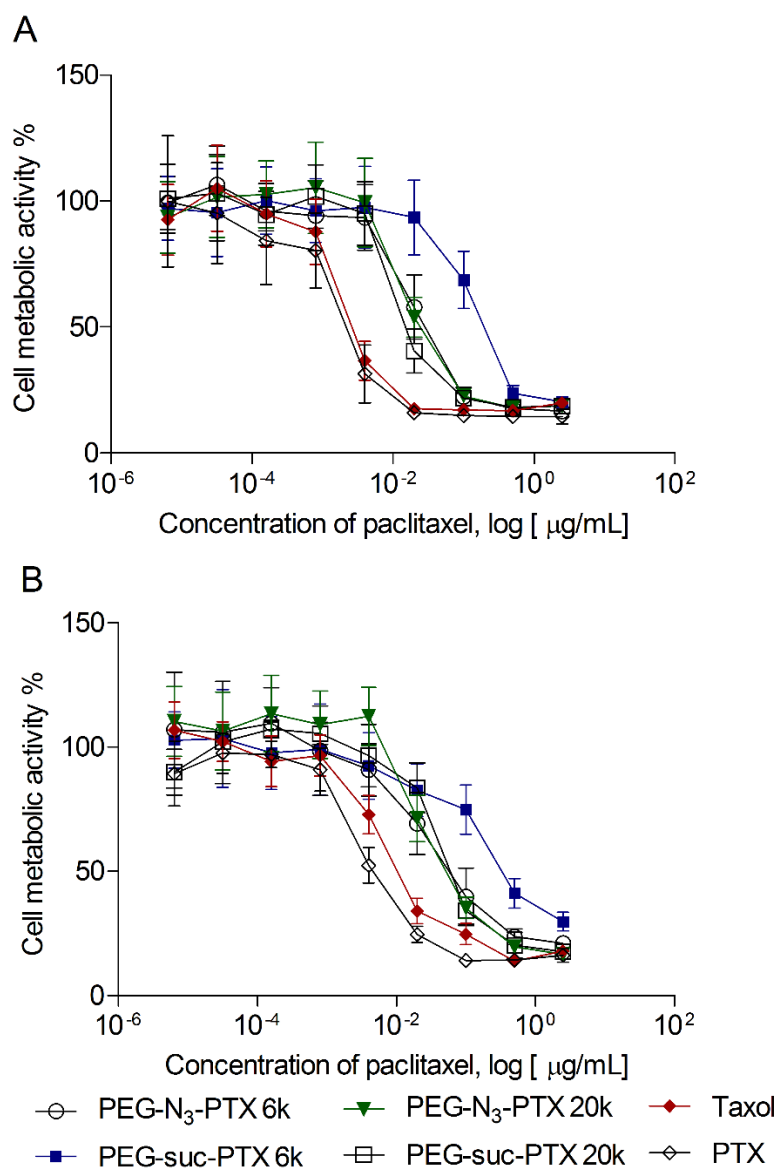


Fig. 17 Cell metabolic activities of PEG-PTX conjugates and Taxol on LL/2 Lewis lung cancer cells (A) and B16-F10 melanoma cells (B). Results are shown as the mean of 3 independent tests (8 measurements each test) and standard deviation.

We assessed the cytotoxicity of the PEG reagents, PEG-suc and PEG-N<sub>3</sub>, on LL/2 cells because as PTX was released, PEG reagents were simultaneously released. The results showed that all the PEG reagents were very slightly toxic to LL/2 cells at the concentration of 2.5 µg/mL (PTX equiv.; Fig. 18), which was the highest concentration used in the cytotoxicity assay for LL/2 cells (Fig. 17). In particular, PEG-suc 20k was slightly toxic to LL/2 cells, with a 15% loss of viability after 72h of contact. In Taxol, paclitaxel is dissolved in Cremophor EL and ethanol (1:1 v/v). Because Cremophor EL is involved in the side effects induced by Taxol, we also tested the cytotoxicity of Cremophor EL with ethanol on LL/2 cells. Results showed that Cremophor EL did not inhibit the growth of LL/2 cells at the concentration of 2.5 µg/mL (PTX equiv.; Fig. 18). This could come from the low concentration of Cremophor EL tested. Therefore, the decrease in cell viability induced by Taxol (Fig. 17) was caused by paclitaxel itself, and not the excipients Cremophor EL and ethanol. To exclude the interference of DMSO used in the stock solution of free PTX, the cytotoxicity of 0.5% DMSO was also tested on LL/2 cells. This amount of DMSO in culture medium was corresponded to the highest PTX concentration 2.5 µg/mL used in this test. Results showed DMSO below this level did not interfere with the cell viability (Fig.18).

To have an idea of the PTX concentrations in the cell culture medium after 72h of incubation of the conjugates, we extracted PTX from the supernatant of the incubation medium of PEG-N<sub>3</sub>-PTX 6 kDa (200 µg/mL PTX equiv.) and assayed it by HPLC. We found that the concentration of PTX was  $23 \pm 4$  µg/mL, which is only 12 % of the total

amount of PTX in the conjugate. In addition, there was only 11% of intact PEG-N<sub>3</sub>-PTX 6 kDa conjugate remaining in the incubation medium. The low level of PTX detected may be due to the uptake and metabolism of PTX by the cells. We suggest that the conjugates were taken up by the cells through endocytosis and then that PTX was released in the cytoplasm and had its cytotoxic effect. This hypothesis might explain the lack of correlation between cytotoxicity and drug release in acellular media. On the other hand, a study in the literature investigated the intracellular fate of polymer-bound anticancer agents and showed that the toxicity of conjugates might appear against the cytoplasmic, endosomal or lysosomal membranes. Then, the disintegration of the cell organization preceded apoptosis (126). Therefore, conjugates themselves could present cytotoxicity without the release of the anticancer drug. In the case of our PEG-PTX conjugates, the results imply that the toxicity of the conjugates was mainly caused by the released PTX or the conjugates themselves, but not by the PEG reagents.

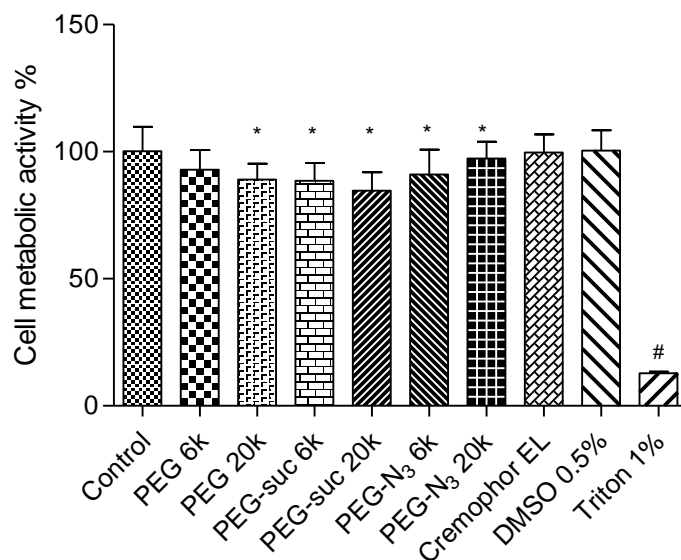


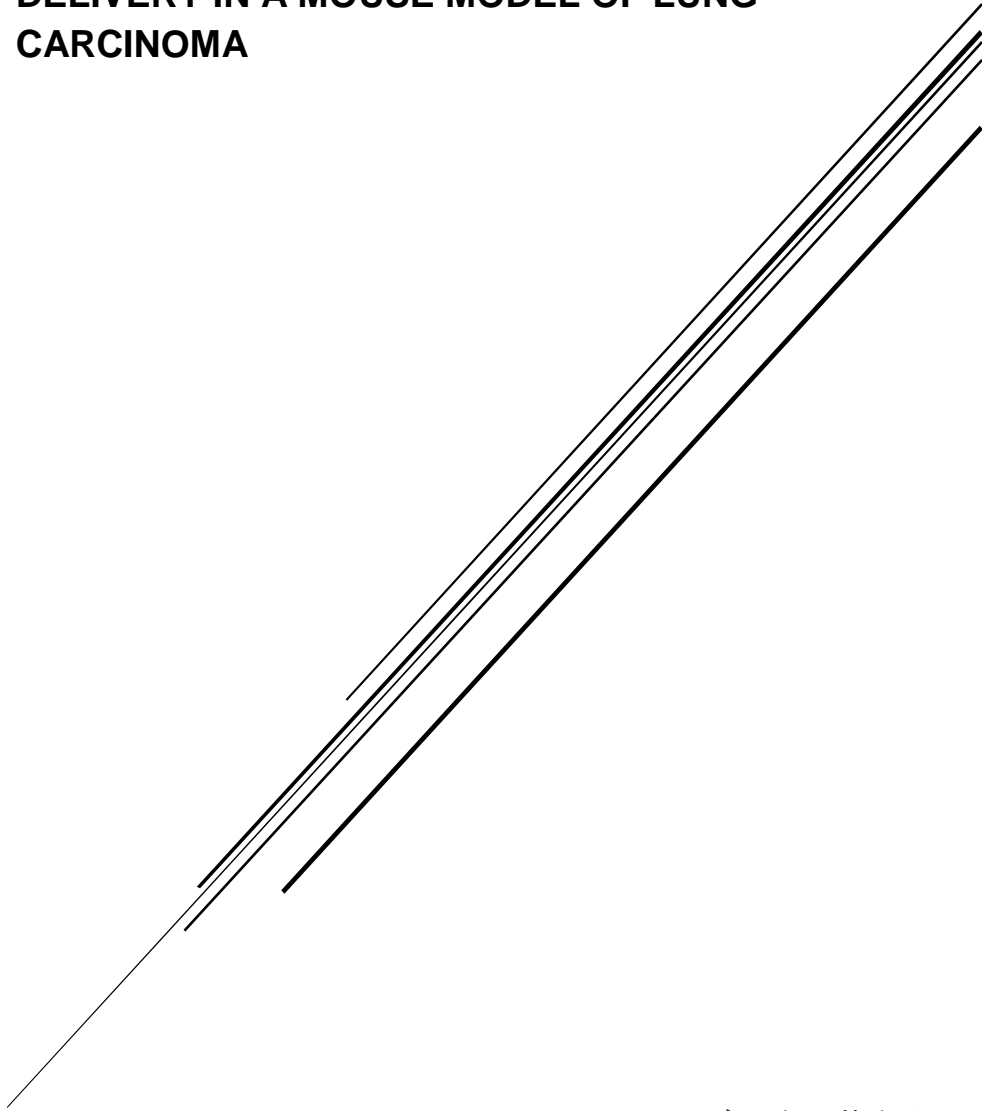
Fig. 18 Cytotoxicity of PEG reagents on LL/2 cells after 72 hour incubation at the concentration of 2.5  $\mu\text{g}/\text{mL}$  (PTX equiv.). Results are shown as the mean of 3 independent tests (8 measurements per test) and standard deviation. \*  $p < 0.05$ , when compared with control group. #  $p < 0.05$ , when compared with triton 1% (Mann-Whitney).

#### 4. Conclusion

Two structures of PEG-PTX conjugates with ester bond as linkage have been produced. Large PEGs with MW of 6 kDa and 20 kDa have been employed for the purpose of sustaining the presence of PTX in the lungs. The conjugates developed by click chemistry demonstrated good stability at the pH of the lung lining fluid and in murine BAL, which is essential for sustaining drug release in the lungs. *In vitro* cytotoxicity

studies on two types of cancer cells showed that the  $IC_{50}$  of all the conjugates were increased due to the formation of the prodrugs at 2'-OH on PTX. To conclude, the delivery system of PEG-PTX conjugates shows the potential to sustain the release of PTX in the lungs. The sustained drug release and the anti-tumor efficacy of the conjugates are currently investigated *in vivo* in the Lewis lung cancer murine model. If efficacy and safety are demonstrated in animal models, these conjugates could possibly be administrated to patients using a nebulizer and a mouthpiece in a cytotoxic chamber in the hospital in preliminary clinical trials.

**CHAPTER 3.  
PEGYLATION OF PACLITAXEL LARGELY  
IMPROVES ITS SAFETY AND ANTI-TUMOR  
EFFICACY FOLLOWING PULMONARY  
DELIVERY IN A MOUSE MODEL OF LUNG  
CARCINOMA**



上善若水，静水流深。  
Still waters run deep.



## **ABSTRACT**

Pulmonary delivery offers an attractive route of administration for chemotherapeutic agents, with the advantages of high drug concentrations locally and low side effects systemically. However, fast clearance mechanisms result in short residence time of small molecule drugs in the lungs. Moreover, the local toxicity induced by antineoplastic drugs is considered a major obstacle for the clinical application of inhaled chemotherapy. In this study, we explored the utility of 6 kDa and 20 kDa polyethylene glycol-paclitaxel (PEG-PTX) conjugates to retain paclitaxel within the lungs, achieve its sustained release locally, and thereby, improve its efficacy and reduce its pulmonary toxicity. The conjugates increased the maximum tolerated dose of paclitaxel by up to 100-fold following intratracheal instillation in healthy mice. PEG-PTX conjugates induced lung inflammation. However, the inflammation was lower than that induced by an equivalent dose of the free drug and it was reversible. Conjugation of paclitaxel to both PEG sizes significantly enhanced its anti-tumor efficacy following intratracheal instillation of a single dose in a Lewis lung carcinoma model in mice. PEG-PTX 20k showed equivalent efficacy as PEG-PTX 6k delivered at a 2.5-fold higher dose, suggesting that the molecular weight of the conjugate plays a role in anti-cancer activity. PEG-PTX 20k conjugate presented a prolonged residency and a sustained paclitaxel release within the lungs. This study showed that PEGylation of paclitaxel offers a potential delivery system for inhalation with improved anti-cancer efficacy, prolonged exposure of lung-resident tumors to the antineoplastic drug and

CHAPTER 3. PEGYLATION OF PACLITAXEL LARGELY IMPROVES ITS SAFETY AND  
ANTI-TUMOR EFFICACY FOLLOWING PULMONARY DELIVERY IN A MOUSE MODEL  
OF LUNG CARCINOMA

---

reduced local toxicity.

*Adapted from: PEGylation of paclitaxel largely decreases toxicity and increases anti-tumor efficacy following pulmonary delivery in a mouse model of lung carcinoma (in revision)*

Authors: Tian Luo, Cristina Loira-Pastoriza, Harshad P. Patil, Bernard Ucakar, Giulio Muccioli, Cynthia Bosquillon, Rita Vanbever

## 1. Introduction

Lung cancer is the leading cause of cancer-related death worldwide (127). Chemotherapy is widely used to treat lung cancer either alone or, combined with surgical resection and radiotherapy (128). However the 5-year survival rate only reaches 17% (129). The poor efficacy of the treatments results from the late diagnosis and from the limited and nonspecific access of chemotherapeutics to lung tumors after intravenous administration (14, 130). Pulmonary delivery is considered an attractive route of administration for chemotherapeutic agents, with the advantages of direct drug deposition at the diseased site and low systemic side effects. However, it is challenging to achieve sustained drug concentrations locally because of the efficient clearance mechanisms in the lungs. Small molecules are absorbed in the bloodstream within minutes and this results in a short residence time of chemotherapeutics in the lungs (45). Moreover, safety issue remains a major consideration for inhaled chemotherapeutics. The inhalation of cytotoxic drugs may cause transient high local drug concentrations, which may lead to toxicity to the lung tissue (47, 94, 131). Therefore, the benefits and the challenges of inhaled chemotherapy have stimulated interests in developing delivery systems for retaining and progressively releasing anti-cancer drugs in the lungs (32, 97).

Polymer-drug conjugates are prodrug systems with one or more drug molecules covalently conjugated to a hydrophilic polymer. They can offer sustained release of drugs and reduced toxicity. Polymer-drug

conjugates of anti-cancer agents have been extensively studied following intravenous administration. The enhanced permeability and retention (EPR) effect favors the passive accumulation of anticancer agents into the tumor tissue when delivered intravenously (132). In general, drugs are conjugated to polymers with biodegradable linkers, which allow the release of the active therapeutics. Conjugates containing ester or amide bonds can be hydrolyzed by non-specific esterase in extracellular environment or within cellular lysosomes.

As an alternative to inhalation of free drug formulations, polymer-drug conjugates would theoretically offer prolonged retention time of anticancer agents in the lungs and reduced toxicity to the lung tissue. In contrast to small molecules, macromolecules present long residence times in the airspaces (45). However, the pulmonary delivery of polymer-drug conjugates in lung cancer has not been thoroughly investigated. Studies on the pulmonary administration of poly-L-glutamic acid paclitaxel conjugate (PGA-PTX) and doxorubicin-conjugated dendrimers have been reported (111, 112, 133). These studies performed in animal lung cancer models showed that polymer-drug conjugates offer potential to improve the tumor exposure to the cytotoxic drug and to provide better tolerance locally.

Large hydrophilic polymers such as polyethylene glycol (PEG) improve the solubility of hydrophobic therapeutics but also increase retention times in the lungs. PEG with large molecular weight (MW > 5 kDa) can be retained in the lungs for up to 7 days (46). This feature could favour the sustained release of drugs conjugated to PEG in the

lungs. Moreover, PEG is nontoxic and it can be eliminated by renal and hepatic pathways. It has already been approved for human use in dosage forms for intravenous, oral and pulmonary applications. In addition, conjugates have relatively high drug loading (10-30%) compared with nanocarrier systems (134). There are various studies about PEGylated anti-cancer drugs by the intravenous route. PEGylated irinotecan, docetaxel, and SN38 (SN 38, 7-ethyl-10-hydroxy-camptothecin) are under phase II or III clinical trials by the intravenous route for the treatment of solid tumors (20, 73, 79). However, the application of PEGylated chemotherapeutics in lung cancer using pulmonary delivery has not been investigated.

Paclitaxel (PTX) has been widely used to treat non-small cell lung cancer. The commercial product is Taxol, which contains the water-insoluble paclitaxel formulated with Cremophor EL and dehydrated alcohol (135). The treatment is currently administered by intravenous infusion in the clinic. However, significant adverse effects such as hypersensitivity reactions, hematologic, neuro toxicities have been reported and some are not only related to paclitaxel but also to Cremophor EL in the formulation (136, 137). In addition, the oily nature of Cremophor will hamper its administration to the lungs. Therefore, developing drug delivery systems for inhaled paclitaxel without using Cremophor EL as solubilizer is critical.

In this study, we explored the possibility of using polyethylene glycol-paclitaxel (PEG-PTX) conjugates for inhaled chemotherapy and assessed the safety and efficacy of their pulmonary administration *in*

*in vivo* in mice. PEG-PTX conjugates with PEG molecular weights of 6 kDa and 20 kDa have previously been produced and characterized *in vitro* (138). The conjugates were synthesized by “click” chemistry and contained hydrolysable ester bonds between PTX and PEG. As the hydrolysis of the ester bonds by non-specific esterase proceeds, PTX is released in an active form. The *in vitro* data showed that PEG-PTX conjugates at both molecular weights were stable in phosphate buffer saline (half-life  $\geq 72$  h) and bronchoalveolar lavage (half-life of 7 to 9 h). The conjugates presented cytotoxicity to B16-F10 melanoma cells and LL/2 Lewis lung cancer cells *in vitro*, but less than Taxol. These data suggests that PEG-PTX conjugates have the potential to prolong the retention time of paclitaxel in the lungs. The prodrug nature of PEG-PTX conjugates is expected to reduce the local toxicity compared with the native drug. Therefore, we hypothesized that PEG-PTX conjugates delivered to the lungs would show improved antitumor efficacy with reduced toxicity *in vivo*.

## **2. Materials and methods**

### **2.1 Materials**

PTX was purchased from Chemieliva (Chongqing, China). PEG 6 kDa and 20 kDa were purchased from Iris Biotech (Marktredwitz, Germany). Taxol was obtained from Bristol-Myers Squibb. Hanks balanced salt solution (HBSS), phosphate buffered saline (PBS), Dulbecco’s modified Eagle’s medium (DMEM), penicillin/streptomycin (Pen Strep), and fetal bovine serum (FBS) were obtained from Life

Technologies (Belgium). Cell culture flasks and microplates were from Corning (Corning® T-75, Sigma-Aldrich, USA). Tissue-Tek® O.C.T. Compound and Cryomold were purchased from Sakura® Finetek (Torrance, CA). Superfrost™ microscope slides and blot were obtained from Gerhard Menzel B.V. & Co.KG (Braunschweig, Germany). Pierce micro BCA protein assay kit and Pierce lactate dehydrogenase (LDH) cytotoxicity assay kit were from Thermo Fisher Scientific (Leuven, Belgium). ONE-glo® luciferase assay kit was purchased from Promega (Leiden, Netherlands). HPLC grade acetonitrile was from Merck (Darmstadt, Germany). Ultrapure water was used throughout and all other reagents were of analytical grade.

## **2.2 PEG-PTX conjugates and Taxol**

PEG-PTX conjugates made of linear PEG 6 kDa or 20 kDa were prepared by conjugating paclitaxel to PEG at both its hydroxyl ends via click chemistry using azide linker triazole rings and ester bonds, as previously described (138). The conjugates were white lyophilized powders and the solutions of conjugates were filtrated through 0.22 µm membrane before lyophilisation. 6k and 20k PEG-PTX conjugates were reconstituted in 37 °C sterile PBS according to the desired doses before administration to mice. Taxol is the commercial formulation of paclitaxel, which is made of 6 mg paclitaxel, 50% of Cremophor EL and 50% of ethanol per mL. Taxol was diluted with sterile PBS according to the desired doses and filtrated through 0.22 µm membrane before administration to mice.

### 2.3 Animals

Female C57BL/6NJR mice (6 to 8 weeks old, Janvier, Le Genest-StIsle, France) were kept on a 12-hour light-dark cycle and were allowed to food and water *ad libitum*. The experimental protocols were approved by the Institutional Animal Care and Use Committee of the Université catholique de Louvain (Permit number: 2012/UCL/MD/006). All studies were performed under anesthesia and all efforts were made to minimize animal suffering.

Mice were anesthetized by intraperitoneal injection of ketamine/xylazine (90/10 mg/kg) before receiving paclitaxel formulations by intratracheal instillation (i.t.). The mouse was fixed to make sure its neck was vertical. After gently pulling the tongue out, treatment solution was pipetted on the top of trachea. The tongue was released after two breaths were completed. Single dose treatments of the different formulations were given in a volume of 50  $\mu$ L per mouse. Blood samples were collected from the orbital sinus and kept at 4 °C overnight. After centrifugation at 12,000 $\times$ g for 10 min, the serum was withdrawn and stored at -20 °C. Bronchoalveolar lavage (BAL) was performed after euthanizing the mice by cervical dislocation. One ml of HBSS was injected into the trachea and left for 15 s. 0.5 mL of the fluid was then withdrawn and re-injected into the lungs. All the BAL liquid was removed from the lungs afterwards. The volume of recovered BAL was recorded. The BAL samples were then centrifuged at 4,500 $\times$ g for 10 min to remove the cells. The supernatants were collected and stored at -20 °C. The lungs were then resected and

kept in 0.5 mL HBSS on ice during the experiment. The lungs were homogenized and centrifuged at 3000xg rpm for 10 min. The supernatants were withdrawn and stored at -20 °C.

#### **2.4 Maximum tolerated doses of PEG-PTX conjugates delivered intratracheally**

To determine the toxicity of PEG-PTX conjugates, the maximum tolerated doses (MTD) of PEG-PTX conjugates and Taxol were assessed following intratracheal instillation in female healthy C57BL/6NJR mice by the method describing at 2.3. PEG-PTX 6k conjugate was delivered by intratracheal instillation at doses of 10, 25, and 50 mg/kg (PTX equiv.). PEG-PTX 20k conjugate was delivered by intratracheal instillation at the dose of 20 mg/kg (PTX equiv.). Taxol was delivered by intratracheal instillation at doses of 0.5, 1.2, 2, 5 mg/kg. Taxol was also injected in the tail vein at doses of 10 mg/kg and 20 mg/kg in 200 µL. Mice were observed for 2 weeks. Symptoms and the numbers of surviving mice were recorded. The appropriate endpoints were defined based on signs of moderate severity, as described in the guidance from the Laboratory Animal Science Association. The MTD was defined as a maximum body weight loss of 20% and neither death nor severe symptoms occurrence within 2 weeks.

#### **2.5 Local toxicity of PEG-PTX conjugates in the lungs**

The local toxicity of the PEG-PTX conjugates and Taxol were assessed in healthy female C57BL/6NJR mice 24 hours, 72 hours and

7 days post intratracheal instillation. PEG-PTX 6k, 20k conjugates and Taxol were delivered by intratracheal instillation in 50  $\mu$ L at their MTDs, i.e., 50 mg/kg, 20 mg/kg, and 0.5 mg/kg, respectively. The local toxicity of PEG-N<sub>3</sub> 6k was also investigated at the equivalent dose of 50 mg/kg PTX. In addition, a low dose of PEG-PTX 6k of 0.5 mg/kg was also assessed 24 hours post intratracheal delivery. Mice were sacrificed at the predetermined time points and about 1 mL bronchoalveolar lavage was recovered and centrifuged immediately according to the procedures described in 2.3. Total protein and lactate dehydrogenase (LDH) in BAL supernatant were analyzed by Pierce BCA protein assay kit and LDH assay kit, respectively. Cell pellets were reconstituted at a concentration of 20,000 cells/mL and total live cells were counted by Türk's solution method (Merck KGaA, Darmstadt, Germany). The differential cell counts were obtained by cytocentrifugation and coloration with Diff Quick<sup>®</sup> (Medion Diagnostics AG, Switzerland).

The lungs were inflated with 1 mL Tissue Tek/PBS (1:1) and carefully removed from mice. The left lobes were embedded into Tissue Tek cryomatrix and then placed into liquid nitrogen to freeze rapidly. Frozen sections (10  $\mu$ m) were performed with Cryostat (Leica Microsystems, Wetzlar, GE) and stained with haematoxylin-eosin (Sakura DRS 601). The sections were examined by Leica slide scanner SCN 400 (Leica Biosystems, Wetzlar, GE).

## **2.6 Anti-tumor efficacy of PEG-PTX conjugates against Lewis lung carcinoma**

Murine Lewis Lung Carcinoma cell line (LL/2-luc-M38 Bioware Cell Line, Caliper Life Sciences, Inc) stably expressing luciferase was a gift from Prof. Didier Cataldo, University of Liege (Belgium). LL/2-luc-M38 was cultured at 37 °C in 5% CO<sub>2</sub>, in DMEM supplemented with 10% FBS, 1 mM sodium pyruvate and 1% Pen Strep.

C57BL/6NJR female mice were randomly assigned to 5 groups according to treatments (n=6). A Lewis lung carcinoma model was established by tail vein injection of Lewis Lung carcinoma cells. On day 0, each C57BL/6NJR female mouse received  $2 \times 10^5$  cells (passage 17 or 18) in 0.1 mL PBS intravenously (i.v.). On day 7, single dose treatments of PEG-PTX 6k, 20k conjugates and Taxol were delivered to 3 groups of mice by intratracheal instillation in 50  $\mu$ L at their MTD, i.e., 50 mg/kg, 20 mg/kg, and 0.5 mg/kg, respectively. The preparation of the conjugates and Taxol solutions followed the procedure described in 2.2. 50  $\mu$ L PBS was administered intratracheally to one group of mice as a control. In addition, one group of mice received 20 mg/kg of Taxol in 200  $\mu$ L by tail vein injection to compare the efficacy of different administration routes. Mice were observed for symptoms and body weights were recorded. On day 14, all mice were euthanized by cervical dislocation. The lungs were immediately taken. Lung weights were recorded. The number of lung metastases were counted using bioluminescence on total resected and grounded lungs. One glo<sup>®</sup> assay was conducted to detect

bioluminescence and LL/2-luc-M38 cells cultured *in vitro* were used as calibration.

## 2.7 Kinetics of *in vivo* distribution in the respiratory tract

PEG-PTX 20k and Taxol were investigated for their release kinetics and biodistribution *in vivo*. Female C57BL/6NJR mice were anesthetized by ketamine/xylazine (90/10 mg/kg) intraperitoneal injection. PEG-PTX 20k conjugates and Taxol were delivered by intratracheal instillation in 50  $\mu$ L at their MTD, i.e., 20 mg/kg and 0.5 mg/kg, respectively. Blood was taken immediately after administration of treatments. Mice were then euthanized. This time point was marked as 0h. 1 mL BAL and lungs were taken according to the procedure described in 2.3. Blood, BAL and lungs were also collected 24h and 48h post intratracheal instillation. To extract paclitaxel from serum, BAL and suspensions of homogenized lungs, acetonitrile was added at 1:1 (v/v) ratio to the samples and vortexed for 15 seconds. The suspensions were then centrifuged at 10,000 $\times$ g for 10 min and the supernatants were withdrawn. The supernatants were then dried under nitrogen flow at room temperature. The resulting residues from blood samples were reconstituted in 100  $\mu$ L water/acetonitrile (1:1 v/v). The residues from BAL and lung samples were reconstituted in 300  $\mu$ L water/acetonitrile (1:1 v/v). The samples were then centrifuged (10000 $\times$ g, 10 min) and 20  $\mu$ L of the supernatant were analyzed by HPLC-MS (for PTX analysis) or by HPLC-UV (for analysis of the remaining PEG-PTX conjugates) by UV absorbance. The use of HPLC-UV for the analysis of PEG-PTX 20k was necessary because

of the lack of proper signal for this large molecule with the LC-MS used in this study.

Briefly, Paclitaxel was analyzed by LC-MS using an LTQ-Orbitrap mass spectrometer coupled to an Accela HPLC system (Thermo Fischer Scientific). Analytic separation was achieved using reverse phase C18 column (LiChrospher 100 RP-18 5  $\mu\text{m}$  particles, 250 x 4 mm, Merck, Darmstadt, Germany). Mobile phases A and B consisted of  $\text{H}_2\text{O}$  / formic acid 99.9:0.1 (v/v) and acetonitrile. The gradient (1 mL/min) was performed as follows: starting at 40% B and reaching linearly 90% B in 13 min. This was followed by 7 min at 90% B before equilibrating at 40% B. An ESI source operated in the positive mode was used for the MS analysis. The ESI spray voltage was set at 5.0 kV and the capillary temperature at 275°C while the sheath gas flow and auxiliary gas flow were set at 20 and 10 arbitrary units, respectively. Paclitaxel was analyzed as the  $[\text{M}+\text{H}]^+$  ion ( $m/z$  854.33823). A standard curve was established in the range of 0.1-50  $\mu\text{g}/\text{mL}$  of PTX in BAL following the extraction method above (correlation coefficient  $R = 0.9999$ , LOD = 0.13  $\mu\text{g}/\text{ml}$ , LOQ = 0.44  $\mu\text{g}/\text{ml}$ , recovery at 10  $\mu\text{g}/\text{mL}$  was 99.6%). Standard curves were also established in homogenized mouse lung suspension and mouse serum in the range of 0.1-10  $\mu\text{g}/\text{mL}$  of PTX following the same extraction method above ( $R = 0.9948$  and  $0.9994$ , recovery at 10  $\mu\text{g}/\text{mL}$  was 101.1% and 93.5% in lungs and serum, respectively).

HPLC was carried out using the Hewlett Packard series 1100 system (Agilent Technologies, Palo Alto, CA) with a reverse phase C18

column (NUCLEOSIL® 300-5 C18 · 5 µm particles · 300 Å pores, 250mm×4.6mm, MACHEREY-NAGEL GmbH & Co. KG, Düren, Germany). The mobile phase was acetonitrile and water eluted at 1 mL/min using a gradient protocol as follows: a linear gradient from acetonitrile 40% to 60% for 20 minutes, a linear gradient from acetonitrile 60% to 40% for 5 minutes. Absorbance of the column effluent was monitored at 227 nm. The areas under the peaks of conjugates were monitored.

## **2.8 Statistics**

Results were shown as mean ± standard error of the mean (SEM). Mann-Whitney test was performed using the software GraphPad Prism to demonstrate statistical differences ( $p < 0.05$ ) between groups.

## **3. Results**

### **3.1 Conjugation to PEG increased the MTD of paclitaxel post-intratracheal delivery**

An acute toxicity study was conducted to assess the MTD of the PEG-PTX conjugates following intratracheal instillation. The maximum doses tested were 50 mg/kg and 20 mg/kg for PEG-PTX 6k and 20k conjugate, respectively, because these doses reached the limits of their solubility in PBS. As controls, the MTD of Taxol was assessed following intratracheal instillation and intravenous injection.

All the intratracheal instillation groups showed body weight loss 1-2 days post-delivery (Fig. 19A, B and C). A maximum of 7% of body weight loss was found in the group of PEG-PTX 6k 50 mg/kg (PTX equiv.) 1 day post-delivery. A maximum of 14% of body weight loss was found in the group of PEG-PTX 20k 20 mg/kg (PTX equiv.) at 2 days post-delivery. However, these weight losses were reversible. All mice from the conjugate groups and Taxol 0.5 mg/kg group recovered their initial body weights within 3-4 days post-delivery.

Subdued behavior, lung noises and hunching were found in the groups of PEG-PTX 6k 50 mg/kg (PTX equiv.), PEG-PTX 20k 20 mg/kg (PTX equiv.) as well as in the group receiving Taxol 0.5 mg/kg. However, these symptoms disappeared after 4-5 days of delivery. Death was found immediately after delivery in the group receiving Taxol 5 mg/kg intratracheally. The mice receiving Taxol 2 mg/kg and 1.2 mg/kg intratracheally survived for 1 day and 2 days post-delivery, respectively. Death was then found on the second and third days post-delivery. Mice were found to have tremors, lung noises, subdued behavior as well as hunching in the groups receiving Taxol 1.2 mg/kg and above. The dead mice of the group receiving Taxol 1.2 mg/kg were examined and lung haemorrhage was found. Therefore, the MTDs of PEG-PTX 6k and 20k following intratracheal instillation were 50 mg/kg (PTX equiv.) and 20 mg/kg (PTX equiv.), respectively (Table 5). These values were 100-fold and 40-fold the MTD of Taxol, i.e., 0.5 mg/kg.

The MTD of Taxol delivered by intravenous injection was also studied. Based on the reports in the literature (134, 139), two doses of 10

mg/kg and 20 mg/kg were delivered. Both groups of mice were found to have transient prostration for 5-10 minutes. The body weights of the 2 groups stably increased for 2 weeks. Therefore, the MTD of Taxol following intravenous injection was 20 mg/kg in this study.

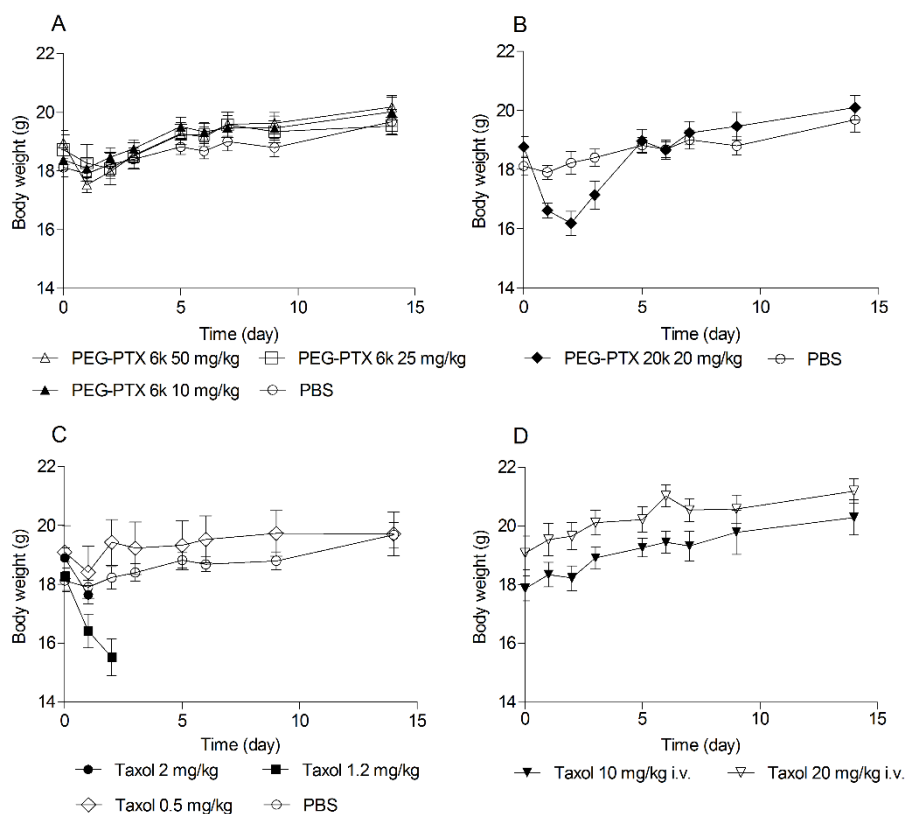


Fig. 19 Body weights of mice receiving PEG-PTX conjugates and Taxol intratracheally and intravenously. (A) PEG-PTX 6k conjugate delivered intratracheally at different doses, (B) PEG-PTX 20k conjugate delivered intratracheally, (C) Taxol delivered intratracheally at different doses, (D) Taxol delivered intravenously at different doses. Mean  $\pm$  SEM are shown, n=6 mice per group.

Table 5. MTD of PEG-paclitaxel conjugates and Taxol post i.t. or i.v. injection.

<b>MTD (PTX equiv.)</b>	
PEG-PTX 6k i.t.	>50 mg/kg
PEG-PTX 20k i.t.	>20 mg/kg
Taxol i.t.	0.5 mg/kg
Taxol i.v.	20 mg/kg

*n=6 mice per group*

### 3.2 Local toxicity studies of PEG-PTX conjugates in the lungs

The local toxicity of the PEG-PTX conjugates to the lungs was assessed in healthy female C57BL/6NJR mice. Conjugates and Taxol were administered at their MTDs. PEG-N<sub>3</sub> 6k was the synthetic material of PEG-PTX 6k. It was tested to verify PEG toxicity to the lung tissue. We also tested Cremophor EL at the corresponding dose of 0.5 mg/kg PTX, which would give a better understanding of the pulmonary toxicity of Taxol.

We analyzed biochemical inflammation markers in BAL in order to check if PEG-PTX induced inflammation in the lungs. Total protein was analyzed to detect the alteration of the alveolar-capillary barrier. Results showed that the groups of Taxol 0.5 mg/kg, PEG-PTX 6k 50 mg/kg (PTX equiv.), PEG-PTX 20k 20 mg/kg (PTX equiv.) and Cremophor EL 0.5 mg/kg (PTX equiv.) induced large increases of total protein levels at 24h and 72h. However, PEG-PTX 6k at a lower dose

of 0.5 mg/kg (PTX equiv.) and PEG-N<sub>3</sub> 6k 50 mg/kg (PTX equiv.) did not induce an increase of total protein levels. At Day 7, the total protein concentrations decreased to the normal levels in the groups of Taxol, PEG-PTX 6k and 20k (Fig. 20A).

The extracellular presence of lactate dehydrogenase (LDH), an intracellular enzyme, can reflect injury to pulmonary cells. Taxol 0.5 mg/kg increased LDH levels in bronchoalveolar lavage 24h after i.t. delivery (Fig. 20B). Cremophor EL delivered i.t. at the corresponding dose of 0.5 mg/kg paclitaxel also showed a significant increase of LDH level. PEG-PTX 6k and 20k at their MTD caused significant increases of LDH in BAL 24h post i.t. delivery. However, PEG-N<sub>3</sub> 6k delivered at the equiv. dose of PEG-PTX 6k 50 mg/kg (PTX equiv.) did not increase LDH level significantly. The LDH level of PEG-PTX 6k at a low dose of 0.5 mg/kg, which was the MTD of Taxol i.t., remained at the same level as the control. At Day 7, the LDH concentration decreased to the normal level in the groups of Taxol, PEG-PTX 20k, and PEG-N<sub>3</sub> 6k. The group of PEG-PTX 6k 50 mg/kg (PTX equiv.) showed decreased LDH concentration compared with 24h and 72h, but it still had higher LDH level than the PBS control group.

CHAPTER 3. PEGYLATION OF PACLITAXEL LARGELY IMPROVES ITS SAFETY AND ANTI-TUMOR EFFICACY FOLLOWING PULMONARY DELIVERY IN A MOUSE MODEL OF LUNG CARCINOMA

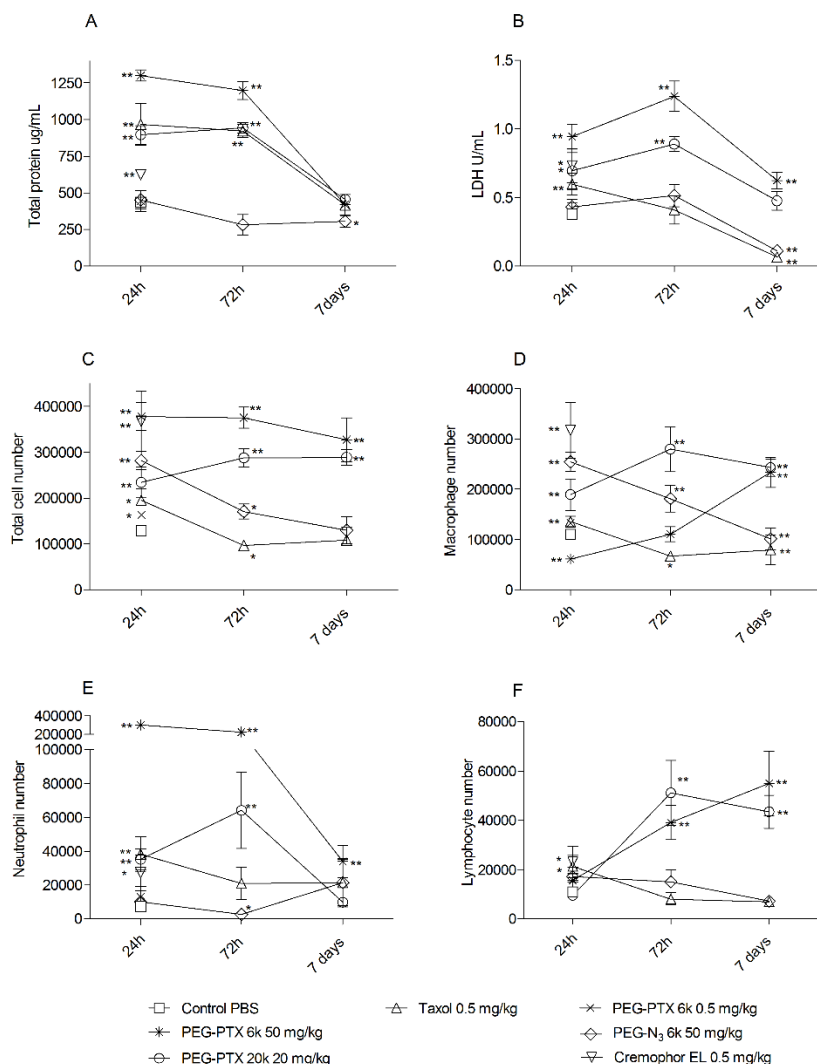


Fig. 20 Local toxicity of PEG-PTX conjugates, Taxol, free PEG-N<sub>3</sub> 6k and Cremophor EL. (A) Total protein (B) LDH level (C) total cell numbers (D) macrophage numbers (E) neutrophil numbers and (F) lymphocyte numbers in BAL at different time points post intratracheal instillation of PEG-PTX conjugates, Taxol, PEG-N<sub>3</sub> 6k and Cremophor EL. Mean and SEM are shown, n=4-6 mice per group, \* p < 0.05, \*\* p < 0.01, compared with control group (Mann-Whitney).

Total cells number and cell distributions in BAL fluid can provide an indication on the degree of pulmonary inflammation. There were large increases of total cell number in PEG-PTX 6k 50 mg/kg and 20k 20 mg/kg groups at 24h, 72h, and 7 days. The total cell number in the Taxol group increased at 24h but decreased to normal level 72h post-delivery (Fig. 20C). The group of PEG-PTX 6k at the low dose of 0.5 mg/kg presented an increase of total cell number at 24h but less than the Taxol group. The group treated with only PEG-N<sub>3</sub> 6k at the corresponding dose of 50 mg/kg PTX had an increase of total cell number at 24h, but the number decreased to normal level at day 7. Cremophor EL also induced a large increase of total cell number in BAL at 24h.

The number of neutrophils in BAL fluid is a cellular marker of inflammation. When PEG-PTX 6k was administered at the high dose of 50 mg/kg (PTX equiv.), the neutrophil number rose significantly to more than 10-fold that of the control group at 24h and 72h, and decreased to normal level at day 7 (Fig. 20E). In the groups of PEG-PTX 20k and Taxol, increases of neutrophil numbers were found at 24h and 72h, but neutrophil numbers were less than that of the PEG-PTX 6k group at all time points tested. The influx of neutrophils contributed to the increase of total cell numbers in these three groups. When PEG-PTX 6k was given at a low dose of 0.5 mg/kg, there was no significant increase of neutrophil number. PEG-N<sub>3</sub> 6k 50 mg/kg (PTX equiv.) did not induce a significant increase of neutrophils at all time points tested. Cremophor EL given at the dose of 0.5 mg/kg (PTX equiv.) showed a significant increase of neutrophils numbers 24h post-

delivery. In addition, foamy macrophages were found in the groups receiving PEG-PTX 6k, 20k at their MTD and PEG-N<sub>3</sub> 6k at 50 mg/kg (PTX equiv.) at all time points (Fig. 21).

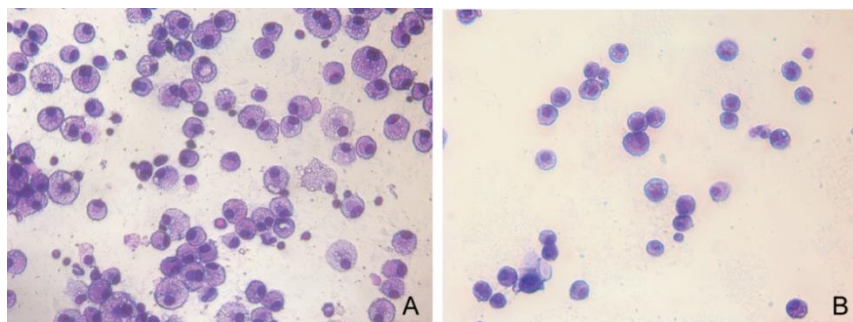


Fig. 21 Representative pictures showing foamy macrophages in (A) PEG-PTX 20k group 7 days post-delivery and their absence in (B) PBS control group (colored by Diff Quick®, magnification × 40 under optical microscope).

Generally, the histological examination showed no significant damages and changes in the structure and morphology of the lung parenchyma in all tested groups 24h post-delivery (Fig. 22). This was probably because obvious damages of lung parenchyma have not been induced yet. The group receiving PEG-PTX 6k at a low dose of 0.5 mg/kg did not show obvious differences in morphology as compared with the PBS control group. There might be damages in the integrity of lung structure in some samples of Taxol 0.5 mg/kg group when compared with the control. The thicknesses of bronchioles and alveolar epithelium appeared to be increased in groups treated with Taxol 0.5 mg/kg, PEG-PTX 6k 50 mg/kg (PTX equiv.), PEG-PTX 20k 20mg/kg (PTX equiv.) and PEG-N<sub>3</sub> 6k 50 mg/kg (PTX equiv.), compared with the negative control. This might reflect an over-production of mucus.

CHAPTER 3. PEGYLATION OF PACLITAXEL LARGELY IMPROVES ITS SAFETY AND ANTI-TUMOR EFFICACY FOLLOWING PULMONARY DELIVERY IN A MOUSE MODEL OF LUNG CARCINOMA

---

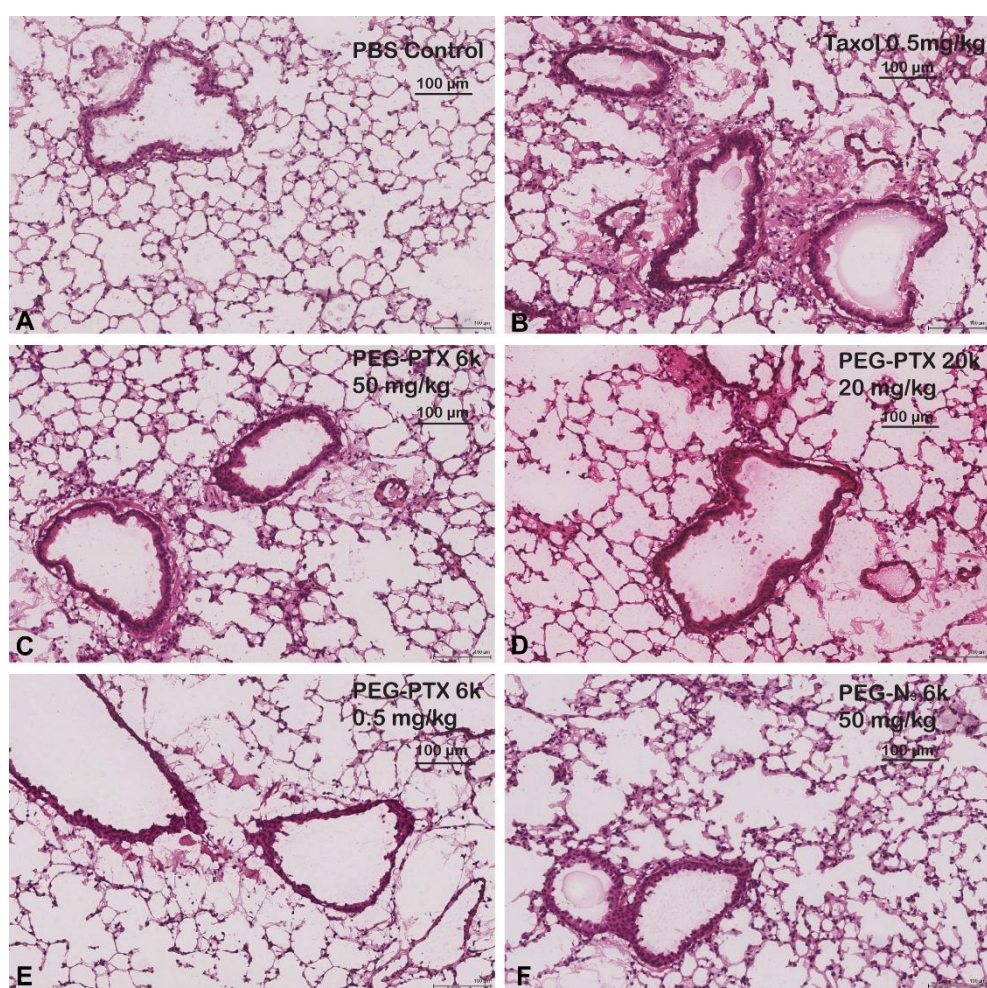


Fig. 22 Representative pictures showing lung morphology post intratracheal delivery of PBS control (A), Taxol 0.5 mg/kg (B), PEG-PTX 6k 50 mg/kg (C), PEG-PTX 20k 20 mg/kg (D), PEG-PTX 0.5 mg/kg (E), and PEG-N<sub>3</sub> 50 mg/kg (F) (Hematoxylin-Eosin staining).

### **3.3 PEG-PTX conjugates increased anti-tumor efficacy in a murine model of lung carcinoma**

Both PEG-PTX 6k and 20k at their MTDs reduced the tumor cell number in the lungs compared to the non-treated control group (Fig. 23). When comparing with Taxol i.t., PEG-PTX 6k and 20k also showed superior efficacy. Taxol delivered i.t. was not able to significantly reduce tumor cells in the lungs. There was no statistical difference between the groups of PEG-PTX 6k and 20k (Fig. 23B), which indicated that same anti-tumor efficacy could be achieved at a lower dose of paclitaxel with higher molecular weight of PEG. Taxol was also injected intravenously to compare the efficacy of different administration routes. However, intravenous Taxol at its MTD was not able to significantly decrease tumor cell number in the lungs. There was a slight and reversible body weight loss 1 and 2 days post-intratracheal instillation in the conjugates and Taxol groups (Fig. 23C).

CHAPTER 3. PEGYLATION OF PACLITAXEL LARGELY IMPROVES ITS SAFETY AND ANTI-TUMOR EFFICACY FOLLOWING PULMONARY DELIVERY IN A MOUSE MODEL OF LUNG CARCINOMA

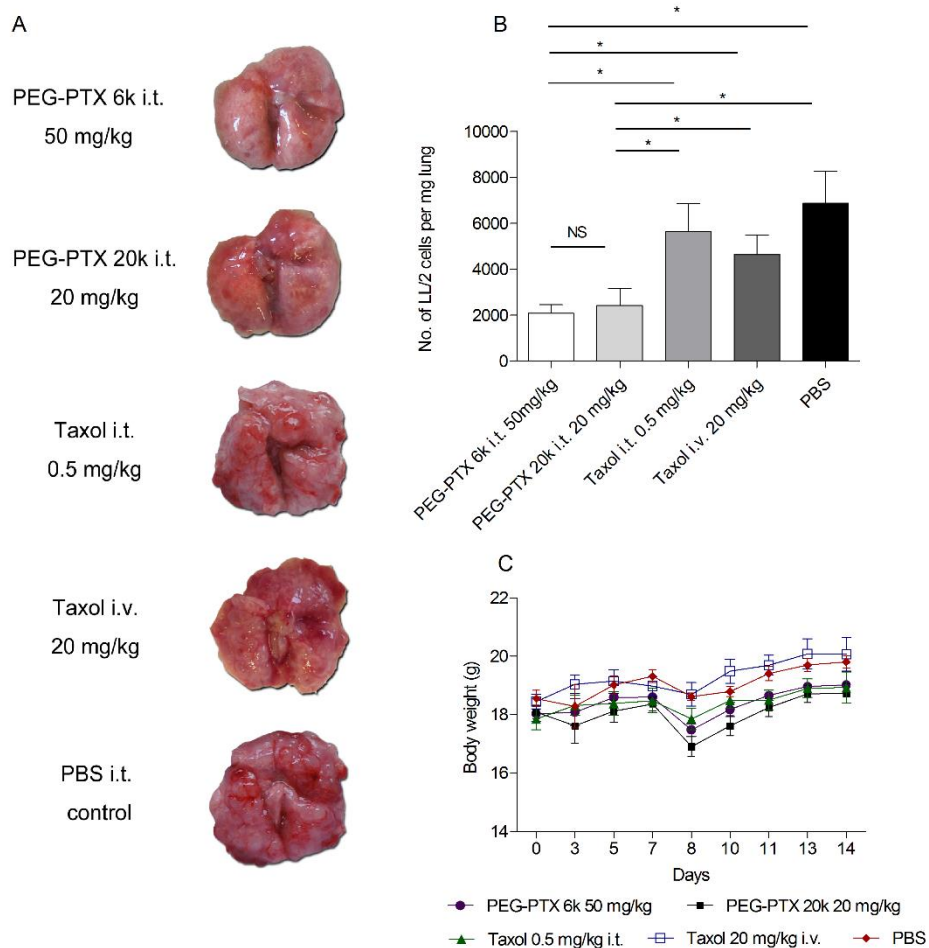


Fig. 23 Efficacy assessment of PEG-PTX conjugates and Taxol delivered by intratracheal instillation or intravenous injection in a murine model of Lewis lung carcinoma. (A) Representative images of mouse lungs. (B) Numbers of LL/2 tumor cells per milligram lung tissue. (C) Body weights of mice. Mean  $\pm$  SEM are given,  $n=6-7$ . \*  $p < 0.05$ ; NS, no significant difference (Mann-Whitney). Similar results were obtained in two independent experiments.

### **3.4 PEG-PTX conjugates prolonged the retention time of paclitaxel in the lungs**

PEG-PTX 20k (20 mg/kg PTX equiv.) presented equivalent anti-cancer efficacy and less local toxicity compared with PEG-PTX 6k at a 2.5 higher dose (50 mg/kg PTX equiv.). Therefore, we selected PEG-PTX 20k to investigate the release of PTX from the conjugate *in vivo* and we used Taxol as a control. PEG-PTX 20k presented a prolonged release of PTX in both BAL and lungs (Fig. 24). Indeed, at 48h post-delivery, PTX amount in BAL was still 40% of the dose recovered at time 0 (Fig. 24C). Most of the PTX released from the conjugate was present in the BAL at all time points, and only a small percentage was present in the lung tissue (Fig. 24C). In serum, the PTX released from conjugate was below limit of quantification at all time points. PEG-PTX 20k showed a long retention time in both BAL and lungs. 43% and 20% of PEG-PTX 20k initial dose remained in BAL and lungs 48h post-delivery, respectively (Fig. 24D). There was no PEG-PTX conjugate detected in serum at all time points. As a contrast, Taxol delivered at the dose of 0.5 mg/kg (10 µg of PTX per mouse) showed a quick clearance from the respiratory tract. Only 3.8 µg and 0.6 µg of PTX were present in BAL and lungs respectively at time 0 (Figs. 24A&B), but in serum the concentration of PTX was below the limit of quantification. PTX was also below the limit of quantification in serum, BAL and lungs 24h and 48h post-delivery.

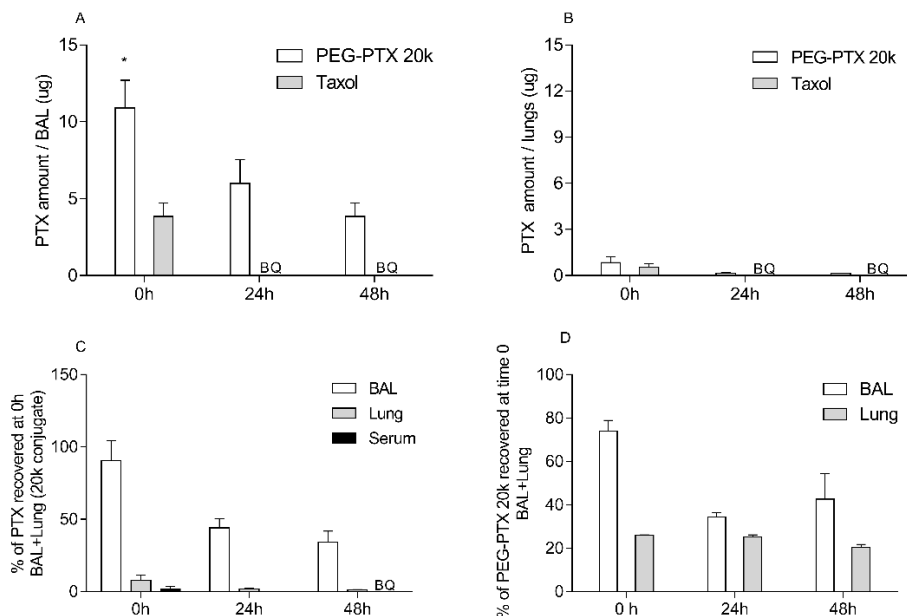


Fig. 24 PTX and PEG-PTX 20k recovered from the respiratory tract 0h, 24h and 48h post intratracheal administration. (A) PTX amount in BAL and (B) PTX amount in the lungs in mice having received PEG-PTX 20k (20 mg/kg PTX equiv.) and Taxol (0.5 mg/kg). (C) Amount of PTX expressed as a percentage of the total dose recovered from BAL, lungs and serum at time 0. (D) Amount of PEG-PTX 20k expressed as a percentage of the total dose recovered from BAL and lungs at time 0. \*  $p < 0.05$ , when compared with Taxol group (Mann-Whitney); BQ, below quantification limit.

#### 4. Discussion

The present study demonstrated that PEG-PTX conjugates had lower toxicity but superior anti-tumor efficacy than Taxol when administered i.t. to mice. We used PEGylation to solubilize PTX instead of Cremophor EL, which reduced the local toxicity. Moreover, the choice of large MW of PEG (20 kDa) prolonged the retention time of paclitaxel

in the lungs, which led to the improved efficacy. These results suggested that PEGylation of chemotherapeutics could be an effective approach to embody inhaled chemotherapy in the future.

Conjugation of PTX to PEG largely increased the MTD following intratracheal instillation. The MTD of PEG-PTX 6k i.t. was 100-fold of Taxol i.t.. This could be attributed to the prodrug nature of PEG-PTX conjugates. Intratracheal delivery of PEG-PTX 6k at a high dose (50 mg/kg PTX equiv.) increased LDH and neutrophils levels in BAL 24h post-delivery. However, delivery of equiv. dose of PEG-N<sub>3</sub> 6k did not increase LDH and neutrophils significantly. Therefore, the toxicity of conjugates mainly came from the high dose of PTX itself. Taxol containing 50% of Cremophor EL was used as the PTX control in this study. Intratracheal delivery of either Taxol or Cremophor EL alone caused increased levels of LDH and neutrophils, which indicated that the pulmonary toxicity was induced by both PTX and the Cremophor EL. Although it is not suitable for pulmonary delivery, Cremophor EL is needed in the formulation to solubilize the desired amount of PTX. Further, PEG-PTX 6k delivered at the same low dose as Taxol (0.5 mg/kg PTX equiv.) did not induce significant toxicity to the lungs. These results suggested that PEGylation reduced the local toxicity of the native drug and that the local toxicity of PEG-PTX conjugates was dose-dependent.

As PEG-PTX 20k presented long retention time in the lungs, toxicological concerns may arise from long-term accumulation of high molecular weight PEG in the lungs. The safety of PEG 3,350 Da has

been proved in rats following 2-week exposure by aerosol (140). However, there is no safety study on large PEG (> 5 kDa) delivered by inhalation. In this study, PEG-N<sub>3</sub> 6k at 200 mg/kg (50 mg/kg PTX equiv.; 5 mg of PEG-N<sub>3</sub> 6k per mouse) presented acceptable safety over 7 days following a single administration dose in the lungs. Generally, PEG is non-toxic and extensively used in drug delivery. It has been approved for human use in intravenous, oral and pulmonary formulations. However, the non-biodegradable property of PEG might be the drawback for application by inhalation. It is anticipated that either PEG-PTX or the free PEG released following the hydrolysis of PEG-PTX would be partially cleared by mucociliary clearance and by alveolar macrophages. The fraction absorbed in the systemic circulation would likely be eliminated by renal clearance (141). Considering the large PEG size and the high doses delivered, long-term safety studies are needed to ascertain the safety of inhaled PEG-PTX.

43% and 20% of the PEG-PTX 20k initial dose were still present in BAL and lungs 48h post-intratracheal instillation, respectively. In previous studies of PEG retention in the lungs, PEG with MW > 5 kDa was not quickly cleared and absorbed into the systemic circulation (46). In addition, 60% of the initial dose of PEG 40 kDa remained in murine lungs 48h post-intratracheal instillation (87). Therefore, the prolonged retention of PEG-PTX 20k was probably due to the large MW of PEG.

As compared with other drug delivery systems, PEG-PTX showed increased retention time of the drug in the lungs. Koshkina *et al.*

investigated the delivery of liposomal PTX by aerosol inhalation (63). PTX was released and reached the concentration peak in the lungs after 30 min of inhalation but it was cleared within 3 hours. Gill *et al.* studied the administration of PTX micelles by the pulmonary route (65). This system showed prolonged drug retention of PTX in the lungs compared to Taxol<sup>®</sup> administered intratracheally. Paclitaxel concentration at 12h post-delivery was found to be 46% of that at 1h post-delivery. Kaminskas *et al.* assessed the pulmonary delivery of a PEGylated polylysine dendrimer of doxorubicin (133). They demonstrated that 20% of the initial dose of the doxorubicin dendrimer was present in the BAL and the lungs 1 day after the intratracheal instillation, respectively.

It is anticipated that the slightly acidic microenvironment of the tumor would lead to accelerated cleavage of PTX from the conjugate backbone compared with the non-tumor area (142, 143). Therefore, the hydrolysis of PEG-PTX could possibly take place prior to the internalization of the conjugates, which possibly resulted in a high proportion of PTX in the interstitial tumor area within the lungs (Fig. 25). On the other hand, there are also opportunities for conjugates to be taken up by the cells via endocytosis, leading to the drug release in cytoplasm. It is likely that the PTX concentrations achieved using PEG-PTX was high enough to improve lung tumor exposure to PTX, because PEG-PTX showed significantly increased tumor regression compared with the intravenously or intratracheally injected Taxol.

The intratracheal delivery of PEGT-PTX 6k and 20k conjugates demonstrated superior anti-tumor efficacy than both i.v. and i.t.

administered Taxol, the formulation of the free drug. This result suggests that both the local delivery and the PEGylation of PTX contributed to the enhanced efficacy. As discussed above, PEG-PTX also demonstrated lower local toxicity than Taxol. Therefore, our hypothesis that PEGylation can improve the anti-tumor efficacy with reduced local toxicity is demonstrated. Moreover, since PEG-PTX 20k at a lower dose than PEG-PTX 6k showed equivalent anti-tumor efficacy but less toxicity, it could be assumed that better efficacy and lower toxicity could be achieved with higher molecular weight of PEG.

As a summary, PEGylated PTX can increase anti-tumor efficacy compared to Taxol post i.t. delivery. PEGylated paclitaxel can also greatly improve the MTD i.t. and decrease local toxicity. The retention time of PTX can be prolonged by conjugation to PEG with large MW. Therefore, PEG-PTX conjugates are a promising system for application in inhaled chemotherapy.

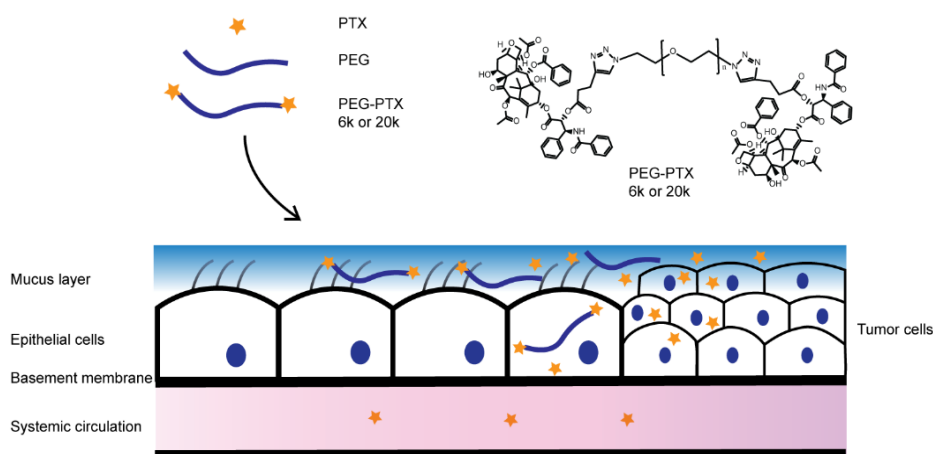
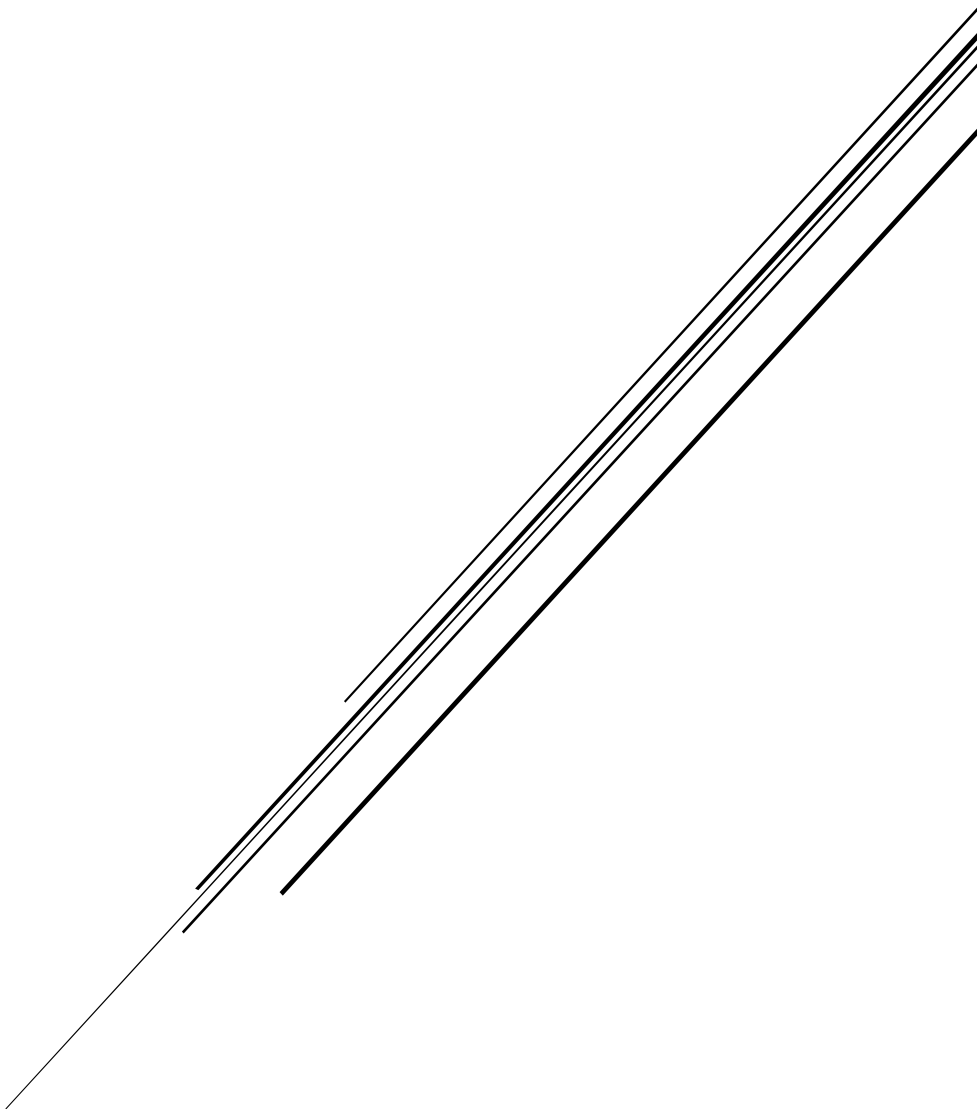


Fig. 25 Illustration of possible release mechanism of PTX from conjugates in the lungs.

## CHAPTER 4. DISCUSSION AND CONCLUSION



善始者善终。

A good beginning makes a good ending.



## **1. Main achievements**

### **1.1 Outcomes of the thesis**

Inhaled chemotherapy can be an alternative to systemic chemotherapy. However, administration of chemotherapeutics directly to the lungs will lead to local toxicity. In addition, the fast clearance mechanisms of the lungs will result in short retention time of anti-cancer drugs in the lungs. These impediments limit the therapeutic efficacy of inhaled chemotherapeutics. The aim of this thesis was to use polymer-drug conjugates to reduce the local toxicity and prolong the retention time of chemotherapeutics in the lungs. The improved anti-cancer efficacy can be achieved by the local retention and sustained release of the chemotherapeutics.

The first part of the thesis focused on the design and synthesis of PEG-PTX conjugates. PTX was conjugated to PEG 6 kDa and 20 kDa by ester bonds in two structures: 1) PEG-N<sub>3</sub>-PTX, via “click” chemistry; 2) PEG-suc-PTX, with a succinic spacer between PEG and PTX. The conjugates were produced and purified at an acceptable yield of 70%. The drug loading reached 20% and 7% (w/w) in all the structures of 6 kDa and 20 kDa conjugates, respectively. The molecular ratio of PTX in PEG-PTX conjugates was approximately 1.8 PTX per PEG molecule in both structures and both molecular weights. All the conjugates largely improved the solubility of PTX by 3-4 orders of magnitude.

In a second step, we evaluated the stability and toxicity of PEG-PTX conjugates *in vitro*. The conjugates showed very good stability in PBS pH 6.9 (pH of lung lining fluid) with half-lives longer than 72 hours. The conjugates also presented good stability in BAL with half-lives between 3 to 9 hours. The PEG-N<sub>3</sub>-PTX conjugates were more stable than the PEG-suc-PTX conjugates. To test the cytotoxicity of these conjugates, the conjugates were incubated with two cancer cell lines. These conjugates were cytotoxic, but less than Taxol, the commercial product of paclitaxel. All these *in vitro* results indicated that PEGylation of PTX has the potential to prolong the retention of PTX in the lungs and reduce local toxicity. PEG-N<sub>3</sub>-PTX conjugates were chosen for the *in vivo* evaluation because of their increased stability.

We were then interested to evaluate whether PEGylation could reduce the toxicity of PTX. Maximum tolerated doses were determined following intratracheal delivery of PEG-PTX to healthy mice. Results showed PEGylation can improve the MTD of PTX by up to 100 fold. To investigate the local toxicity of PEG-PTX conjugates, several inflammation markers including total protein, lactate dehydrogenase, and cell components were examined in the lungs following intratracheal delivery of PEG-PTX conjugates. PEG-PTX conjugates at high doses (MTDs) induced local toxicity, but at a lower dose, the toxicity was largely reduced to an acceptable level. This was due to the prodrug nature of the PEG-PTX conjugates which could avoid the transient high concentration of chemotherapeutics in the lungs.

Based on the MTD of conjugates, the anti-tumor efficacy was evaluated in a mouse model of Lewis lung carcinoma. We compared the efficacy of PEGylated PTX at different molecular weights with native PTX following intratracheal or intravenous delivery. Both PEG-PTX 6k and 20k demonstrated superior efficacy compared with Taxol delivered either intratracheally or intravenously. Therefore, PEGylation is an effective method to improve anticancer efficacy of inhaled chemotherapeutics.

To further understand the impact of PEGylation on the residence time of PTX, *in vivo* release of PTX from the conjugates were evaluated. PEGylated PTX appeared to significantly prolong its residence time in the lungs compared to the non-PEGylated free drug. The large 20 kDa PEG contributed greatly in the improving the residence time of the conjugate.

To the best of our knowledge, this is the first study about PEGylation of chemotherapeutics for pulmonary delivery in lung cancer. The main contributions of thesis are the improvement of the anti-cancer efficacy and the large reduction of toxicity of inhaled chemotherapeutics by PEGylation.

## **1.2 Synthesis of PEG-conjugated paclitaxel with cleavable linkage for pulmonary application**

Initially, we use the strategy of adding an amino acid spacer between PEG and PTX. N, N'-disuccinimidyl carbonate (DSC) was used to activate PEG and then the activated PEG-DSC was supposed to react

with glycine. However, the method was not successful mainly due to the low yield and low substitution rate of PTX on PEG terminals. Therefore, this method was not pursued.

Afterwards, we performed “click” chemistry to conjugate alkyne modified PTX to azide activated PEG. Thanks to this efficient reaction, a high yield of PEG-N<sub>3</sub>-PTX conjugates were obtained with high substitution rate. The structure of the PEG-N<sub>3</sub>-PTX conjugate is novel with a hydrolysable ester bond and a stable triazole link between PEG and PTX. The ester bond ensures that paclitaxel can be released in an intact form and the triazole link enhances the stability of the conjugate. Although various polymer-paclitaxel conjugates have been prepared, few studies have been performed in the field of pulmonary drug delivery. To the best of our knowledge, this study is the first to report PEGylation of PTX using “click” chemistry in pulmonary delivery. In the case of the pulmonary delivery of chemotherapeutics, sustained local drug concentrations are crucial to achieve anti-tumor efficacy. Therefore, a long residence time of the conjugates in the lungs is necessary. Herein, high molecular weight PEG (6 kDa and 20 kDa) were used with the expectation of long drug residency in the lungs (46). Then, because of the hydrolysable ester bonds between PEG and PTX, PTX will be released progressively to take anti-tumor effect.

### **1.3 Increased anti-tumor efficacy and prolonged lung retention of chemotherapeutics**

The PEGylated PTX 6k and 20k delivered intratracheally demonstrated superior anti-tumor efficacy than the free drug formulation Taxol when delivered both intratracheally and intravenously. The results indicated pulmonary delivery increased accumulation of PEG-PTX conjugates just in the lungs, which resulted in the relatively higher drug concentration in tumors than that of the intravenously administered Taxol. Moreover, PEGylation played a very important role in the achievement of improved anti-tumor efficacy. These results were consistent with our hypothesis that PEGylation offers the sustained release of PTX, which enables the single high dose treatment to demonstrate prolonged the anti-tumor efficacy with low toxicity. In the literature, previously work of polyglutamic acid paclitaxel conjugate (PGA-PTX) delivered intratracheally showed better anti-tumor efficacy than Taxol but with reduced toxicity (111, 112, 144, 145). This promising result was also a proof of concept that polymer drug conjugates would be a reasonable strategy for inhaled chemotherapy.

43 % and 20% of the initial dose of the PEG-PTX 20k conjugate remained in BAL and lung tissue 48h post-delivery, respectively. This prolonged effect was probably due to the large MW of PEG. As PEG with MW > 5 kDa could not be cleared and absorbed into systemic circulation quickly (46), it offered the opportunity for the drug conjugated to have a long retention time. Moreover, since PEG-PTX

20k at a lower dose showed equivalent anti-tumor efficacy as PEG-PTX 6k, it could be assumed that higher molecular weight of PEG would demonstrate longer retention in the lungs, thus better anti-tumor efficacy could be achieved. As compared with other delivery systems such as liposome, micelle and dendrimer of chemotherapeutics, PEG-PTX showed longer retention time of drug in the lungs (63, 65, 133). This indicated that PEGylation with large PEG is a very effective method to achieve sustained release of anti-cancer drug in the lungs

#### **1.4 Improved MTD and reduced local toxicity for inhaled chemotherapy**

Delivery of native chemotherapeutics would lead to unexpected acute local toxicity in the lungs. A study of inhalation solutions of doxorubicin (dissolved in 20% ethanol) in pet dogs with spontaneously occurred lung cancer showed pneumonitis and fibrosis (33). In our study, administration of both 6k and 20k PEG-PTX at MTD increased LDH level and neutrophil number, though these markers could return to normal levels after 7 days. As the dose decreased to 0.5 mg/kg (PTX equiv.) of PEG-PTX 6k, no inflammation was found. The intratracheal delivery of only PEG-N<sub>3</sub> 6k did not induce the rise of inflammatory markers, which indicated the toxicity was a result of high dose of PTX (50 mg/kg PTX equiv.). Although there was still inflammation, PEGylation of PTX improved the MTD by up to 100-fold compared with Taxol. PTX could be delivered at high doses in a tolerated manner. As the sustained release feature of PEG-PTX, the treatment could be given with reduced frequency. Therefore, the overall toxicity of PEG-

PTX was much lower than the native PTX formulation. The local bioavailability was improved.

### **1.5 Summary**

The present thesis demonstrates that PEGylation of chemotherapeutics with large PEG enhances the anti-tumor efficacy and reduces the local toxicity after administration to the respiratory tract. Further, it shows that PEGylation prolongs the residence time of chemotherapeutics in the lungs.

## 2. Perspectives

### 2.1 Long-term toxicity

In this study, we evaluated the acute and local toxicity of PEGylated PTX. PEG-PTX largely improved the MTD of PTX following intratracheal delivery. Inflammation was found at the high doses of PEG-PTX (50 and 20 mg/kg PTX equiv.), which have significant anti-tumor efficacy. We followed the toxicity of inhaled PEG-PTX at MTD for 7 days with a single dose treatment. The results showed acceptable toxicity. Given that repeated doses and relatively long term treatments are usually needed in chemotherapy, the chronic toxicity of inhaled PEG-PTX is noteworthy to investigate. More precisely, the long-term tolerability of the lungs to repeated doses of the PEGylated PTX versus the unconjugated free drug should be evaluated by examining biochemical and cellular components in broncho-alveolar lavage in extended time periods, for instance 1 to 3 months. Further, it would be interesting to investigate the local toxic effect of different sizes of PEG-PTX to provide further understanding of inhalable PEGylated chemotherapeutics.

Generally, PEG is considered to be devoid of toxicity except at high parenteral doses where renal failure has been observed (146). Klonne *et al.* studied the toxicity of 3.4 kDa PEG at a daily dose of 1.8 g/m<sup>3</sup> delivered by inhalation for 2 weeks, and found little toxicity in rat lungs (140). No toxicity study on large PEG (> 5 kDa) in the lungs was found in the literature. Large PEGs were found to have long retention times in the lungs (46, 87). The fact that large PEG could remain for long

times within the lungs generates concerns of long-term safety, thus the importance to investigate the chronic toxicology of PEG-PTX cannot be neglected.

## **2.2 Improvement of polymer-drug conjugation strategy**

We used linear PEG 6 kDa and 20 kDa for the PEGylation of PTX in this study, which provided drug loading percentages of 20% and 7%, respectively. However, the drug loading percentage could be further improved by using multi-branched PEG. The branched PEG will provide more reactive terminal hydroxyl for PEGylation, which could increase the drug molecules on each PEG. With increased drug content in the conjugate, less PEG will be delivered to the lungs. For instance, PEGylated docetaxel (NKTR-105) now in clinical trial was produced with multi-arm PEG (84). Obstacles may be the characterization and detection of these branched conjugates *in vitro* and *in vivo*. Radio labeling could be an option to follow the fate of these conjugates *in vivo* as this technology has been used in one study of doxorubicin dendrimer (133).

To further explore the pulmonary application of polymer-drug conjugates, other biodegradable polymers can also be considered to replace PEG. The most commonly used natural polymers are polysaccharides, chitosan, gelatin and hyaluronic acid. In addition, some synthetic biodegradable polymers such as poly lactic acid (PLA), poly vinyl alcohol (PVA), and poly lactic glycolic acid (PLGA) can also be options to synthesize polymer-drug conjugates (147). By choosing appropriate molecular weight and structure, long retention time as well

as reduced toxicity of chemotherapeutics could be achieved. As the polymers are biodegradable, the safety concerns of elimination would be minimized as compared with PEG.

### **2.3 Mechanisms involved in the lung retention of PEGylated paclitaxel**

In this study, we hypothesized that PEG-PTX conjugates presented long retention time in the lungs because of the large molecular weight of PEG. It would be essential to further investigate the parameters that influence the retention of PEGylated PTX.

*PEG molecular weight.* In this work, Kinetics of *in vivo* distribution of PEG-PTX conjugates in the respiratory tract showed that 43% of initially dosed PEG-PTX 20k stayed in murine lungs 48h post-delivery. Moreover, Koussoroplis *et al.* found that 60 % of initial dosed PEG 40 kDa stays in murine lungs 48h post-delivery. One study about retention of dendrimers in the lungs showed that approximately 20–30% of the dose of relatively small (<22 kDa) dendrimers were systemically absorbed compared to only 2% absorption for a larger (78 kDa) PEGylated dendrimer 48h post-delivery (148). These data suggested that the retention time of polymer in the lungs is highly related to the molecular weight. In addition, mucoadhesion might be one reason that large PEG would possess long retention time in the lungs. However, the mucoadhesive effect might be more significant with large (> 20 kDa) PEG. Above all, it would be interesting to varying polymer size to observe the relation between retention time and polymer size in murine lungs. The retention time of unconjugated PEG should also be

investigated.

*Administration site.* Conjugates can be delivered using different techniques to reach specific regions of the respiratory tract. Different administration sites may result in different depositing position of the conjugates in the respiratory tract. As the rate of mucociliary clearance decreases from the proximal to the distal lungs, the deposition sites of the conjugates might have influence on the retention time. If the conjugates are delivered to the deep lungs, the retention time is assumed to be prolonged. Nasal lavage, bronchoalveolar lavage and lung tissues could be collected post-administration of the conjugates and the concentration of PEG-PTX could be analyzed to study the retention time.



## APPENDIX

### Supporting information

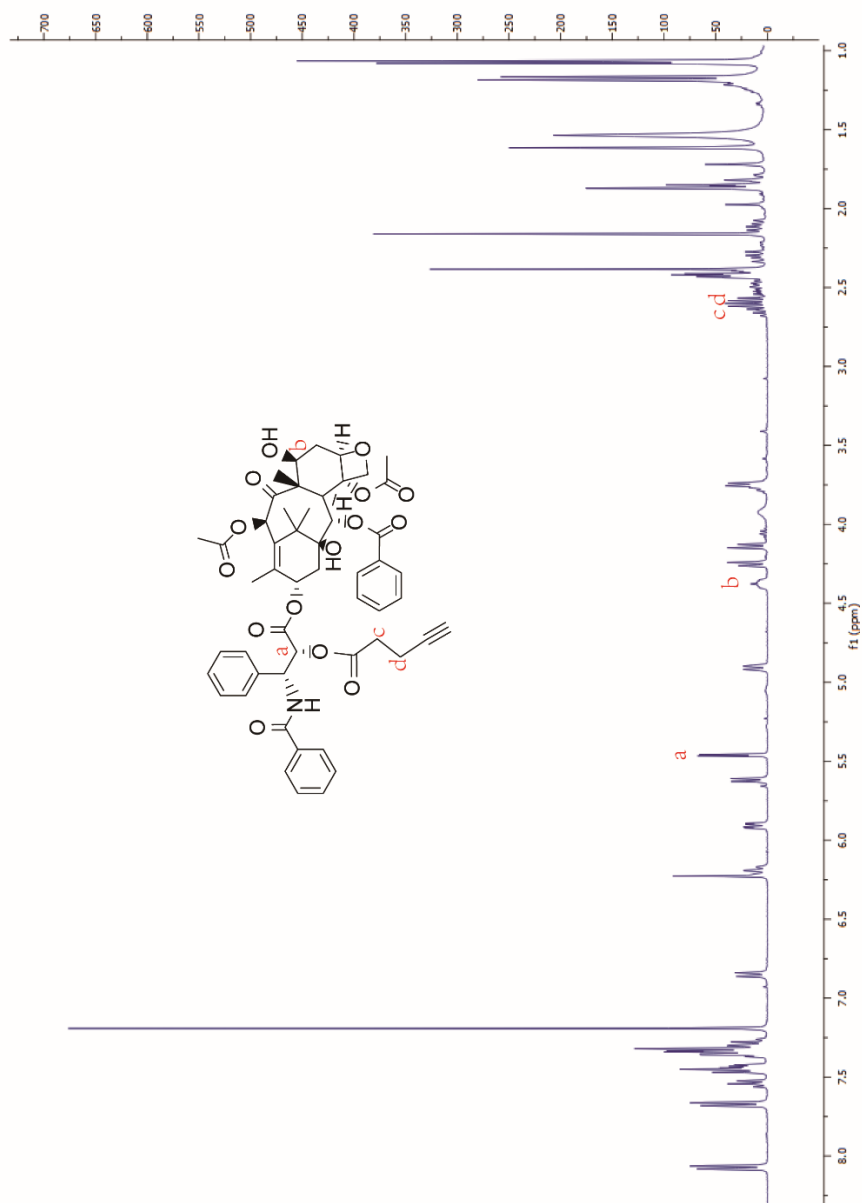


**Figure S 1**  $^1\text{H}$  NMR spectrum of PTX alkyne. Signals of “a”, “c”, and “d” confirmed that pentynoic group was covalently linked to PTX.

Openlynx Report - Johannes  
 Date: 01-Oct-2013  
 ID: tian-ptx-alkyne  
 Method: C:\MassLynx200\_1500\pos.olp  
 Printed: Tue Oct 01 13:36:15 2013

File: johannes1-2  
 Sample: 2

Page 2

Time: 13:30:41  
 Vial: 1-4

1: TOF MS ES+ : TIC Smooth (SG, 2x3) 4.6e+004

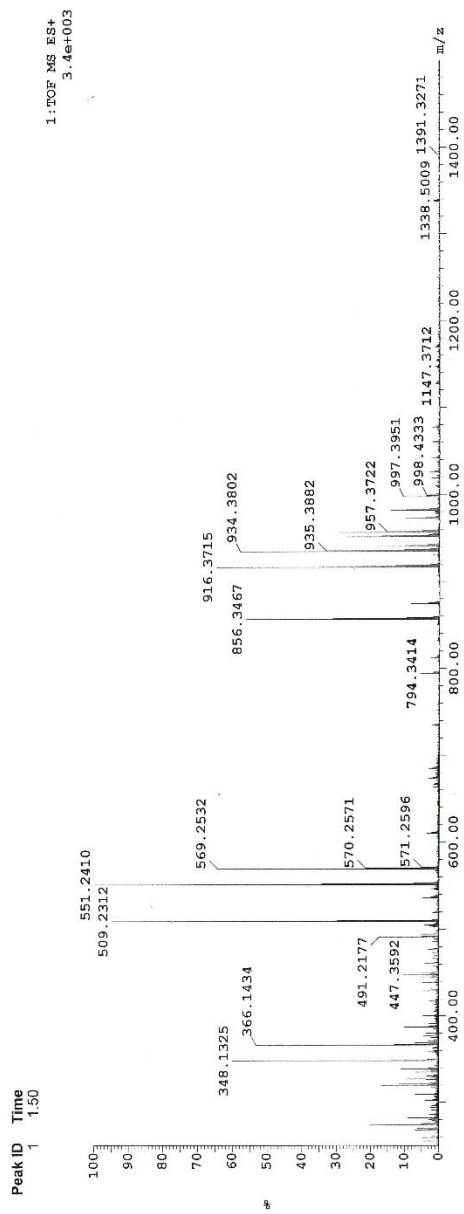
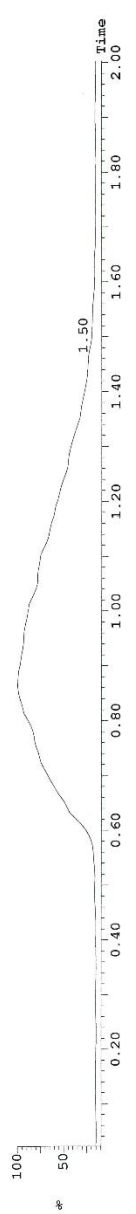


Figure S 2 Mass spectrum of PTX alkyne. 934.4 (M+H<sup>+</sup>, PTX-alkyne + H<sup>+</sup>)

## REFERENCES

1. Cancer fact sheet N°297: World Health Organization; 2013. Available from: <http://www.who.int/mediacentre/factsheets/fs297/en/>.
2. Non-small Cell Lung Cancer Collaborative G. Chemotherapy for non-small cell lung cancer. *Cochrane Database Syst Rev.* 2000(2):CD002139.
3. Jemal A, Bray F, Center MM, Ferlay J, Ward E, Forman D. Global cancer statistics. *CA Cancer J Clin.* 2011;61(2):69-90.
4. Nesbitt JC, Putnam JB, Jr., Walsh GL, Roth JA, Mountain CF. Survival in early-stage non-small cell lung cancer. *Ann Thorac Surg.* 1995;60(2):466-72.
5. Manser R, Wright G, Hart D, Byrnes G, Campbell D, Wainer Z, et al. Surgery for local and locally advanced non-small cell lung cancer. *Cochrane Database of Systematic Reviews.* 2005( 1).
6. Kaskowitz L, Graham MV, Emami B, Halverson KJ, Rush C. Radiation therapy alone for stage I non-small cell lung cancer. *Int J Radiat Oncol Biol Phys.* 1993;27(3):517-23.
7. Rowell NP, Williams CJ. Radical radiotherapy for stage I/II non-small cell lung cancer in patients not sufficiently fit for or declining surgery (medically inoperable). *Cochrane Database Syst Rev.* 2001(2):CD002935.
8. Schaake-Koning C, van den Bogaert W, Dalesio O, Festen J, Hoogenhout J, van Houtte P, et al. Effects of concomitant cisplatin and radiotherapy on inoperable non-small-cell lung cancer. *N Engl J Med.* 1992;326(8):524-30.
9. Cavalli F, Hasen HH, Kaye SB. *Textbook of Medical Oncology.* UK2004.
10. Bonfill X, Serra C, Sacristan M, Nogue M, Losa F, Montesinos J. Second-line chemotherapy for non-small cell lung cancer. *Cochrane Database Syst Rev.* 2002(2):CD002804.
11. Biersack B, Schobert R. Current State of Metal-Based Drugs for the

- Efficient Therapy of Lung Cancers and Lung Metastases. *Adv Exp Med Biol.* 2016;893:211-24.
12. Spiro SG, Silvestri GA. The treatment of advanced non-small cell lung cancer. *Curr Opin Pulm Med.* 2005;11(4):287-91.
  13. Einhorn LH. First-line chemotherapy for non-small-cell lung cancer: is there a superior regimen based on histology? *J Clin Oncol.* 2008;26(21):3485-6.
  14. Minchinton AI, Tannock IF. Drug penetration in solid tumours. *Nat Rev Cancer.* 2006;6(8):583-92.
  15. Coates A, Abraham S, Kaye SB, Sowerbutts T, Frewin C, Fox RM, et al. On the receiving end—patient perception of the side-effects of cancer chemotherapy. *European Journal of Cancer and Clinical Oncology.* 1983;19(2):203-8.
  16. Barenholz Y. Doxil(R)--the first FDA-approved nano-drug: lessons learned. *J Control Release.* 2012;160(2):117-34.
  17. Dranitsaris G, Yu B, Wang L, Sun W, Zhou Y, King J, et al. Abraxane(R) versus Taxol(R) for patients with advanced breast cancer: A prospective time and motion analysis from a Chinese health care perspective. *J Oncol Pharm Pract.* 2016;22(2):205-11.
  18. Miele E, Spinelli GP, Miele E, Tomao F, Tomao S. Albumin-bound formulation of paclitaxel (Abraxane ABI-007) in the treatment of breast cancer. *Int J Nanomedicine.* 2009;4:99-105.
  19. Iwamoto T. Clinical application of drug delivery system in cancer chemotherapy: review of efficacy and side effects of approved drugs. *Biol Pharm Bull.* 2013;36(5):715-8.
  20. Pang X, Du HL, Zhang HQ, Zhai YJ, Zhai GX. Polymer-drug conjugates: present state of play and future perspectives. *Drug Discov Today.* 2013;18(23-24):1316-22.
  21. Egusquiaguirre SP, Igartua M, Hernandez RM, Pedraz JL. Nanoparticle

delivery systems for cancer therapy: advances in clinical and preclinical research. *Clin Transl Oncol.* 2012;14(2):83-93.

22. Rusch V, Klimstra D, Venkatraman E, Pisters PW, Langenfeld J, Dmitrovsky E. Overexpression of the epidermal growth factor receptor and its ligand transforming growth factor alpha is frequent in resectable non-small cell lung cancer but does not predict tumor progression. *Clin Cancer Res.* 1997;3(4):515-22.

23. Schreiber RD, Old LJ, Smyth MJ. Cancer immunoediting: integrating immunity's roles in cancer suppression and promotion. *Science.* 2011;331(6024):1565-70.

24. Motz GT, Coukos G. Deciphering and reversing tumor immune suppression. *Immunity.* 2013;39(1):61-73.

25. Zugazagoitia J, Guedes C, Ponce S, Ferrer I, Molina-Pinelo S, Paz-Ares L. Current Challenges in Cancer Treatment. *Clin Ther.* 2016.

26. Homet Moreno B, Ribas A. Anti-programmed cell death protein-1/ligand-1 therapy in different cancers. *Br J Cancer.* 2015;112(9):1421-7.

27. Strebhardt K, Ullrich A. Paul Ehrlich's magic bullet concept: 100 years of progress. *Nat Rev Cancer.* 2008;8(6):473-80.

28. Tatsumura T, Yamamoto K, Murakami A, Tsuda M, Sugiyama S. Nclinical Pharmacokineticsew chemotherapeutic method for the treatment of tracheal and bronchial cancers--nebulization chemotherapy. *Gan No Rinsho.* 1983;29(7):765-70.

29. Tatsumura T, Koyama S, Tsujimoto M, Kitagawa M, Kagamimori S. Further study of nebulisation chemotherapy, a new chemotherapeutic method in the treatment of lung carcinomas: fundamental and clinical. *Br J Cancer.* 1993;68(6):1146-9.

30. Verschraegen CF, Gilbert BE, Loyer E, Huaranga A, Walsh G, Newman RA, et al. Clinical evaluation of the delivery and safety of aerosolized liposomal 9-nitro-20(s)-camptothecin in patients with advanced pulmonary

- malignancies. *Clin Cancer Res.* 2004;10(7):2319-26.
31. Otterson GA, Villalona-Calero MA, Sharma S, Kris MG, Imondi A, Gerber M, et al. Phase I study of inhaled Doxorubicin for patients with metastatic tumors to the lungs. *Clin Cancer Res.* 2007;13(4):1246-52.
32. Roa WH, Azarmi S, Al-Hallak MH, Finlay WH, Magliocco AM, Lobenberg R. Inhalable nanoparticles, a non-invasive approach to treat lung cancer in a mouse model. *J Control Release.* 2011;150(1):49-55.
33. Hershey AE, Kurzman ID, Forrest LJ, Bohling CA, Stonerook M, Placke ME, et al. Inhalation chemotherapy for macroscopic primary or metastatic lung tumors: proof of principle using dogs with spontaneously occurring tumors as a model. *Clin Cancer Res.* 1999;5(9):2653-9.
34. Otterson GA, Villalona-Calero MA, Hicks W, Pan X, Ellerton JA, Gettinger SN, et al. Phase I/II study of inhaled doxorubicin combined with platinum-based therapy for advanced non-small cell lung cancer. *Clin Cancer Res.* 2010;16(8):2466-73.
35. Weibel ER, Gomez DM. Architecture of the human lung. Use of quantitative methods establishes fundamental relations between size and number of lung structures. *Science.* 1962;137(3530):577-85.
36. Labiris NR, Dolovich MB. Pulmonary drug delivery. Part I: physiological factors affecting therapeutic effectiveness of aerosolized medications. *Br J Clin Pharmacol.* 2003;56(6):588-99.
37. Usmani OS, Biddiscombe MF, Barnes PJ. Regional lung deposition and bronchodilator response as a function of beta2-agonist particle size. *Am J Respir Crit Care Med.* 2005;172 (2005) 1497-1504.
38. Heyder J. Deposition of inhaled particles in the human respiratory tract and consequences for regional targeting in respiratory drug delivery. *Proc Am Thorac Soc.* 2004;1(4):315-20.
39. Hinds WC. *Aerosol technology: properties, behavior, and measurement of airborne particles.* New York, NY, USA1999.

40. Cone RA. Barrier properties of mucus. *Adv Drug Deliv Rev.* 2009;61(2):75-85.
41. Semmler-Behnke M, Takenaka S, Fertsch S, Wenk A, Seitz J, Mayer P, et al. Efficient elimination of inhaled nanoparticles from the alveolar region: evidence for interstitial uptake and subsequent reentrainment onto airways epithelium. *Environ Health Perspect.* 2007;115(5):728-33.
42. Darwiche K, Zarogoulidis P, Karamanos NK, Domvri K, Chatzaki E, Constantinidis TC, et al. Efficacy versus safety concerns for aerosol chemotherapy in non-small-cell lung cancer: a future dilemma for micro-oncology. *Future Oncol.* 2013;9(4):505-25.
43. Olmsted SS, Padgett JL, Yudin AI, Whaley KJ, Moench TR, Cone RA. Diffusion of macromolecules and virus-like particles in human cervical mucus. *Biophys J.* 2001;81(4):1930-7.
44. Lai SK, O'Hanlon DE, Harrold S, Man ST, Wang YY, Cone R, et al. Rapid transport of large polymeric nanoparticles in fresh undiluted human mucus. *Proc Natl Acad Sci U S A.* 2007;104(5):1482-7.
45. Patton JS, Fishburn CS, Weers JG. The lungs as a portal of entry for systemic drug delivery. *Proc Am Thorac Soc.* 2004;1(4):338-44.
46. Gursahani H, Riggs-Sauthier J, Pfeiffer J, Lechuga-Ballesteros D, Fishburn CS. Absorption of polyethylene glycol (PEG) polymers: the effect of PEG size on permeability. *J Pharm Sci.* 2009;98(8):2847-56.
47. Zarogoulidis P, Chatzaki E, Porpodis K, Domvri K, Hohenforst-Schmidt W, Goldberg EP, et al. Inhaled chemotherapy in lung cancer: future concept of nanomedicine. *Int J Nanomedicine.* 2012;7:1551-72.
48. Hickey AJ. *Inhalation aerosols - physical and biological basis for therapy.* New Yorker 1996.
49. Maestrelli P, Schlunssen V, Mason P, Sigsgaard T. Contribution of host factors and workplace exposure to the outcome of occupational asthma. *Eur Respir Rev.* 2012;21(124):88-96.

- 
50. Rosenow EC, 3rd, Myers JL, Swensen SJ, Pisani RJ. Drug-induced pulmonary disease. An update. *Chest*. 1992;102(1):239-50.
  51. Schwaiblmair M, Behr W, Haeckel T, Markl B, Foerg W, Berghaus T. Drug induced interstitial lung disease. *Open Respir Med J*. 2012;6:63-74.
  52. Oberdörster G. Toxicology of ultrafine particles: in vivo studies. *Philosophical Transactions of the Royal Society of London Series A: Mathematical, Physical and Engineering Sciences*. 2000;358(1775):2719-40.
  53. Ballou B, Lagerholm BC, Ernst LA, Bruchez MP, Waggoner AS. Noninvasive Imaging of Quantum Dots in Mice. *Bioconjugate Chemistry*. 2003;15(1):79-86.
  54. Oberdorster G, Sharp Z, Atudorei V, Elder A, Gelein R, Kreyling W, et al. Translocation of inhaled ultrafine particles to the brain. *Inhal Toxicol*. 2004;16(6-7):437-45.
  55. Ferin J, Oberdoster G, Soderholm SC, Gelein R. Pulmonary tissue access of ultrafine particle. *Journal of Aerosol Medicine*. Spring 1991(4(1): 57-68).
  56. Card JW, Zeldin DC, Bonner JC, Nestmann ER. Pulmonary applications and toxicity of engineered nanoparticles. *American Journal of Physiology - Lung Cellular and Molecular Physiology*. 2008;295(3):L400-L11.
  57. Sayes CM, Marchione AA, Reed KL, Warheit DB. Comparative pulmonary toxicity assessments of C60 water suspensions in rats: few differences in fullerene toxicity in vivo in contrast to in vitro profiles. *Nano Lett*. 2007;7(8):2399-406.
  58. Sayes CM, Reed KL, Warheit DB. Assessing toxicity of fine and nanoparticles: comparing in vitro measurements to in vivo pulmonary toxicity profiles. *Toxicol Sci*. 2007;97(1):163-80.
  59. Wang T-H, Wang H-S, Soong Y-K. Paclitaxel-induced cell death. *Cancer*. 2000;88(11):2619-28.
  60. Malik S, Cusidó RM, Mirjalili MH, Moyano E, Palazón J, Bonfill M.

- Production of the anticancer drug taxol in *Taxus baccata* suspension cultures: A review. *Process Biochemistry*. 2011;46(1):23-34.
61. Guenard D, Gueritte-Voegelein F, Potier P. Taxol and taxotere: discovery, chemistry, and structure-activity relationships. *Accounts of Chemical Research*. 1993;26(4):160-7.
62. van Zuylen L, Verweij J, Sparreboom A. Role of formulation vehicles in taxane pharmacology. *Invest New Drugs*. 2001;19(2):125-41.
63. Koshkina NV, Waldrep JC, Roberts LE, Golunski E, Melton S, Knight V. Paclitaxel liposome aerosol treatment induces inhibition of pulmonary metastases in murine renal carcinoma model. *Clin Cancer Res*. 2001;7(10):3258-62.
64. Pasut G, Veronese FM. PEG conjugates in clinical development or use as anticancer agents: an overview. *Adv Drug Deliv Rev*. 2009;61(13):1177-88.
65. Gill KK, Nazzal S, Kaddoumi A. Paclitaxel loaded PEG5000–DSPE micelles as pulmonary delivery platform: Formulation characterization, tissue distribution, plasma pharmacokinetics, and toxicological evaluation. *European Journal of Pharmaceutics and Biopharmaceutics*. 2011;79(2):276-84.
66. Tang BC, Fu J, Watkins DN, Hanes J. Enhanced efficacy of local etoposide delivery by poly(ether-anhydride) particles against small cell lung cancer in vivo. *Biomaterials*. 2010;31(2):339-44.
67. Sakagami M, Byron P. Respirable Microspheres for Inhalation. *Clinical Pharmacokinetics*. 2005;44(3):263-77.
68. Edwards DA, Hanes J, Caponetti G, Hrkach J, Ben-Jebria A, Eskew ML, et al. Large Porous Particles for Pulmonary Drug Delivery. *Science*. 1997;276(5320):1868-72.
69. Weers J, Metzheiser B, Taylor G, Warren S, Meers P, Perkins WR. A gamma scintigraphy study to investigate lung deposition and clearance of

- inhaled amikacin-loaded liposomes in healthy male volunteers. *J Aerosol Med Pulm Drug Deliv.* 2009;22(2):131-8.
70. Ben-Jebria A, Chen D, Eskew M, Vanbever R, Langer R, Edwards D. Large Porous Particles for Sustained Protection from Carbachol-Induced Bronchoconstriction in Guinea Pigs. *Pharmaceutical Research.* 1999;16(4):555-61.
71. Vanbever R, Ben-Jebria A, Mintzes JD, Langer R, Edwards DA. Sustained release of insulin from insoluble inhaled particles. *Drug Development Research.* 1999;48(4):178-85.
72. Gilani K, Moazeni E, Ramezanli T, Amini M, Fazeli MR, Jamalifar H. Development of respirable nanomicelle carriers for delivery of amphotericin B by jet nebulization. *J Pharm Sci.* 2011;100(1):252-9.
73. Pasut G, Veronese FM. PEG conjugates in clinical development or use as anticancer agents: An overview. *Adv Drug Deliv Rev.* 2009;61(13):1177-88.
74. Veronese FM, Pasut G. PEGylation, successful approach to drug delivery. *Drug Discov Today.* 2005;10(21):1451-8.
75. Kopecek J. Polymer-drug conjugates: origins, progress to date and future directions. *Adv Drug Deliv Rev.* 2013;65(1):49-59.
76. Kratz F, Beyer U, Schutte MT. Drug-polymer conjugates containing acid-cleavable bonds. *Crit Rev Ther Drug Carrier Syst.* 1999;16(3):245-88.
77. Li W, Zhan P, De Clercq E, Lou H, Liu X. Current drug research on PEGylation with small molecular agents. *Progress in Polymer Science.* 2013;38(3-4):421-44.
78. Fang J, Nakamura H, Maeda H. The EPR effect: Unique features of tumor blood vessels for drug delivery, factors involved, and limitations and augmentation of the effect. *Adv Drug Deliv Rev.* 2011;63(3):136-51.
79. <http://ir.nektar.com/releasedetail.cfm?ReleaseID=342650>:Nektar Therapeutics.

- 
80. Greenwald RB, Gilbert CW, Pendri A, Conover CD, Xia J, Martinez A. Drug delivery systems: water soluble taxol 2'-poly(ethylene glycol) ester prodrugs-design and in vivo effectiveness. *J Med Chem.* 1996;39(2):424-31.
81. Enzon Reports on Clinical Development Program: The Free Library. Available from: <http://www.thefreelibrary.com/Enzon+Reports+on+Clinical+Development+Program.-a096056271>.
82. Pendri A, Conover CD, Greenwald RB. Antitumor activity of paclitaxel-2'-glycinate conjugated to poly(ethylene glycol): a water-soluble prodrug. *Anticancer Drug Des.* 1998;13(5):387-95.
83. Xie Z, Lu T, Chen X, Lu C, Zheng Y, Jing X. Triblock poly(lactic acid)-b-poly(ethylene glycol)-b-poly(lactic acid)/paclitaxel conjugates: Synthesis, micellization, and cytotoxicity. *Journal of Applied Polymer Science.* 2007;105(4):2271-9.
84. Calvo E, Hoch U, Maslyar DJ, Tolcher AW. Dose-escalation phase I study of NKTR-105, a novel pegylated form of docetaxel. *J Clin Oncol.* 2010;28 (15 suppl.):abstr TPS160.
85. Eliasof S, Crawford TC, Gangal G, Reiter LA, Ng P-S, inventors Polymer-agent conjugates, particles, compositions, and related methods of use. US patent US 2011/0189092 A1.
86. Khafagy E-S, Morishita M, Onuki Y, Takayama K. Current challenges in non-invasive insulin delivery systems: A comparative review. *Adv Drug Deliv Rev.* 2007;59(15):1521-46.
87. Koussoroplis SJ, Paulissen G, Tyteca D, Goldansaz H, Todoroff J, Barilly C, et al. PEGylation of antibody fragments greatly increases their local residence time following delivery to the respiratory tract. *J Control Release.* 2014;187:91-100.
88. Morris CJ, Beck K, Fox MA, Ulaeto D, Clark GC, Gumbleton M. Pegylation of Antimicrobial Peptides Maintains the Active Peptide Conformation, Model Membrane Interactions, and Antimicrobial Activity

- while Improving Lung Tissue Biocompatibility following Airway Delivery. *Antimicrobial Agents and Chemotherapy*. 2012;56(6):3298-308.
89. Sheth P, Myrdal P. Excipients Utilized for Modifying Pulmonary Drug Release. In: Smyth HDC, Hickey AJ, editors. *Controlled Pulmonary Drug Delivery. Advances in Delivery Science and Technology*: Springer New York; 2011. p. 237-63.
90. Ryan GM, Kaminskis LM, Kelly BD, Owen DJ, McIntosh MP, Porter CJH. Pulmonary Administration of PEGylated Polylysine Dendrimers: Absorption from the Lung versus Retention within the Lung Is Highly Size-Dependent. *Molecular Pharmaceutics*. 2013.
91. Bayard FJ, Thielemans W, Pritchard DI, Paine SW, Young SS, Backman P, et al. Polyethylene glycol-drug ester conjugates for prolonged retention of small inhaled drugs in the lung. *J Control Release*. 2013;171(2):234-40.
92. Torre LA, Bray F, Siegel RL, Ferlay J, Lortet-Tieulent J, Jemal A. Global cancer statistics, 2012. *CA Cancer J Clin*. 2015;65(2):87-108.
93. Patton JS, Fishburn CS, Weers JG. The lungs as a portal of entry for systemic drug delivery. *Proc Am Phorac Soc* 2004;1(4):338-44.
94. Zarogoulidis P, Giraleli C, Karamanos NK. Inhaled chemotherapy in lung cancer: safety concerns of nanocomplexes delivered. *Ther Deliv*. 2012; 3 1021–3.
95. Loira-Pastoriza C, Todoroff J, Vanbever R. Delivery strategies for sustained drug release in the lungs. *Adv Drug Deliv Rev*. 2014;75:81-91.
96. Garbuzenko OB, Saad M, Betigeri S, Zhang M, Vetcher AA, Soldatenkov VA, et al. Intratracheal versus intravenous liposomal delivery of siRNA, antisense oligonucleotides and anticancer drug. *Pharm Res*. 2009;26(2):382-94.
97. Waite CL, Roth CM. Nanoscale drug delivery systems for enhanced drug penetration into solid tumors: current progress and opportunities. *Crit Rev Biomed Eng*. 2012;40(1):21-41.

- 
98. Jain RK. Transport of molecules in the tumor interstitium: a review. *Cancer Res.* 1987;47(12):3039-51.
99. Gursahani H, Riggs-Sauthier J, Pfeiffer J, Lechuga-Ballesteros D, Fishburn. CS. Absorption of polyethylene glycol (PEG) polymers: the effect of PEG size on permeability. *J Pharm Sci.* 2009;98:2847-56.
100. Duncan R, Vicent MJ, Greco F, Nicholson RI. Polymer-drug conjugates: towards a novel approach for the treatment of endocrine-related cancer. *Endocr Relat Cancer.* 2005;12 Suppl 1:S189-99.
101. Vicent MJ. Polymer-drug conjugates as modulators of cellular apoptosis. *AAPS J.* 2007;9(2):E200-7.
102. Krishna R, Mayer LD. Multidrug resistance (MDR) in cancer. Mechanisms, reversal using modulators of MDR and the role of MDR modulators in influencing the pharmacokinetics of anticancer drugs. *European Journal of Pharmaceutical Sciences.* 2000;11(4):265-83.
103. Cole SP, Bhardwaj G, Gerlach JH, Mackie JE, Grant CE, Almquist KC, et al. Overexpression of a transporter gene in a multidrug-resistant human lung cancer cell line. *Science.* 1992;258(5088):1650-4.
104. Danhier F, Danhier P, De Saedeleer CJ, Fruytier AC, Schleich N, Rieux A, et al. Paclitaxel-loaded micelles enhance transvascular permeability and retention of nanomedicines in tumors. *Int J Pharm.* 2015;479(2):399-407.
105. Sparreboom A, van Tellingen O, Nooijen WJ, Beijnen JH. Nonlinear pharmacokinetics of paclitaxel in mice results from the pharmaceutical vehicle Cremophor EL. *Cancer Res.* 1996;56(9):2112-5.
106. Gelderblom H, Verweij J, Nooter K, Sparreboom A. Cremophor EL: the drawbacks and advantages of vehicle selection for drug formulation. *Eur J Cancer.* 2001;37(13):1590-8.
107. Kiss L, Walter FR, Bocsik A, Veszelka S, Ozsvari B, Puskas LG, et al. Kinetic analysis of the toxicity of pharmaceutical excipients Cremophor EL and RH40 on endothelial and epithelial cells. *J Pharm Sci.* 2013;102(4):1173-

- 81.
108. Chen S, Li L, Zhao C, Zheng J. Surface hydration: Principles and applications toward low-fouling/nonfouling biomaterials. *Polymer*. 2010;51:5283-93.
109. Branca C, Magazu S. Hydration Study of PEG/Water Mixtures by Quasi Elastic Light Scattering, Acoustic and Rheological Measurements. *J Phys Chem B*. 2002;106:10272-6.
110. Navath RS, Wang B, Kannan S, Romero R, Kannan RM. Stimuli-responsive star poly(ethylene glycol) drug conjugates for improved intracellular delivery of the drug in neuroinflammation. *J Control Release*. 2010;142(3):447-56.
111. Li C, Price JE, Milas L, Hunter NR, Ke S, Yu DF, et al. Antitumor activity of poly(L-glutamic acid)-paclitaxel on syngeneic and xenografted tumors. *Clin Cancer Res*. 1999;5(4):891-7.
112. Zou Y, Fu H, Ghosh S, Farquhar D, Klostergaard J. Antitumor activity of hydrophilic Paclitaxel copolymer prodrug using locoregional delivery in human orthotopic non-small cell lung cancer xenograft models. *Clin Cancer Res*. 2004;10(21):7382-91.
113. Greenwald RB. PEG drugs: an overview. *J Control Release*. 2001;74(1-3):159-71.
114. Greenwald RB, Choe YH, McGuire J, Conover CD. Effective drug delivery by PEGylated drug conjugates. *Adv Drug Deliv Rev*. 2003;55(2):217-50.
115. Khandare JJ, Jayant S, Singh A, Chandna P, Wang Y, Vorsa N, et al. Dendrimer versus linear conjugate: Influence of polymeric architecture on the delivery and anticancer effect of paclitaxel. *Bioconjug Chem*. 2006;17(6):1464-72.
116. Arpicco S, Stella B, Schiavon O, Milla P, Zonari D, Cattel L. Preparation and characterization of novel poly(ethylene glycol) paclitaxel derivatives. *Int*

- J Pharm. 2013;454(2):653-9.
117. Pilkington-Miksa M, Arosio D, Battistini L, Belvisi L, De Matteo M, Vasile F, et al. Design, synthesis, and biological evaluation of novel cRGD-paclitaxel conjugates for integrin-assisted drug delivery. *Bioconjug Chem.* 2012;23(8):1610-22.
118. Greenwald RB, Pendri A, Bolikal D. Highly Water Soluble Taxol Derivatives: 7-Polyethylene Glycol Carbamates and Carbonates. *J Org Chem.* 1995;60 331-6.
119. Deutsch HM, Glinski JA, Hernandez M, Haugwitz RD, Narayanan VL, Suffness M, et al. Synthesis of congeners and prodrugs. 3. Water-soluble prodrugs of taxol with potent antitumor activity. *J Med Chem.* 1989;32(4):788-92.
120. de Groot FM, van Berkomp LW, Scheeren HW. Synthesis and biological evaluation of 2'-carbamate-linked and 2'-carbonate-linked prodrugs of paclitaxel: selective activation by the tumor-associated protease plasmin. *J Med Chem.* 2000;43(16):3093-102.
121. Ng AW, Bidani A, Heming TA. Innate host defense of the lung: effects of lung-lining fluid pH. *Lung.* 2004;182(5):297-317.
122. Rocks N, Bekaert S, Coia I, Paulissen G, Gueders M, Evrard B, et al. Curcumin–cyclodextrin complexes potentiate gemcitabine effects in an orthotopic mouse model of lung cancer. *British Journal of Cancer.* 2012;107:1083–92.
123. Sorrentino R, Morello S, Luciano A, Crother TR, Maiolino P, Bonavita E, et al. Plasmacytoid dendritic cells alter the antitumor activity of CpG-oligodeoxynucleotides in a mouse model of lung carcinoma. *J Immunol.* 2010;185(8):4641-50.
124. Yoshiura K, Nishishita T, Nakaoka T, Yamashita N, Yamashita N. Inhibition of B16 melanoma growth and metastasis in C57BL mice by vaccination with a syngeneic endothelial cell line. *J Exp Clin Cancer Res.*

2009;28:13.

125. Li W, Zhang P, De Clercq E, Lou H, X. L. Current drug research on PEGylation with small molecular agents. *Progress in Polymer Science*. 2013;38(3-4):421-44.

126. Hovorka O, St'astny M, Etrych T, Subr V, Strohalm J, Ulbrich K, et al. Differences in the intracellular fate of free and polymer-bound doxorubicin. *J Control Release*. 2002;80(1-3):101-17.

127. Siegel RL, Miller KD, Jemal A. Cancer statistics, 2015. *CA Cancer J Clin*. 2015;65(1):5-29.

128. Bonfill X, Serra C, Sacristan M, Nogue M, Losa F, Montesinos J. Second-line chemotherapy for non-small cell lung cancer. *Cochrane Database Syst Rev*. 2001(4):CD002804.

129. Carbone DP, Minna JD. Chemotherapy for non-small cell lung cancer. *BMJ*. 1995;311(7010):889-90.

130. Kyle AH, Baker JH, Gandolfo MJ, Reinsberg SA, Minchinton AI. Tissue penetration and activity of camptothecins in solid tumor xenografts. *Mol Cancer Ther*. 2014;13(11):2727-37.

131. Zarogoulidis P, Eleftheriadou E, Sapardanis I, Zarogoulidou V, Lithoxopoulou H, Kontakiotis T, et al. Feasibility and effectiveness of inhaled carboplatin in NSCLC patients. *Invest New Drugs*. 2012;30(4):1628-40.

132. Maeda H, Nakamura H, Fang J. The EPR effect for macromolecular drug delivery to solid tumors: Improvement of tumor uptake, lowering of systemic toxicity, and distinct tumor imaging in vivo. *Adv Drug Deliv Rev*. 2013;65(1):71-9.

133. Kaminskas LM, McLeod VM, Ryan GM, Kelly BD, Haynes JM, Williamson M, et al. Pulmonary administration of a doxorubicin-conjugated dendrimer enhances drug exposure to lung metastases and improves cancer therapy. *J Control Release*. 2014;183:18-26.

134. Danhier F, Magotteaux N, Ucakar B, Lecouturier N, Brewster M, Preat

- V. Novel self-assembling PEG-p-(CL-co-TMC) polymeric micelles as safe and effective delivery system for paclitaxel. *Eur J Pharm Biopharm.* 2009;73(2):230-8.
135. Singla AK, Garg A, Aggarwal D. Paclitaxel and its formulations. *Int J Pharm.* 2002;235(1-2):179-92.
136. Quasthoff S, Hartung HP. Chemotherapy-induced peripheral neuropathy. *J Neurol.* 2002;249(1):9-17.
137. Carvalho TC, Carvalho SR, McConville JT. Formulations for pulmonary administration of anticancer agents to treat lung malignancies. *J Aerosol Med Pulm Drug Deliv.* 2011;24(2):61-80.
138. Luo T, Magnusson J, Preat V, Frederick R, Alexander C, Bosquillon C, et al. Synthesis and In Vitro Evaluation of Polyethylene Glycol-Paclitaxel Conjugates for Lung Cancer Therapy. *Pharm Res.* 2016.
139. Eiseman JL, Eddington ND, Leslie J, MacAuley C, Sentz DL, Zuhowski M, et al. Plasma pharmacokinetics and tissue distribution of paclitaxel in CD2F1 mice. *Cancer Chemother Pharmacol.* 1994;34(6):465-71.
140. Klonne DR, Dodd DE, Losco PE, Troup CM, Tyler TR. Two-week aerosol inhalation study on polyethylene glycol (PEG) 3350 in F-344 rats. *Drug Chem Toxicol.* 1989;12(1):39-48.
141. Webster R, Didier E, Harris P, Siegel N, Stadler J, Tilbury L, et al. PEGylated proteins: evaluation of their safety in the absence of definitive metabolism studies. *Drug Metab Dispos.* 2007;35(1):9-16.
142. Tannock IF, Rotin D. Acid pH in tumors and its potential for therapeutic exploitation. *Cancer Res.* 1989;49(16):4373-84.
143. Estrella V, Chen T, Lloyd M, Wojtkowiak J, Cornell HH, Ibrahim-Hashim A, et al. Acidity generated by the tumor microenvironment drives local invasion. *Cancer Res.* 2013;73(5):1524-35.
144. Li C, Yu DF, Newman RA, Cabral F, Stephens LC, Hunter N, et al. Complete regression of well-established tumors using a novel water-soluble

- poly(L-glutamic acid)-paclitaxel conjugate. *Cancer Res.* 1998;58(11):2404-9.
145. Li C, Ke S, Wu QP, Tansey W, Hunter N, Buchmiller LM, et al. Tumor irradiation enhances the tumor-specific distribution of poly(L-glutamic acid)-conjugated paclitaxel and its antitumor efficacy. *Clin Cancer Res.* 2000;6(7):2829-34.
146. Veronese FM. PEGylated protein drugs: Basic science and clinical applications. Birkhauser, Basel, Switzerland 2009.
147. Sheth P, Myrdal PB. Controlled Pulmonary Drug Delivery. Smyth HDC, Hickey AJ, editors. New York, NY, USA,: Controlled Release Society & Springer; 2011.
148. Ryan GM, Kaminskis LM, Kelly BD, Owen DJ, McIntosh MP, Porter CJ. Pulmonary administration of PEGylated polylysine dendrimers: absorption from the lung versus retention within the lung is highly size-dependent. *Mol Pharm.* 2013;10(8):2986-95.